

# Power System Analysis

Power Flow Analysis

Fault Analysis

Power System Dynamics and Stability

Lecture 227-0526-00, ITET ETH Zürich

Göran Andersson

EEH - Power Systems Laboratory

ETH Zürich

September 2011



Eidgenössische Technische Hochschule Zürich  
Swiss Federal Institute of Technology Zurich



# Contents

Preface	vii
<b>I Static Analysis</b>	<b>1</b>
<b>1 Introduction</b>	<b>1</b>
1.1 Power Flow Analysis . . . . .	1
1.2 Fault Current Analysis . . . . .	3
1.3 Literature . . . . .	3
<b>2 Network Models</b>	<b>5</b>
2.1 Lines and Cables . . . . .	6
2.2 Transformers . . . . .	9
2.2.1 In-Phase Transformers . . . . .	10
2.2.2 Phase-Shifting Transformers . . . . .	12
2.2.3 Unified Branch Model . . . . .	14
2.3 Shunt Elements . . . . .	16
2.4 Loads . . . . .	17
2.5 Generators . . . . .	18
2.5.1 Stator Current Heating Limit . . . . .	18
2.5.2 Field Current Heating Limit . . . . .	20
2.5.3 Stator End Region Heating Limit . . . . .	20
<b>3 Active and Reactive Power Flows</b>	<b>21</b>
3.1 Transmission Lines . . . . .	21
3.2 In-phase Transformers . . . . .	23
3.3 Phase-Shifting Transformer with $\mathbf{a}_{km} = \mathbf{1}$ . . . . .	24
3.4 Unified Power Flow Equations . . . . .	25
<b>4 Nodal Formulation of the Network Equations</b>	<b>27</b>
<b>5 Basic Power Flow Problem</b>	<b>31</b>
5.1 Basic Bus Types . . . . .	31
5.2 Equality and Inequality Constraints . . . . .	32

5.3	Problem Solvability . . . . .	34
<b>6</b>	<b>Solution of the Power Flow Problem</b>	<b>37</b>
6.1	Solution by Gauss-Seidel Iteration . . . . .	37
6.2	Newton-Raphson Method . . . . .	39
6.2.1	Unidimensional case . . . . .	40
6.2.2	Quadratic Convergence . . . . .	41
6.2.3	Multidimensional Case . . . . .	42
6.3	Newton-Raphson applied to the Power Flow Equations . . . . .	44
6.4	$P\theta - QU$ Decoupling . . . . .	45
6.5	Approximative Solutions of the Power Flow Problem . . . . .	49
6.5.1	Linearization . . . . .	49
6.5.2	Matrix Formulation of DC Power Flow Equations . . . . .	52
<b>7</b>	<b>Fault Analysis</b>	<b>57</b>
7.1	Transients on a transmission line . . . . .	61
7.2	Short circuit of a synchronous machine . . . . .	63
7.3	Algorithms for short circuit studies . . . . .	66
7.3.1	Generator model . . . . .	66
7.3.2	Simplifications . . . . .	66
7.3.3	Solving the linear system equations . . . . .	67
7.3.4	The superposition technique . . . . .	69
7.3.5	The Takahashi method . . . . .	71
<b>II</b>	<b>Power System Dynamics and Stability</b>	<b>77</b>
<b>8</b>	<b>Classification and Definitions of Power System Stability</b>	<b>79</b>
8.1	Dynamics in Power Systems . . . . .	80
8.1.1	Classification of Dynamics . . . . .	80
8.1.2	Modelling . . . . .	81
8.2	Power System Stability . . . . .	82
8.2.1	Definition of Stability . . . . .	82
8.2.2	Classification of Power System Stability . . . . .	84
8.3	Literature on Power System Dynamics and Stability . . . . .	87
<b>9</b>	<b>Synchronous Machine Models</b>	<b>89</b>
9.1	Design and Operating Principle . . . . .	89
9.1.1	Rotor Types . . . . .	90
9.1.2	Stator Field . . . . .	91
9.1.3	Magnetic Torque . . . . .	94
9.2	Stationary Operation . . . . .	95
9.2.1	Stationary Single Phase Equivalent Circuit . . . . .	95
9.2.2	Phasor diagram . . . . .	97

9.2.3	Operational Limits . . . . .	98
9.3	Dynamic Operation . . . . .	100
9.3.1	Transient Single Phase Equivalent Circuit . . . . .	100
9.3.2	Simplified Mechanical Model . . . . .	100
<b>10</b>	<b>The Swing Equation</b>	<b>103</b>
10.1	Derivation of the Swing Equation . . . . .	103
10.2	Analysis of the Swing Equation . . . . .	105
10.3	Swing Equation as System of First Order Differential Equations	106
<b>11</b>	<b>Power Swings in a Simple System</b>	<b>109</b>
11.1	The Swing Equation and its Solutions . . . . .	109
11.1.1	Qualitative Analysis . . . . .	111
11.1.2	Stable and Unstable Solutions . . . . .	113
11.2	Equal Area Criterion . . . . .	121
11.3	Lyapunov Stability Criterion . . . . .	123
11.4	Small Signal Analysis . . . . .	124
11.5	Methods to Improve System Stability . . . . .	127
<b>12</b>	<b>Power Oscillations in Multi-Machine Systems</b>	<b>131</b>
12.1	Classical Model for Systems with Several Machines . . . . .	131
12.2	General Model for Electro-Mechanical Oscillations . . . . .	134
<b>13</b>	<b>Voltage Stability</b>	<b>137</b>
13.1	Mechanisms of Voltage Instability . . . . .	137
13.1.1	Long Term Voltage Instability . . . . .	138
13.1.2	Short Term Voltage Instability . . . . .	138
13.2	Simple Systems for Analysis of Voltage Stability . . . . .	139
13.3	Analysis of Voltage Stability . . . . .	142
13.3.1	Stability Indicators . . . . .	143
13.3.2	Analysis of Simple System . . . . .	144
<b>14</b>	<b>Control of Electric Power Systems</b>	<b>153</b>
14.1	Control of Active Power and Frequency . . . . .	155
14.1.1	Spinning reserve . . . . .	156
14.1.2	Supplementary Reserves . . . . .	158
14.1.3	Back-Up Reserves . . . . .	159
14.2	Control of Reactive Power and Voltage . . . . .	159
14.2.1	Reactive Power Control . . . . .	159
14.2.2	Voltage Control . . . . .	160
14.3	Supervisory Control of Electric Power Systems . . . . .	162
<b>A</b>	<b>Phase-Shifting Transformers</b>	<b>165</b>

<b>B</b>	<b>Protections in Electric Power Systems</b>	<b>169</b>
B.1	Design of Protections . . . . .	169
B.2	Distance Protections . . . . .	171
B.2.1	General Principles . . . . .	171
B.2.2	Automatic Re-Closure . . . . .	173
B.3	Out of Step Protections . . . . .	174
B.4	System Protections . . . . .	174

# Preface

These notes are intended to be used in the lecture *Power System Analysis* (Lecture number ETH Zürich 227-0526-00) (*Modellierung und Analyse elektrischer Netze*) given at ETH Zürich in Information Technology and Electrical Engineering. In these lectures three main topics are covered, i.e.

- Power flow analysis
- Fault current calculations
- Power systems dynamics and stability

In Part I of these notes the two first items are covered, while Part II gives an introduction to dynamics and stability in power systems. In appendices brief overviews of phase-shifting transformers and power system protections are given.

The notes start with a derivation and discussion of the models of the most common power system components to be used in the power flow analysis. A derivation of the power flow equations based on physical considerations is then given. The resulting non-linear equations are for realistic power systems of very large dimension and they have to be solved numerically. The most commonly used techniques for solving these equations are reviewed. The role of power flow analysis in power system planning, operation, and analysis is discussed.<sup>1</sup>

The next topic covered in these lecture notes is fault current calculations in power systems. A systematic approach to calculate fault currents in meshed, large power systems will be derived. The needed models will be given and the assumptions made when formulating these models discussed. It will be demonstrated that algebraic models can be used to calculate the dimensioning fault currents in a power system, and the mathematical analysis has similarities with the power flow analysis, so it is natural to put these two items in Part I of the notes.

In Part II the dynamic behaviour of the power system during and after disturbances (faults) will be studied. The concept of power system stability is defined, and different types of power system instabilities are discussed. While the phenomena in Part I could be studied by algebraic equations,

---

<sup>1</sup>As stated above, the presentation of the power flow problem is in these lecture notes based on physical considerations. However, for implementation of these equations in computer software, an object oriented approach is more suitable. Such an approach is presented in the lecture notes *Modellierung und Analyse elektrischer Netze*, by Rainer Bacher. In those lecture notes the techniques for handling large but sparse matrices are also reviewed.

the description of the power system dynamics requires models based on differential equations.

These lecture notes provide only a basic introduction to the topics above. To facilitate for readers who want to get a deeper knowledge of and insight into these problems, bibliographies are given in the text.

I want to thank numerous assistants, PhD students, and collaborators of Power Systems Laboratory at ETH Zürich, who have contributed in various ways to these lecture notes.

Zürich, September 2011

Göran Andersson

Part I

**Static Analysis**



# 1

## Introduction

*This chapter gives a motivation why an algebraic model can be used to describe the power system in steady state. It is also motivated why an algebraic approach can be used to calculate fault currents in a power system.*

A POWER SYSTEM is predominantly in steady state operation or in a state that could with sufficient accuracy be regarded as steady state. In a power system there are always small load changes, switching actions, and other transients occurring so that in a strict mathematical sense most of the variables are varying with the time. However, these variations are most of the time so small that an algebraic, i.e. not time varying model of the power system is justified.

A short circuit in a power system is clearly not a steady state condition. Such an event can start a variety of different dynamic phenomena in the system, and to study these dynamic models are needed. However, when it comes to calculate the fault currents in the system, steady state (static) models with appropriate parameter values can be used. A fault current consists of two components, a transient part, and a steady state part, but since the transient part can be estimated from the steady state one, fault current analysis is commonly restricted to the calculation of the steady state fault currents.

### 1.1 Power Flow Analysis

It is of utmost importance to be able to calculate the voltages and currents that different parts of the power system are exposed to. This is essential not only in order to design the different power system components such as generators, lines, transformers, shunt elements, etc. so that these can withstand the stresses they are exposed to during steady state operation without any risk of damages. Furthermore, for an economical operation of the system the losses should be kept at a low value taking various constraints into account, and the risk that the system enters into unstable modes of operation must be supervised. In order to do this in a satisfactory way the *state* of the system, i.e. all (complex) voltages of all nodes in the system, must be known. With these known, all currents, and hence all active and

reactive power flows can be calculated, and other relevant quantities can be calculated in the system.

Generally the power flow, or load flow, problem is formulated as a non-linear set of equations

$$\mathbf{f}(\mathbf{x}, \mathbf{u}, \mathbf{p}) = 0 \quad (1.1)$$

where

$\mathbf{f}$  is an  $n$ -dimensional (non-linear) function

$\mathbf{x}$  is an  $n$ -dimensional vector containing the state variables, or states, as components. These are the unknown voltage magnitudes and voltage angles of nodes in the system

$\mathbf{u}$  is a vector with (known) control outputs, e.g. voltages at generators with voltage control

$\mathbf{p}$  is a vector with the parameters of the network components, e.g. line reactances and resistances

The power flow problem consists in formulating the equations  $\mathbf{f}$  in eq. (1.1) and then solving these with respect to  $\mathbf{x}$ . This will be the subject dealt with in the first part of these lectures. A necessary condition for eq. (1.1) to have a physically meaningful solution is that  $\mathbf{f}$  and  $\mathbf{x}$  have the same dimension, i.e. that we have the same number of unknowns as equations. But in the general case there is no unique solution, and there are also cases when no solution exists.

If the states  $\mathbf{x}$  are known, all other system quantities of interest can be calculated from these and the known quantities, i.e.  $\mathbf{u}$  and  $\mathbf{p}$ . System quantities of interest are active and reactive power flows through lines and transformers, reactive power generation from synchronous machines, active and reactive power consumption by voltage dependent loads, etc.

As mentioned above, the functions  $\mathbf{f}$  are non-linear, which makes the equations harder to solve. For the solution of the equations, the linearization

$$\frac{\partial \mathbf{f}}{\partial \mathbf{x}} \Delta \mathbf{x} = \Delta \mathbf{y} \quad (1.2)$$

is quite often used and solved. These equations give also very useful information about the system. The Jacobian matrix  $\frac{\partial \mathbf{f}}{\partial \mathbf{x}}$ , whose elements are given by

$$\left( \frac{\partial \mathbf{f}}{\partial \mathbf{x}} \right)_{ij} = \frac{\partial f_i}{\partial x_j} \quad (1.3)$$

can be used for many useful computations, and it is an important indicator of the system conditions. This will also be elaborated on.

## 1.2 Fault Current Analysis

In the lectures *Elektrische Energiesysteme* it was studied how to calculate fault currents, e.g. short circuit currents, for simple systems. This analysis will now be extended to deal with realistic systems including several generators, lines, loads, and other system components. Generators (synchronous machines) are important system components when calculating fault currents and their modelling will be elaborated on and discussed.

## 1.3 Literature

The material presented in these lectures constitutes only an introduction to the subject. Further studies can be recommended in the following text books:

1. *Power Systems Analysis*, second edition, by Artur R. Bergen and Vijay Vittal. (Prentice Hall Inc., 2000, ISBN 0-13-691990-1, 619 pages)
2. *Computational Methods for Large Sparse Power Systems, An object oriented approach*, by S.A. Soma, S.A. Khaparde, Shubba Pandit (Kluwer Academic Publishers, 2002, ISBN 0-7923-7591-2, 333 pages)



# 2

## Network Models

*In this chapter models of the most common network elements suitable for power flow analysis are derived. These models will be used in the subsequent chapters when formulating the power flow problem.*

ALL ANALYSIS in the engineering sciences starts with the formulation of appropriate models. A model, and in power system analysis we almost invariably then mean a mathematical model, is a set of equations or relations, which appropriately describes the interactions between different quantities in the time frame studied and with the desired accuracy of a physical or engineered component or system. Hence, depending on the purpose of the analysis different models of the same physical system or components might be valid. It is recalled that the general model of a transmission line was given by the telegraph equation, which is a partial differential equation, and by assuming stationary sinusoidal conditions the long line equations, ordinary differential equations, were obtained. By solving these equations and restricting the interest to the conditions at the ends of the lines, the lumped-circuit line models ( $\pi$ -models) were obtained, which is an algebraic model. This gives us three different models each valid for different purposes.

In principle, the complete telegraph equations could be used when studying the steady state conditions at the network nodes. The solution would then include the initial switching transients along the lines, and the steady state solution would then be the solution after the transients have decayed. However, such a solution would contain a lot more information than wanted and, furthermore, it would require a lot of computational effort. An algebraic formulation with the lumped-circuit line model would give the same result with a much simpler model at a lower computational cost.

In the above example it is quite obvious which model is the appropriate one, but in many engineering studies the selection of the “correct” model is often the most difficult part of the study. It is good engineering practice to use as simple models as possible, but of course not too simple. If too complicated models are used, the analysis and computations would be unnecessarily cumbersome. Furthermore, generally more complicated models need more parameters for their definition, and to get reliable values of these requires often extensive work.

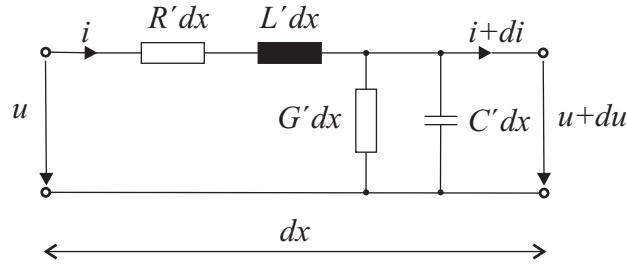


**Figure 2.1.** Equivalent circuit of a line element of length  $dx$

In the subsequent sections algebraic models of the most common power system components suitable for power flow calculations will be derived. If not explicitly stated, symmetrical three-phase conditions are assumed in the following.

## 2.1 Lines and Cables

The equivalent  $\pi$ -model of a transmission line section was derived in the lectures *Electric Power Systems (Elektrische Energiesysteme)*, 227-0122-00L. The general distributed model is characterized by the series parameters

$$R' = \text{series resistance/km per phase } (\Omega/\text{km})$$

$$X' = \text{series reactance/km per phase } (\Omega/\text{km})$$

and the shunt parameters

$$B' = \text{shunt susceptance/km per phase (siemens/km)}$$

$$G' = \text{shunt conductance/km per phase (siemens/km)}$$

as depicted in Figure 2.1. The parameters above are specific for the line or cable configuration and are dependent on conductors and geometrical arrangements.

From the circuit in Figure 2.1 the telegraph equation is derived, and from this the lumped-circuit line model for symmetrical steady state conditions, Figure 2.2. This model is frequently referred to as the  $\pi$ -model, and it is characterized by the parameters

$$Z_{km} = R_{km} + jX_{km} = \text{series impedance } (\Omega)$$

$$Y_{km}^{sh} = G_{km}^{sh} + jB_{km}^{sh} = \text{shunt admittance (siemens)}^1$$

<sup>1</sup>In Figure 2.2 the two shunt elements are assumed to be equal, which is true for

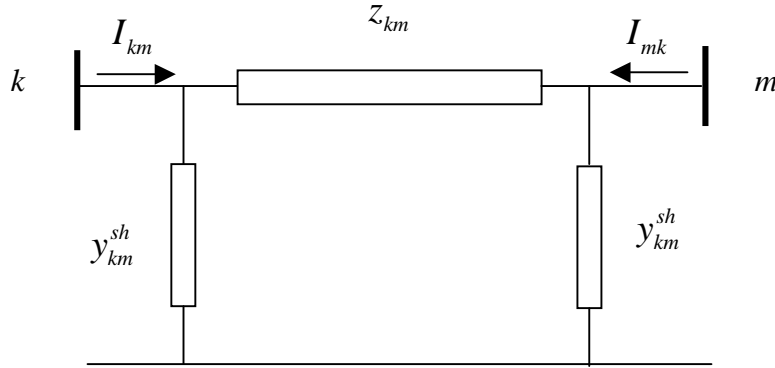


**Figure 2.2.** Lumped-circuit model ( $\pi$ -model) of a transmission line between nodes  $k$  and  $m$ .

**Note.** In the following most analysis will be made in the p.u. system. For impedances and admittances, capital letters indicate that the quantity is expressed in ohms or siemens, and lower case letters that they are expressed in p.u.

**Note.** In these lecture notes complex quantities are not explicitly marked as underlined. This means that instead of writing  $\underline{z}_{km}$  we will write  $z_{km}$  when this quantity is complex. However, it should be clear from the context if a quantity is real or complex. Furthermore, we will not always use specific type settings for vectors. Quite often vectors will be denoted by bold face type setting, but not always. It should also be clear from the context if a quantity is a vector or a scalar.

When formulating the network equations the node admittance matrix will be used and the series admittance of the line model is needed

$$y_{km} = z_{km}^{-1} = g_{km} + jb_{km} \quad (2.1)$$

with

$$g_{km} = \frac{r_{km}}{r_{km}^2 + x_{km}^2} \quad (2.2)$$

and

$$b_{km} = -\frac{x_{km}}{r_{km}^2 + x_{km}^2} \quad (2.3)$$

---

homogenous lines, i.e. a line with equal values of the line parameters along its length, but this might not be true in the general case. In such a case the shunt elements are replaced by  $Y_{km}^{sh}$  and  $Y_{mk}^{sh}$  with  $Y_{km}^{sh} \neq Y_{mk}^{sh}$  with obvious notation. A general model is presented in sect. 2.2.3, which takes asymmetric conditions into account.

For actual transmission lines the series reactance  $x_{km}$  and the series resistance  $r_{km}$  are both positive, and consequently  $g_{km}$  is positive and  $b_{km}$  is negative. The shunt susceptance  $y_{km}^{sh}$  and the shunt conductance  $g_{km}^{sh}$  are both positive for real line sections. In many cases the value of  $g_{km}^{sh}$  is so small that it could be neglected.

The complex currents  $I_{km}$  and  $I_{mk}$  in Figure 2.2 can be expressed as functions of the complex voltages at the branch terminal nodes  $k$  and  $m$ :

$$I_{km} = y_{km}(E_k - E_m) + y_{km}^{sh}E_k \quad (2.4)$$

$$I_{mk} = y_{km}(E_m - E_k) + y_{km}^{sh}E_m \quad (2.5)$$

where the complex voltages are

$$E_k = U_k e^{j\theta_k} \quad (2.6)$$

$$E_m = U_m e^{j\theta_m} \quad (2.7)$$

This can also be written in matrix form as

$$\begin{pmatrix} I_{km} \\ I_{mk} \end{pmatrix} = \begin{pmatrix} y_{km} + y_{km}^{sh} & -y_{km} \\ -y_{km} & y_{km} + y_{km}^{sh} \end{pmatrix} \begin{pmatrix} E_k \\ E_m \end{pmatrix} \quad (2.8)$$

As seen the matrix on the right hand side of eq. (2.8) is symmetric and the diagonal elements are equal. This reflects that the lines and cables are symmetrical elements.

**Example 2.1.** *The series impedance of a 138 kV transmission line section is*

$$z = r + jx = 0.0062 + j0.0360 \text{ p.u.}$$

*The total shunt susceptance (double the susceptance that appears in the equivalent  $\pi$ -model) is*

$$b^{sh} = 0.0105 \text{ p.u.}$$

*and the shunt conductance is ignored. Calculate the series conductance and series susceptance and the ratio between the series and shunt susceptances.*

**Solution** The series conductance is given by

$$g = \frac{r}{r^2 + x^2} = \frac{0.0062}{0.0062^2 + 0.0360^2} = 4.64 \text{ p.u.}$$

and the series susceptance by

$$b = -\frac{x}{r^2 + x^2} = -\frac{0.0360}{0.0062^2 + 0.0360^2} = -27.0 \text{ p.u.}$$

The  $b/b^{sh}$  ratio is given by

$$b/b^{sh} = \frac{-27.0}{0.0105} = -2596$$

Of interest is also the ratio  $x/r$

$$x/r = \frac{0.036}{0.0062} = 5.8$$



**Example 2.2.** *The series impedance and the total shunt impedance of a 750 kV line section are*

$$z = r + jx = 0.00072 + j0.0175 \text{ p.u.}$$

$$b^{sh} = 8.77 \text{ p.u.}$$

*Calculate the series conductance and series susceptance and the ratio between the series and shunt susceptances and the  $x/r$  ratio.*

**Solution** The series conductance and susceptance are given by

$$g = \frac{0.00072}{0.00072^2 + 0.0175^2} = 2.35 \text{ p.u.}$$

$$b = -\frac{0.0175}{0.00072^2 + 0.0175^2} = -57 \text{ p.u.}$$

The  $x/r$  ratio and  $b/b^{sh}$  ratio are

$$x/r = \frac{0.0175}{0.00072} = 24.3$$

$$b/b^{sh} = \frac{-57}{8.77} = -6.5$$



**Note.** *The 750 kV line has a much higher  $x/r$  ratio than the 138 kV line and, at the same time, a much smaller (in magnitude)  $b/b^{sh}$  ratio. (Why?) Higher  $x/r$  ratios mean better decoupling between active and reactive parts of the power flow problem, while smaller (in magnitude)  $b/b^{sh}$  ratios may indicate the need for some sort of compensation, shunt or series, or both.*

## 2.2 Transformers

We will start with a simplified model of a transformer where we neglect the magnetizing current and the no-load losses <sup>2</sup>. In this case the transformer

---

<sup>2</sup>Often the magnetizing current and no-load losses are modelled by a shunt impedance, with much higher impedance than the leakage impedance. The inductive part of this impedance is then determined by the value of the magnetizing current and the resistive part by the no load losses.

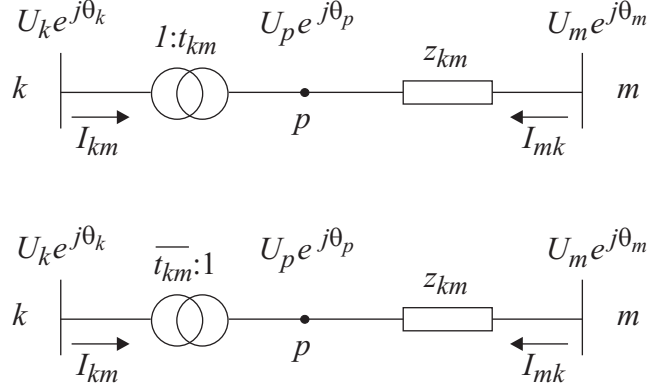


**Figure 2.3.** Transformer model with complex ratio  $t_{km} = a_{km}e^{j\varphi_{km}}$   
( $\bar{t}_{km} = a_{km}^{-1}e^{-j\varphi_{km}}$ )

can be modelled by an ideal transformer with turns ratio  $t_{km}$  in series with a series impedance  $z_{km}$  which represents resistive (load-dependent) losses and the leakage reactance, see Figure 2.3. Depending on whether  $t_{km}$  is real or non-real (complex) the transformer is in-phase or phase-shifting, respectively.

### 2.2.1 In-Phase Transformers

Figure 2.4 shows an in-phase transformer model indicating the voltage at the internal – non-physical – node  $p$ . In this model the ideal voltage magnitude ratio (turns ratio) is

$$\frac{U_p}{U_k} = a_{km} \quad (2.9)$$

Since  $\theta_k = \theta_p$ , this is also the ratio between the complex voltages at nodes  $k$  and  $p$ ,

$$\frac{E_p}{E_k} = \frac{U_p e^{j\theta_p}}{U_k e^{j\theta_k}} = a_{km} \quad (2.10)$$

There are no power losses (neither active nor reactive) in the ideal transformer (the  $k$ - $p$  part of the model), which yields

$$E_k I_{km}^* + E_p I_{mk}^* = 0 \quad (2.11)$$

Then applying eqs. (2.9) and (2.10) gives

$$\frac{I_{km}}{I_{mk}} = -\frac{|I_{km}|}{|I_{mk}|} = -a_{km}, \quad (2.12)$$

which means that the complex currents  $I_{km}$  and  $I_{mk}$  are out of phase by  $180^\circ$  since  $a_{km} \in \mathbb{R}$ .

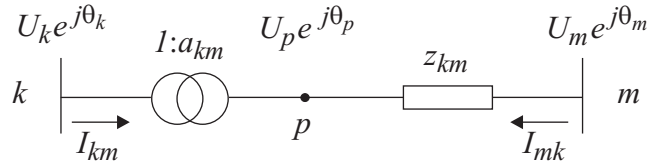


Figure 2.4. In-phase transformer model

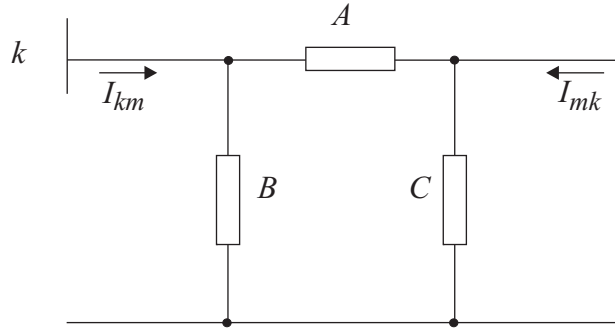
Figure 2.5. Equivalent  $\pi$ -model for in-phase transformer

Figure 2.5 represents the equivalent  $\pi$ -model for the in-phase transformer in Figure 2.4. Parameters  $A$ ,  $B$ , and  $C$  of this model can be obtained by identifying the coefficients of the expressions for the complex currents  $I_{km}$  and  $I_{mk}$  associated with the models of Figures 2.4 and 2.5. Figure 2.4 gives

$$I_{km} = -a_{km}y_{km}(E_m - E_p) = (a_{km}^2 y_{km})E_k + (-a_{km}y_{km})E_m \quad (2.13)$$

$$I_{mk} = y_{km}(E_m - E_p) = (-a_{km}y_{km})E_k + (y_{km})E_m \quad (2.14)$$

or in matrix form

$$\begin{pmatrix} I_{km} \\ I_{mk} \end{pmatrix} = \begin{pmatrix} a_{km}^2 y_{km} & -a_{km}y_{km} \\ -a_{km}y_{km} & y_{km} \end{pmatrix} \begin{pmatrix} E_k \\ E_m \end{pmatrix} \quad (2.15)$$

As seen the matrix on the right hand side of eq. (2.15) is symmetric, but the diagonal elements are not equal when  $a_{km}^2 \neq 1$ . Figure 2.5 provides now the following:

$$I_{km} = (A + B)E_k + (-A)E_m \quad (2.16)$$

$$I_{mk} = (-A)E_k + (A + C)E_m \quad (2.17)$$

or in matrix form

$$\begin{pmatrix} I_{km} \\ I_{mk} \end{pmatrix} = \begin{pmatrix} A + B & -A \\ -A & A + C \end{pmatrix} \begin{pmatrix} E_k \\ E_m \end{pmatrix} \quad (2.18)$$

Identifying the matrix elements from the matrices in eqs. (2.15) and (2.18) yields

$$A = a_{km}y_{km} \quad (2.19)$$

$$B = a_{km}(a_{km} - 1)y_{km} \quad (2.20)$$

$$C = (1 - a_{km})y_{km} \quad (2.21)$$

**Example 2.3.** *A 138/69 kV in-phase transformer with a series resistance of zero, a 0.23 p.u. series reactance, and p.u. turns ratio of 1 : 1.030 (from the model in Figure 2.4) Calculate the equivalent  $\pi$ -model parameters.*

**Solution**

$$A = a_{km}y_{km} = 1.030(j0.230)^{-1} = -j4.48 \text{ p.u.}$$

$$B = a_{km}(a_{km} - 1)y_{km} = 1.030(1.030 - 1)(j0.230)^{-1} = -j0.13 \text{ p.u.}$$

$$C = (1 - a_{km})y_{km} = (1 - 1.030)(j0.230)^{-1} = j0.13 \text{ p.u.}$$

Hence, since  $A$ ,  $B$ , and  $C$  denote admittances,  $A$  and  $B$  are inductive, and  $C$  is capacitive.  $\blacklozenge$

**Example 2.4.** *A 500/750 kV in-phase transformer with a series resistance of zero, a 0.00623 p.u. series reactance, and p.u. turns ratio of 1 : 0.950 (from the model in Figure 2.4) Calculate the parameters for the equivalent  $\pi$ -model. (100 MVA base)*

**Solution** As in the previous example one obtains:

$$A = -j152.5 \text{ p.u.}$$

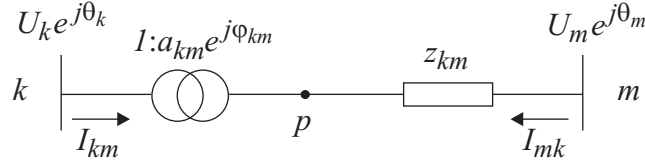
$$B = j7.62 \text{ p.u.}$$

$$C = -j8.03 \text{ p.u.}$$

i.e., parameter  $B$  is capacitive and parameter  $C$  is inductive (762 Mvar and  $-803$  Mvar, respectively, assuming nominal voltage magnitudes and a 100 MVA base).  $\blacklozenge$

## 2.2.2 Phase-Shifting Transformers

Phase-shifting transformers, such as the one represented in Figure 2.6, are used to control active power flows; the control variable is the phase angle and the controlled quantity can be, among other possibilities, the active power flow in the branch where the shifter is placed. In Appendix A the physical design of phase-shifting transformer is described.



$$\theta_p = \theta_k + \varphi_{km}$$

$$U_p = a_{km} U_k$$

**Figure 2.6.** Phase-shifting transformer with  $t_{km} = a_{km} e^{j\varphi_{km}}$ .

A phase-shifting transformer affects both the phase and magnitude of the complex voltages  $E_k$  and  $E_p$ , without changing their ratio, i.e.,

$$\frac{E_p}{E_k} = t_{km} = a_{km} e^{j\varphi_{km}} \quad (2.22)$$

Thus,  $\theta_p = \theta_k + \varphi_{km}$  and  $U_p = a_{km} U_k$ , using eqs. (2.11) and (2.22),

$$\frac{I_{km}}{I_{mk}} = -t_{km}^* = -a_{km} e^{-j\varphi_{km}} \quad (2.23)$$

As with in-phase transformers, the complex currents  $I_{km}$  and  $I_{mk}$  can be expressed in terms of complex voltages at the phase-shifting transformer terminals:

$$I_{km} = -t_{km}^* y_{km} (E_m - E_p) = (a_{km}^2 y_{km}) E_k + (-t_{km}^* y_{km}) E_m \quad (2.24)$$

$$I_{mk} = y_{km} (E_m - E_p) = (-t_{km} y_{km}) E_k + (y_{km}) E_m \quad (2.25)$$

or in matrix form

$$\begin{pmatrix} I_{km} \\ I_{mk} \end{pmatrix} = \begin{pmatrix} a_{km}^2 y_{km} & -t_{km}^* y_{km} \\ -t_{km} y_{km} & y_{km} \end{pmatrix} \begin{pmatrix} E_k \\ E_m \end{pmatrix} \quad (2.26)$$

As seen this matrix is not symmetric if  $t_{km}$  is non-real, and the diagonal matrix elements are not equal if  $a_{km}^2 \neq 1$ . There is no way to determine parameters  $A$ ,  $B$ , and  $C$  of the equivalent  $\pi$ -model from these equations, since the coefficient  $-t_{km}^* y_{km}$  of  $E_m$  in eq. (2.24) differs from  $-t_{km} y_{km}$  in eq. (2.25), as long as there is nonzero phase shift, i.e.  $t_{km} \notin \mathbb{R}$ . A phase-shifting transformer can thus not be represented by a  $\pi$ -model.

**Example 2.5.** A 230/138 kV transformer (Figure 2.6) has a series resistance of zero, a 0.0127 p.u. series reactance, and a complex turns ratio of  $1 : 1.007e^{j30^\circ}$  (Y- $\Delta$  connection).

Show that this transformer can be seen to consist of a series connection of two transformers: an ideal in-phase transformer with a turns ratio of 1 : 1.007 (constant voltage phase) and a phase-shifting transformer with a complex turns ratio of 1 :  $e^{j30^\circ}$  (constant voltage amplitude) and a series reactance of 0.0127 p.u.

**Note.** If no parallel paths exist, the phase-shifting has no significance. The introduced phase-shift can in such a case be seen as a shift of the phase angle of the reference node. Y- $\Delta$  connected transformers are often used to provide zero-sequence de-coupling between two parts of the system, and not for active power flow. For active power flow control usually phase-shifting much lower than  $30^\circ$  is needed. Often the phase-shifting could be varied to cope with different loading situations in the system.

**Example 2.6.** Consider two transformers connected in parallel according to Figure 2.7. Transformer A has a turns-ratio of 1:1 (p.u./p.u.) while the turns-ratio of transformer B will be varied as described below. The transformers are feeding a load at bus 2,  $I_{load} = 1.05 \angle -45^\circ$  p.u. and  $E_2 = 1 \angle 0^\circ$  p.u. The reactances of the transformers are given in the figure.

Calculate the complex power through the transformers when the turns-ratios of transformer B are ( $t_{12} = a_{12}e^{j\varphi_{12}}$ )

(a)  $a_{12} = 1, \varphi_{12} = 0^\circ$

(b)  $a_{12} = 1.05, \varphi_{12} = 0^\circ$

(c)  $a_{12} = 1, \varphi_{12} = 3^\circ$

Comments!

### 2.2.3 Unified Branch Model

The expressions for the complex currents  $I_{km}$  and  $I_{mk}$  for both transformers and shifters derived above depend on the side where the tap is located; i.e., they are not symmetrical. It is however possible to develop unified complex expressions which can be used for lines, transformers, and phase-shifters, regardless of the side on which the tap is located (or even in the case when there are taps on both sides of the device). Consider initially the model in Figure 2.8 in which shunt elements have been temporarily ignored and  $t_{km} = a_{km}e^{j\varphi_{km}}$  and  $t_{mk} = a_{mk}e^{j\varphi_{mk}}$ . In this case

$$I_{km} = t_{km}^* I_{pq} = t_{km}^* (E_p - E_q) y_{km} = t_{km}^* (t_{km} E_k - t_{mk} E_m) y_{km} \quad (2.27)$$

and

$$I_{mk} = t_{mk}^* I_{qp} = t_{mk}^* (E_q - E_p) y_{km} = t_{mk}^* (t_{mk} E_m - t_{km} E_k) y_{km} \quad (2.28)$$

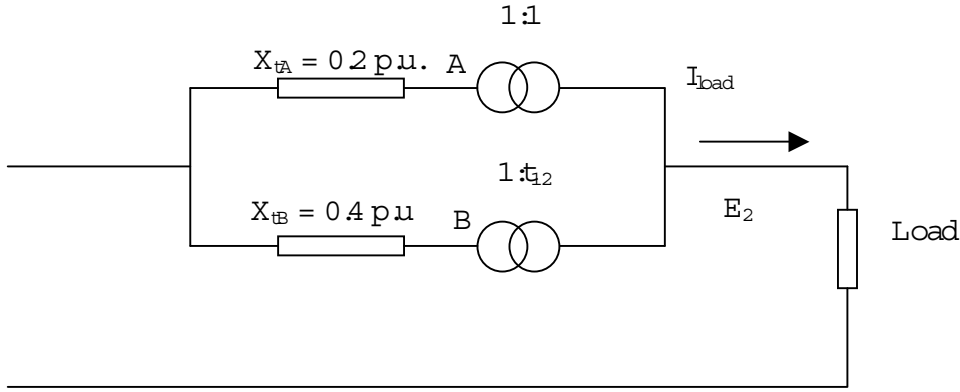


Figure 2.7. System for Example 2.6.

which together yield

$$I_{km} = (a_{km}^2 E_k - t_{km}^* t_{mk} E_m) y_{km} \quad (2.29)$$

and

$$I_{mk} = (a_{mk}^2 E_m - t_{mk}^* t_{km} E_k) y_{km} \quad (2.30)$$

(These expressions are symmetrical in the sense that if  $k$  and  $m$  are interchanged, as in the expression for  $I_{km}$ , the result is the expression for  $I_{mk}$ , and vice-versa.)

Figure 2.9 shows the unified branch model. All the devices studied above can be derived from this general model by establishing the appropriate definitions of the parameters that appear in the unified model. Thus, for instance, if  $t_{km} = t_{mk} = 1$  is assumed, the result is an equivalent  $\pi$ -model of a transmission line; or, if the shunt elements are ignored, and  $t_{km} = 1$  and  $t_{mk} = a_{mk} e^{-j\varphi_{mk}}$  is assumed, then the result is a phase shifting transformer with the tap located on the bus  $m$  side. The general expressions for  $I_{km}$  and  $I_{mk}$  can be obtained from the model in Figure 2.9:

$$I_{km} = (a_{km}^2 E_k - t_{km}^* t_{mk} E_m) y_{km} + y_{km}^{sh} a_{km}^2 E_k \quad (2.31)$$

and

$$I_{mk} = (a_{mk}^2 E_m - t_{mk}^* t_{km} E_k) y_{km} + y_{mk}^{sh} a_{mk}^2 E_m \quad (2.32)$$

or

$$\begin{pmatrix} I_{km} \\ I_{mk} \end{pmatrix} = \begin{pmatrix} a_{km}^2 (y_{km} + y_{km}^{sh}) & -t_{km}^* t_{mk} y_{km} \\ -t_{mk}^* t_{km} y_{km} & a_{mk}^2 (y_{km} + y_{km}^{sh}) \end{pmatrix} \begin{pmatrix} E_k \\ E_m \end{pmatrix} \quad (2.33)$$

The transformers modelled above were all two-winding transformers. In power systems there are also three-winding and  $N$ -winding ( $N > 3$ ) transformers, and they can be modelled in a similar way. Instead of linear relationships between two complex currents and two complex voltages, we will

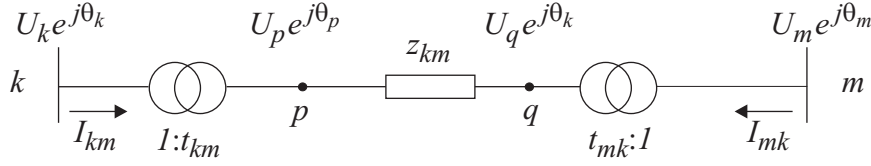


**Figure 2.8.** Transformer symmetrical model.

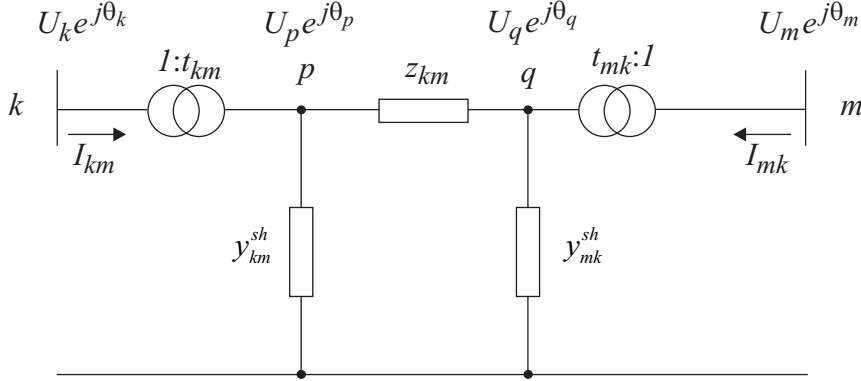


**Figure 2.9.** Unified branch model extended ( $\pi$ -model).

have linear relationships between these quantities modelled by  $N \times N$  matrices. It should be noted that for  $N$ -winding transformers there are leakage reactances between each pair of windings, i.e. in total  $N(N-1)/2$  reactances. Since the power ratings of the different windings are not necessarily equal, as in the two-winding case, it should be noted that the power bases for expressing the reactances in p.u. are not always equal.

## 2.3 Shunt Elements

The modelling of shunt elements in the network equations is straightforward and the main purpose here is to introduce the notation and the sign convention to be used when formulating the network equations in the coming chapters. As seen from Figure 2.10 the current from a shunt is defined as positive when injected into the bus. This means that

$$I_k^{sh} = -y_k^{sh} E_k \quad (2.34)$$

with  $E_k$  being the complex voltage at node  $k$ . Shunts are in all practical cases either shunt capacitors or reactors. From eq. (2.34) the injected complex

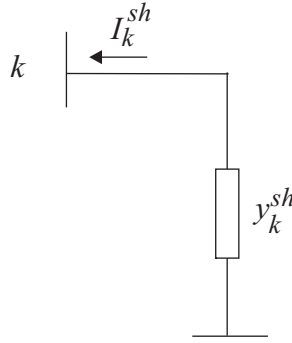


**Figure 2.10.** A shunt connected to bus  $k$ .

power is

$$S_k^{sh} = P_k^{sh} + jQ_k^{sh} = -(y_k^{sh})^* |E_k|^2 = -(y_k^{sh})^* U_k^2 \quad (2.35)$$

## 2.4 Loads

Load modelling is an important topic in power system analysis. When formulating the load flow equations for high voltage systems, a load is most often the infeed of power to a network at a lower voltage level, e.g. a distribution network. Often the voltage in the distribution systems is kept constant by controlling the tap-positions of the distribution transformers which means that power, active and reactive, in most cases can be regarded as independent of the voltage on the high voltage side. This means that the complex power  $E_k(I_k^{load})^*$  is constant, i.e. independent of the voltage magnitude  $U_k$ . Also in this case the current is defined as positive when injected into the bus, see Figure 2.11. In the general case the complex load current can be written as

$$I_k^{load} = I_k^{load}(U_k) \quad (2.36)$$

where the function  $I_k^{load}(\cdot)$  describes the load characteristics.<sup>3</sup> More often the load characteristics are given for the active and reactive powers

$$P_k^{load} = P_k^{load}(U_k) \quad (2.37)$$

$$Q_k^{load} = Q_k^{load}(U_k) \quad (2.38)$$

---

<sup>3</sup>This refers to the steady state model of the load. For transient conditions other load models apply. These are usually formulated as differential equations and might also involve the frequency.

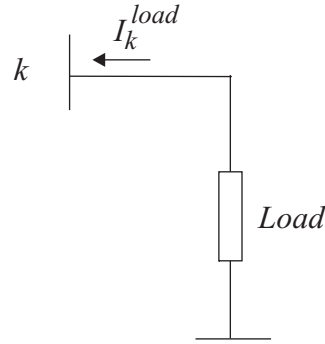


Figure 2.11. Model of a load connected to bus  $k$ .

## 2.5 Generators

Generators are in load flow analysis modelled as current injections, see Figure 2.12. In steady state a generator is commonly controlled so that the active power injected into the bus and the voltage at the generator terminals are kept constant. This will be elaborated later when formulating the load flow equations. Active power from the generator is determined by the turbine control and must of course be within the capability of the turbine-generator system. Voltage is primarily determined by the reactive power injection into the node, and since the generator must operate within its reactive capability curve it is not possible to control the voltage outside certain limits. The reactive capability of a generator depends on a number of quantities, such as active power, bus voltage and other operating conditions, and a typical example is shown in Figure 2.13. The shape of the generator capability curve is specific for each generator and depends on design characteristics, type of generator, hydro or steam turbine, stability constraints, etc. In Figure 2.13 it is also indicated what imposes the different limits for this particular generator. These are briefly discussed below. These limits are also discussed in Chapter 9.

### 2.5.1 Stator Current Heating Limit

The losses in the armature windings are given by  $R_t I_t^2$ , with obvious notation. These losses result in a temperature rise in the armature windings, and this must be limited to a given value otherwise the generator is damaged or its life time is reduced. Since the complex power is given by  $S = P + jQ = U_t I_t^*$  it means that for a given terminal voltage,  $U_t$ , circles in the  $P - Q$ -plane with centre at the origin correspond to constant value of the magnitude of the armature current  $I_t$ . The stator current limit for a given terminal voltage is thus a circle with the centre at the origin. At high

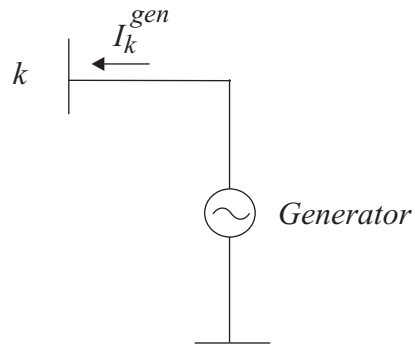


**Figure 2.12.** Model of a generator connected to bus  $k$ .

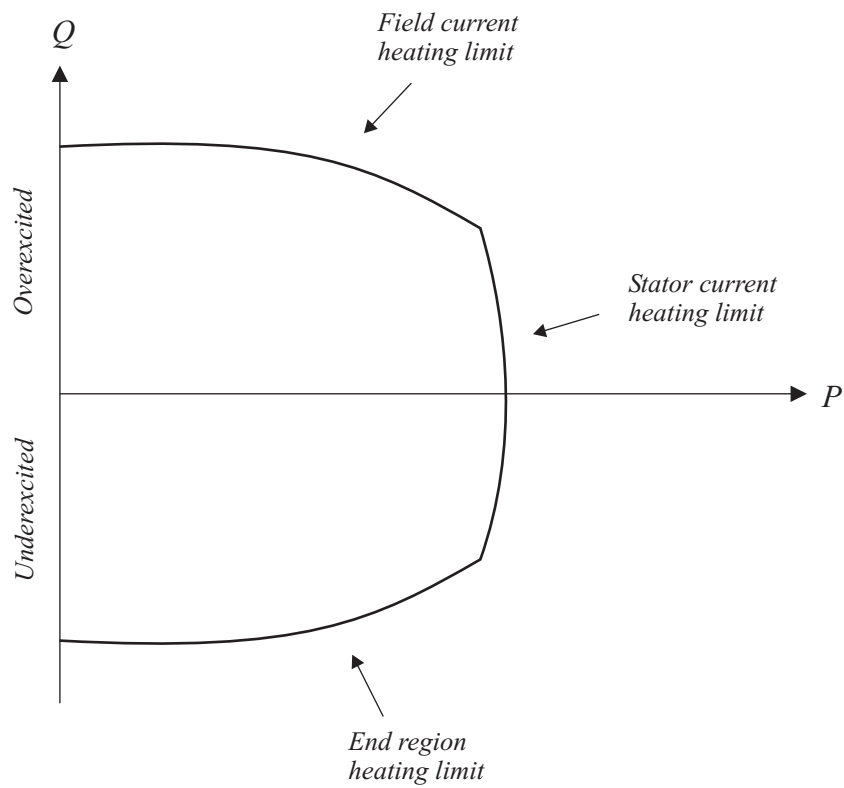


**Figure 2.13.** Reactive capability curve of a turbo generator.

loading of the generator, this is usually determining the reactive capability of the synchronous machine.

### 2.5.2 Field Current Heating Limit

The reactive power that can be generated at low load is determined by the field current heating limit. It can be shown that the locus for constant field current is a circle with the centre on the  $Q$ -axis at  $-E_t^2/X_s$ , where  $E_t$  is the terminal voltage and  $X_s$  is the synchronous reactance. The radius is given by machine parameters and typical behaviour is shown in Figure 2.13. The field current heating is usually limiting at overexcited operation at low load.

### 2.5.3 Stator End Region Heating Limit

When the synchronous machine is underexcited the armature end leakage flux is increased. This flux enters and leaves in a direction perpendicular to the stator laminations causing eddy currents in the laminations, and hence heating. This can limit the capability, particularly for round rotor machines. A typical example of such a limitation is shown in Figure 2.13.

The limits on reactive power generation and absorption given in this subsection and the two previous ones are imposed by internal synchronous machine design. As seen they are dependent on the terminal voltage of the generator. There are also other considerations that can further limit the reactive capability of the synchronous machine. These are stability limits that could further limit the operation of the machine in underexcited operation.

# 3

## Active and Reactive Power Flows

*In this chapter the expressions for the active and reactive power flows in transmission lines, transformers, phase-shifting transformers, and unified branch models are derived.*

THE SYSTEM COMPONENTS dealt with in this chapter are linear in the sense that the relations between voltages and currents are linear<sup>1</sup>. However, since one usually is interested rather in powers, active and reactive, than currents, the resulting equations will be non-linear, which introduces a complication when solving the resulting equations.

### 3.1 Transmission Lines

Consider the complex current  $I_{km}$  in a transmission line

$$I_{km} = y_{km}(E_k - E_m) + jb_{km}^{sh} E_k \quad (3.1)$$

with quantities defined according to Figure 2.2. The complex power,  $S_{km} = P_{km} + jQ_{km}$ , is

$$S_{km} = E_k I_{km}^* = y_{km}^* U_k e^{j\theta_k} (U_k e^{-j\theta_k} - U_m e^{-j\theta_m}) - jb_{km}^{sh} U_k^2 \quad (3.2)$$

where the conductance of  $y_{km}^{sh}$  has been neglected.

The expressions for  $P_{km}$  and  $Q_{km}$  can be determined by identifying the corresponding coefficients of the real and imaginary parts of eq. (3.2), which yields

$$P_{km} = U_k^2 g_{km} - U_k U_m g_{km} \cos \theta_{km} - U_k U_m b_{km} \sin \theta_{km} \quad (3.3)$$

$$Q_{km} = -U_k^2 (b_{km} + b_{km}^{sh}) + U_k U_m b_{km} \cos \theta_{km} - U_k U_m g_{km} \sin \theta_{km} \quad (3.4)$$

where the notation  $\theta_{km} = \theta_k - \theta_m$  is introduced.

---

<sup>1</sup>This is at least true for the models analyzed here. Different non-linear phenomena, e.g. magnetic saturation, can sometimes be important, but when studying steady state conditions the devices to be discussed in this chapter are normally within the region of linearity.

The active and reactive power flows in opposite directions,  $P_{mk}$  and  $Q_{mk}$ , can be obtained in the same way, resulting in:

$$P_{mk} = U_m^2 g_{km} - U_k U_m g_{km} \cos \theta_{mk} + U_k U_m b_{km} \sin \theta_{mk} \quad (3.5)$$

$$Q_{mk} = -U_m^2 (b_{km} + b_{km}^{sh}) + U_k U_m b_{km} \cos \theta_{mk} + U_k U_m g_{km} \sin \theta_{mk} \quad (3.6)$$

From these expressions the active and reactive power losses of the lines are easily obtained as:

$$\begin{aligned} P_{km} + P_{mk} &= g_{km}(U_k^2 + U_m^2 - 2U_k U_m \cos \theta_{km}) \\ &= g_{km}|E_k - E_m|^2 \end{aligned} \quad (3.7)$$

$$\begin{aligned} Q_{km} + Q_{mk} &= -b_{km}^{sh}(U_k^2 + U_m^2) - b_{km}(U_k^2 + U_m^2 - 2U_k U_m \cos \theta_{km}) \\ &= -b_{km}^{sh}(U_k^2 + U_m^2) - b_{km}|E_k - E_m|^2 \end{aligned} \quad (3.8)$$

Note that  $|E_k - E_m|$  represents the magnitude of the voltage drop across the line,  $g_{km}|E_k - E_m|^2$  represents the active power losses,  $-b_{km}^{sh}|E_k - E_m|^2$  represents the reactive power losses; and  $-b_{km}^{sh}(U_k^2 + U_m^2)$  represents the reactive power generated by the shunt elements of the equivalent  $\pi$ -model (assuming actual transmission line sections, i.e. with  $b_{km} < 0$  and  $b_{km}^{sh} > 0$ ).

**Example 3.1.** A 750 kV transmission line section has a series impedance of  $0.00072 + j0.0175$  p.u., a total shunt impedance of 8.775 p.u., a voltage magnitude at the terminal buses of 0.984 p.u. and 0.962 p.u., and a voltage angle difference of  $22^\circ$ . Calculate the active and reactive power flows.

**Solution** The active and reactive power flows in the line are obtained by applying eqs. (3.3) and (3.4), where  $U_k = 0.984$  p.u.,  $U_m = 0.962$  p.u., and  $\theta_{km} = 22^\circ$ . The series impedance and admittances are as follows:

$$z_{km} = 0.00072 + j0.0175 \text{ p.u.}$$

$$y_{km} = g_{km} + jb_{km} = z_{km}^{-1} = 2.347 - j57.05 \text{ p.u.}$$

The  $\pi$ -model shunt admittances (100 MVA base) are:

$$b_{km}^{sh} = 8.775/2 = 4.387 \text{ p.u.}$$

and

$$P_{km} = 0.984^2 \cdot 2.347 - 0.984 \cdot 0.962 \cdot 2.347 \cos 22^\circ + 0.984 \cdot 0.962 \cdot 57.05 \sin 22^\circ \text{ p.u.}$$

$$Q_{km} = -0.984^2 \cdot (-57.05 + 4.39) - 0.984 \cdot 0.962 \cdot 57.05 \cos 22^\circ - 0.984 \cdot 0.962 \cdot 2.347 \sin 22^\circ \text{ p.u.}$$

which yield

$$P_{km} = 2044 \text{ MW} \quad Q_{km} = 8.5 \text{ Mvar}$$

In similar way one obtains:

$$P_{mk} = -2012 \text{ MW} \quad Q_{mk} = -50.5 \text{ Mvar}$$

It should be noted that powers are positive when injected into the line. ♦

## 3.2 In-phase Transformers

The complex current  $I_{km}$  in an in-phase transformer is expressed as in eq. (2.13)

$$I_{km} = a_{km} y_{km} (a_{km} E_k - E_m)$$

The complex power,  $S_{km} = P_{km} + jQ_{km}$ , is given by

$$S_{km} = E_k I_{km}^* = y_{km}^* a_{km} U_k e^{j\theta_k} (a_{km} U_k e^{-j\theta_k} - U_m e^{-j\theta_m}) \quad (3.9)$$

Separating the real and imaginary parts of this latter expression yields the active and reactive power flow equations:

$$P_{km} = (a_{km} U_k)^2 g_{km} - a_{km} U_k U_m g_{km} \cos \theta_{km} - a_{km} U_k U_m b_{km} \sin \theta_{km} \quad (3.10)$$

$$Q_{km} = -(a_{km} U_k)^2 b_{km} + a_{km} U_k U_m b_{km} \cos \theta_{km} - a_{km} U_k U_m g_{km} \sin \theta_{km} \quad (3.11)$$

These same expressions can be obtained by comparing eqs. (3.9) and (3.2); in eq. (3.9) the term  $j b_{km}^{sh} U_k^2$  is not present, and  $U_k$  is replaced by  $a_{km} U_k$ . Hence, the expressions for the active and reactive power flows on in-phase transformers are the same expressions derived for a transmission line, except the for two modifications: ignore  $b_{km}^{sh}$ , and replace  $U_k$  with  $a_{km} U_k$ .

**Example 3.2.** A 500/750 kV transformer with a tap ratio of 1.050:1.0 on the 500 kV side, see Figure 2.4, has negligible series resistance and a leakage reactance of 0.00623 p.u., terminal voltage magnitudes of 1.023 p.u. and 0.968 p.u., and an angle spread of 5.3°. Calculate the active and reactive power flows in the transformer.

**Solution** The active and reactive power flows in the transformer are given by eqs. (3.10) and (3.11), where  $U_k = 1.023$  p.u.,  $U_m = 0.968$  p.u.,  $\theta_{km} = 5.3^\circ$ , and  $a_{km} = 1.0/1.05 = 0.9524$ . The series reactance and susceptance are as follows:

$$x_{km} = 0.00623 \text{ p.u.}$$

$$b_{km} = -x_{km}^{-1} = -160.51 \text{ p.u.}$$

The active and reactive power flows can be expressed as

$$P_{km} = -0.9524 \cdot 1.023 \cdot 0.968 \cdot (-160.51) \sin 5.3^\circ \text{ p.u.}$$

$$Q_{km} = -(0.952 \cdot 1.023)^2 (-160.51) + 0.952 \cdot 1.023 \cdot 0.968 \cdot (-160.51) \cos 5.3^\circ \text{ p.u.}$$

which yield

$$P_{km} = 1398 \text{ MW} \quad Q_{km} = 163 \text{ Mvar}$$

The reader is encouraged to calculate  $P_{mk}$  and  $Q_{mk}$ . (The value of  $P_{mk}$  should be obvious.) ♦

### 3.3 Phase-Shifting Transformer with $a_{km} = 1$

The complex current  $I_{km}$  in a phase shifting transformer with  $a_{km} = 1$  is as follows, see Figure 2.6:

$$I_{km} = y_{km}(E_k - e^{-j\varphi_{km}} E_m) = y_{km} e^{-j\varphi_{km}} (E_k e^{j\varphi_{km}} - E_m) \quad (3.12)$$

and the complex power,  $S_{km} = P_{km} + jQ_{km}$ , is thus

$$S_{km} = E_k I_{km}^* = y_{km}^* U_k e^{j(\theta_k + \varphi_{km})} (U_k e^{-j(\theta_k + \varphi_{km})} - U_m e^{-j\theta_m}) \quad (3.13)$$

Separating the real and imaginary parts of this expression, yields the active and reactive power flow equations, respectively:

$$\begin{aligned} P_{km} &= U_k^2 g_{km} - U_k U_m g_{km} \cos(\theta_{km} + \varphi_{km}) \\ &\quad - U_k U_m b_{km} \sin(\theta_{km} + \varphi_{km}) \end{aligned} \quad (3.14)$$

$$\begin{aligned} Q_{km} &= -U_k^2 b_{km} + U_k U_m b_{km} \cos(\theta_{km} + \varphi_{km}) \\ &\quad - U_k U_m g_{km} \sin(\theta_{km} + \varphi_{km}) \end{aligned} \quad (3.15)$$

As with in-phase transformers, these expressions could have been obtained through inspection by comparing eqs. (3.2) and (3.13): in eq. (3.13), the term  $j b_{km}^{sh} U_k^2$  is not present, and  $\theta_{km}$  is replaced with  $\theta_{km} + \varphi_{km}$ . Hence, the expressions for the active and reactive power flows in phase-shifting transformers are the same expressions derived for the transmission line, albeit with two modifications: ignore  $b_{km}^{sh}$  and replace  $\theta_{km}$  with  $\theta_{km} + \varphi_{km}$ .

**Example 3.3.** A  $\Delta$ -Y, 230/138 kV transformer presents a  $30^\circ$  phase angle shift. Series resistance is neglected and series reactance is 0.0997 p.u. Terminal voltage magnitudes are 0.882 p.u. and 0.989 p.u., and the total angle difference is  $-16.6^\circ$ . Calculate the active and reactive power flows in the transformer.

**Solution** The active and reactive power flows in the phase-shifting transformer are given by eqs. (3.14) and (3.15), where  $U_k = 0.882$  p.u.,  $U_m = 0.989$  p.u.,  $\theta_{km} = -16.6^\circ$ , and  $\varphi_{km} = 30^\circ$ . The series reactance and susceptance are as follows:

$$\begin{aligned}x_{km} &= 0.0997 \text{ p.u.} \\b_{km} &= -x_{km}^{-1} = -10.03 \text{ p.u.}\end{aligned}$$

The active and reactive power flows can be expressed as

$$P_{km} = -0.882 \cdot 0.989 \cdot (-10.03) \cdot (-160.51) \sin(-16.6^\circ + 30^\circ) \text{ p.u.}$$

$$Q_{km} = -0.882^2(-10.03) + 0.882 \cdot 0.989 \cdot (-10.03) \cos(-16.6^\circ + 30^\circ) \text{ p.u.}$$

which yield

$$P_{km} = 203 \text{ MW} \quad Q_{km} = -70.8 \text{ Mvar}$$

The reader is encouraged to calculate  $P_{mk}$  and  $Q_{mk}$ . (The value of  $P_{mk}$  should be obvious.) ♦

### 3.4 Unified Power Flow Equations

The expressions for active and reactive power flows on transmission lines, in-phase transformers, and phase shifting transformers, see Figure 2.9, can be expressed in the following unified forms:

$$\begin{aligned}P_{km} &= (a_{km}U_k)^2 g_{km} \\&\quad - (a_{km}U_k)(a_{mk}U_m)g_{km} \cos(\theta_{km} + \varphi_{km} - \varphi_{mk}) \\&\quad - (a_{km}U_k)(a_{mk}U_m)b_{km} \sin(\theta_{km} + \varphi_{km} - \varphi_{mk})\end{aligned} \quad (3.16)$$

$$\begin{aligned}Q_{km} &= (a_{km}U_k)^2 (b_{km} + b_{km}^{sh}) \\&\quad + (a_{km}U_k)(a_{mk}U_m)b_{km} \cos(\theta_{km} + \varphi_{km} - \varphi_{mk}) \\&\quad - (a_{km}U_k)(a_{mk}U_m)g_{km} \sin(\theta_{km} + \varphi_{km} - \varphi_{mk})\end{aligned} \quad (3.17)$$

Where, for the transmission lines like the one represented in Figure 2.2,  $a_{km} = a_{mk} = 1$  and  $\varphi_{km} = \varphi_{mk} = 0$ ; for in-phase transformers such as the one represented in Figure 2.4,  $y_{km}^{sh} = y_{mk}^{sh} = 0$ ,  $a_{mk} = 1$  and  $\varphi_{km} = \varphi_{mk} = 0$ ; and for a phase-shifting transformer such as the one in Figure 2.6,  $y_{km}^{sh} = y_{mk}^{sh} = 0$ ,  $a_{mk} = 1$  and  $\varphi_{mk} = 0$ .



# 4

## Nodal Formulation of the Network Equations

*In this chapter the basic network equations are derived from Kirchhoff's Current Law (KCL) and put into forms that are suitable for the formulation of the power flow equations in the subsequent chapter*

THE NET COMPLEX current injection at a network bus, see Figure 4.1, is related to the current flows in the branches connected to the bus. Applying Kirchhoff's Current Law (KCL) yields

$$I_k + I_k^{sh} = \sum_{m \in \Omega_k} I_{km}, \quad \text{for } k = 1, \dots, N \quad (4.1)$$

where  $k$  is a generic node,  $I_k$  is the net current injection from generators and loads,  $I_k^{sh}$  is the current injection from shunts,  $m$  is a node adjacent to  $k$ ,  $\Omega_k$  is the set of nodes adjacent to  $k$ , and  $N$  is the number of nodes in the network.

The complex current  $I_{km}$  in the unified branch model, Figure 2.9, is

$$I_{km} = (a_{km}^2 E_k - t_{km}^* t_{mk} E_m) y_{km} + y_{km}^{sh} a_{km}^2 E_k \quad (4.2)$$

where  $t_{km} = a_{km} e^{j\varphi_{km}}$  and  $t_{mk} = a_{mk} e^{j\varphi_{mk}}$ .

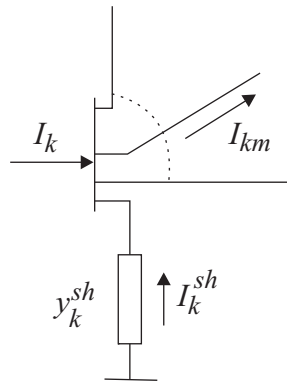


**Figure 4.1.** Generic bus with sign conventions for currents and power flows.

Equations (4.1) and (4.2) yield

$$I_k = \left( y_k^{sh} + \sum_{m \in \Omega_k} a_{km}^2 (y_{km}^{sh} + y_{km}) \right) E_k - \sum_{m \in \Omega_k} (t_{km}^* t_{mk} y_{km}) E_m \quad (4.3)$$

for  $k = 1, \dots, N$ . This expression can be written as

$$\mathbf{I} = \mathbf{Y}\mathbf{E} \quad (4.4)$$

where

- $\mathbf{I}$  is the injection vector with elements  $I_k$ ,  $k = 1, \dots, N$
- $\mathbf{E}$  is the nodal voltage vector with elements  $E_k = U_k e^{j\theta_k}$
- $\mathbf{Y} = \mathbf{G} + j\mathbf{B}$  is the nodal admittance matrix, with the following elements

$$Y_{km} = -t_{km}^* t_{mk} y_{km} \quad (4.5)$$

$$Y_{kk} = y_k^{sh} + \sum_{m \in \Omega_k} a_{km}^2 (y_{km}^{sh} + y_{km}) \quad (4.6)$$

We see that the nodal admittance matrix defined by eqs. (4.5) and (4.6) is modified as compared with the nodal admittance matrix without transformers. Particularly it should be noted that  $\mathbf{Y}$  as defined above is not necessarily symmetric.

For large practical networks this matrix is usually very sparse. The degree of sparsity (percentage of zero elements) normally increases with the dimensions of the network: e.g., a network with 1000 buses and 1500 branches typically presents a degree of sparsity greater than 99 %, i.e. less than 1 % of the matrix elements have non-zero values.

The  $k$ th component of  $\mathbf{I}$ ,  $I_k$ , defined in eq. (4.3), can, by using eqs. (4.5) and (4.6), be written as

$$I_k = Y_{kk} E_k + \sum_{m \in \Omega_k} Y_{km} E_m = \sum_{m \in K} Y_{km} E_m \quad (4.7)$$

where  $K$  is the set of buses adjacent to bus  $k$ , including bus  $k$ , and  $\Omega_k$  is the set of buses adjacent to bus  $k$ , excluding bus  $k$ . Now considering that  $Y_{km} = G_{km} + jB_{km}$  and  $E_m = U_m e^{j\theta_m}$ , eq. (4.7) can be rewritten as

$$I_k = \sum_{m \in K} (G_{km} + jB_{km}) (U_m e^{j\theta_m}) \quad (4.8)$$

The complex power injection at bus  $k$  is

$$S_k = P_k + jQ_k = E_k I_k^* \quad (4.9)$$

and by applying eqs. (4.8) and (4.9) this gives

$$S_k = U_k e^{j\theta_k} \sum_{m \in K} (G_{km} - jB_{km})(U_m e^{-j\theta_m}) \quad (4.10)$$

The expressions for active and reactive power injections are obtained by identifying the real and imaginary parts of eq. (4.10), yielding

$$P_k = U_k \sum_{m \in K} U_m (G_{km} \cos \theta_{km} + B_{km} \sin \theta_{km}) \quad (4.11)$$

$$Q_k = U_k \sum_{m \in K} U_m (G_{km} \sin \theta_{km} - B_{km} \cos \theta_{km}) \quad (4.12)$$



# 5

## Basic Power Flow Problem

*In this chapter the basic power flow problem is formulated and the basic bus types are defined. Also, the conditions for solvability of the problem are discussed*

THE POWER FLOW PROBLEM can be formulated as a set of non-linear algebraic equality/inequality constraints. These constraints represent both Kirchhoff's laws and network operation limits. In the basic formulation of the power flow problem, four variables are associated to each bus (network node)  $k$ :

- $U_k$ : voltage magnitude
- $\theta_k$ : voltage angle
- $P_k$ : net active power (algebraic sum of generation and load)
- $Q_k$ : net reactive power (algebraic sum of generation and load)

### 5.1 Basic Bus Types

Depending on which of the above four variables are known (given) and which ones are unknown (to be calculated), two basic types of buses can be defined:

- PQ bus:  $P_k$  and  $Q_k$  are specified;  $U_k$  and  $\theta_k$  are calculated
- PU bus:  $P_k$  and  $U_k$  are specified;  $Q_k$  and  $\theta_k$  are calculated

PQ buses are normally used to represent load buses without voltage control, and PU buses are used to represent generation buses with voltage control in power flow calculations<sup>1</sup>. Synchronous compensators<sup>2</sup> are also treated as PU buses. A third bus is also needed:

---

<sup>1</sup>Synchronous machines are often equipped with Automatic Voltage Regulators (AVRs), which controls the excitation of the machine so that the terminal voltage, or some other voltage close to the machine, is kept at the set value.

<sup>2</sup>Synchronous compensators, sometimes also called synchronous condensers, are synchronous machines without any active power generation or load (except for losses) used for reactive power and voltage control.

- $U\theta$  bus:  $U_k$  and  $\theta_k$  are specified;  $P_k$  and  $Q_k$  are calculated

The  $U\theta$  bus, also called reference bus or slack bus, has double functions in the basic formulation of the power flow problem:

1. It serves as the voltage angle reference
2. Since the active power losses are unknown in advance, the active power generation of the  $U\theta$  bus is used to balance generation, load, and losses

In “normal” power systems PQ-buses or load buses are the far most common, typically comprising more than 80% of all buses.

Other possible bus types are P, U, and PQU, with obvious definitions. The use of multiple  $U\theta$  buses may also be required for certain applications. In more general cases, the given values are not limited to the specific set of buses (P, Q, U,  $\theta$ ), and branch related variables can also be specified.

**Example 5.1.** *Figure 5.1 shows a 5-bus network with four transmission lines and two transformers. Generators, with voltage control, are connected at buses 1, 3, and 5, and loads are connected at buses 4 and 5, and at bus 4 a shunt is also connected. Classify the buses according to the bus types PU, PQ and  $U\theta$ .*

**Solution** Buses 1, 3, and 5 are all candidates for PU or  $U\theta$  bus types. Since only one could be  $U\theta$  bus, we select (arbitrarily) bus 5 as  $U\theta$ . In a practical system usually a generator, or generator station, that could produce power within a large range is selected as reference or slack bus. It should be noted that even if a load is connected to bus 5 it can only be a PU or  $U\theta$  bus, since voltage control is available at the bus. The reference angle is set at bus 5, usually to 0. Bus 2 is a transition bus in which both  $P$  and  $Q$  are equal to zero, and this bus is consequently of type PQ. Bus 4 is a load bus to which is also connected a shunt susceptance: since shunts are modelled as part of the network, see next section, the bus is also classified as a PQ bus. ♦

## 5.2 Equality and Inequality Constraints

Eqs. (4.11) and (4.12) can be rewritten as follows

$$P_k = \sum_{m \in \Omega_k} P_{km}(U_k, U_m, \theta_k, \theta_m) \quad (5.1)$$

$$Q_k + Q_k^{sh}(U_k) = \sum_{m \in \Omega_k} Q_{km}(U_k, U_m, \theta_k, \theta_m) \quad (5.2)$$

where

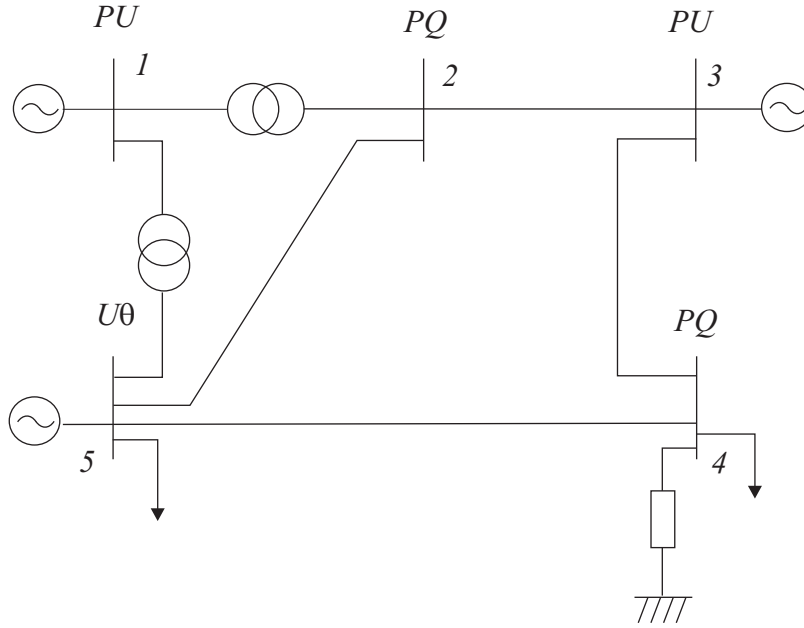


**Figure 5.1.** 5-bus system

- $k = 1, \dots, N$  ( $N$  is the number of buses in the network)
- $\Omega_k$ : set of buses adjacent to  $k$
- $U_k, U_m$ : voltage magnitudes at the terminal buses of branch  $k - m$
- $\theta_k, \theta_m$ : voltage angles at the terminal buses of branch  $k - m$
- $P_{km}$ : active power flow from bus  $k$  to bus  $m$
- $Q_{km}$ : reactive power flow from bus  $k$  to bus  $m$
- $Q_k^{sh}$ : component of reactive power injection due to the shunt element at bus  $k$  ( $Q_k^{sh} = b_k^{sh} U_m^2$ ), where  $b_k^{sh}$  is the shunt susceptance.<sup>3</sup>

A set of inequality constraints imposes operating limits on variables such as the reactive power injections at PU buses (generator buses), see section 2.5, and voltage magnitudes at PQ buses:

$$Q_k^{min} \leq Q_k \leq Q_k^{max} \quad (5.3)$$

$$U_k^{min} \leq U_k \leq U_k^{max} \quad (5.4)$$

<sup>3</sup>It is assumed here that all shunts are reactive without losses. If shunts with resistive components should be included, then eq. (5.1) must be modified accordingly.

When no inequality constraints are violated, nothing is affected in the power flow equations, but if a limit is violated, the bus status is changed and it is enforced as an equality constraint at the limiting value. This normally requires a change in bus type: if, for example, a  $Q$  limit of a PU bus is violated, the bus is transformed into an PQ bus ( $Q$  is specified and the  $U$  becomes a problem unknown). A similar procedure is adopted for backing-off when ever appropriate. What is crucial is that bus type changes must not affect solvability. Various other types of limits are also considered in practical implementations, including branch current flows, branch power flows, active power generation levels, transformer taps, phase shifter angles, and area interchanges.

### 5.3 Problem Solvability

One problem in the definition of bus type (bus classification) is to guarantee that the resulting set of power flow equations contains the same number of equations as unknowns, as are normally necessary for solvability, although not always sufficient. Consider a system with  $N$  buses, where  $N_{PU}$  are of type PU,  $N_{PQ}$  are of type PQ, and one is of type  $U\theta$ . To fully specify the state of the system we need to know the voltage magnitudes and voltage angles of all buses, i.e. in total  $2N$  quantities. But the voltage angle and voltage magnitude of the slack bus are given together with the voltage magnitudes of  $N_{PU}$  buses. Unknown are thus the voltage magnitudes of the PQ buses, and the voltage angles of the PU and the PQ buses, giving a total of  $N_{PU} + 2N_{PQ}$  unknown states. From the PU buses we get  $N_{PU}$  balance equations regarding active power injections, and from the PQ buses  $2N_{PQ}$  equations regarding active and reactive power injections, thus in total  $N_{PU} + 2N_{PQ}$  equations, and hence equal to the number of unknowns, and the necessary condition for solvability has been fulfilled.

Similar necessary conditions for solvability can be established when other types of buses, such as P, U, and PQU buses, are used in the formulation of the power flow problem.

**Example 5.2.** *Consider again the 5-bus in Figure 5.1. Formulate the equality constraints of the system and the inequality constraints for the generator buses.*

**Solution** In this case  $N = 5$ ,  $N_{PQ} = 2$ ,  $N_{PU} = 2$ , and of course  $N_{U\theta} = 1$ . The number of equations are thus:  $N_{PU} + 2N_{PQ} = 2 + 2 \cdot 2 = 6$ , and these

are:

$$\begin{aligned}
 P_1 &= P_{12} + P_{15} \\
 P_2 &= P_{21} + P_{23} + P_{25} \\
 Q_2 &= Q_{21} + Q_{23} + Q_{25} \\
 P_3 &= P_{32} + P_{34} \\
 P_4 &= P_{43} + P_{45} \\
 Q_4 + Q_4^{sh} &= Q_{43} + Q_{45}
 \end{aligned}$$

In the above equations  $P_1$ ,  $P_2$ ,  $P_3$ ,  $P_4$ ,  $Q_2$ , and  $Q_4$  are given. All the other quantities are functions of the bus voltage magnitudes and phase angles, of which  $U_1$ ,  $U_3$ , and  $U_5$  and  $\theta_5$  are given. The other six, i.e.  $U_2$ ,  $U_4$ ,  $\theta_1$ ,  $\theta_2$ ,  $\theta_3$ ,  $\theta_4$ , in total 6 unknowns, can be solved from the above equations, and from these all power flows and injections can be calculated.

The inequality constraints of the generator buses are:

$$\begin{aligned}
 Q_1^{min} &\leq Q_1 \leq Q_1^{max} \\
 Q_3^{min} &\leq Q_3 \leq Q_3^{max} \\
 Q_5^{min} &\leq Q_5 \leq Q_5^{max}
 \end{aligned}$$

The reactive limits above are derived from the generator capability curves as explained in section 2.5. For the slack bus it must also be checked that the injected active and reactive powers are within the range of the generator. If not, the power generation of the other generators must be changed or the voltage settings of these. ♦



# 6

## Solution of the Power Flow Problem

*In this chapter the basic methods to solve the non-linear power flow equations are reviewed. Solution methods based on the observation that active and reactive power flows are not so strongly coupled are introduced.*

IN ALL REALISTIC CASES the power flow problem cannot be solved analytically, and hence iterative solutions implemented in computers must be used. In this chapter we will review two solutions methods, Gauss iteration with a variant called Gauss-Seidel iterative method, and the Newton-Raphson method.

### 6.1 Solution by Gauss-Seidel Iteration

Consider the power flow equations (5.1) and (5.2) which could be written in complex form as

$$S_k = E_k \sum_{m \in K} Y_{km}^* E_m^*, \quad k = 1, 2, \dots, N \quad (6.1)$$

which is the same as eq. (4.10). The set  $K$  is the set of buses adjacent (connected) to bus  $k$ , including bus  $k$ , and hence shunt admittances are included in the summation. Furthermore  $E_k = U_k e^{j\theta_k}$ . This equation can be rewritten as

$$E_k^* = \frac{1}{Y_{kk}^*} \left[ \frac{S_k}{E_k} - \sum_{m \in \Omega_k} Y_{km}^* E_m^* \right], \quad k = 1, 2, \dots, N \quad (6.2)$$

where  $\Omega_k$  is the set of all buses connected to bus  $k$  excluding bus  $k$ . Taking the complex conjugate of eq. (6.2) yields

$$E_k = \frac{1}{Y_{kk}} \left[ \frac{S_k^*}{E_k^*} - \sum_{m \in \Omega_k} Y_{km} E_m \right], \quad k = 1, 2, \dots, N \quad (6.3)$$

Thus we get  $N - 1$  algebraic (complex) equations in the complex variables  $E_k$  in the form

$$\begin{aligned} E_2 &= h_2(E_1, E_2, \dots, E_N) \\ E_3 &= h_3(E_1, E_2, \dots, E_N) \\ &\vdots \\ E_N &= h_N(E_1, E_2, \dots, E_N) \end{aligned} \quad (6.4)$$

where the functions  $h_i$  are given by eq. (6.3). It is assumed here that bus number 1 is the  $U\theta$  bus, and hence  $E_1$  is given and we have no equation for node 1. For PQ buses both the magnitude and angle of  $E_k$  are unknown, while for PU buses only the angle is unknown. For PQ buses  $S_k$  is known, while for PU buses only  $P_k$  is known. This will be discussed below in more detail. In vector form eq. (6.4) can be written as

$$\mathbf{x} = \mathbf{h}(\mathbf{x}) \quad (6.5)$$

and based on this equation the following iterative scheme is proposed

$$\mathbf{x}^{\nu+1} = \mathbf{h}(\mathbf{x}^\nu), \quad \nu = 0, 1, \dots \quad (6.6)$$

where the superscript indicates the iteration number. Thus starting with an initial value  $\mathbf{x}^0$ , the sequence

$$\mathbf{x}^0, \mathbf{x}^1, \mathbf{x}^2, \dots \quad (6.7)$$

is generated. If the sequence converges, i.e.  $\mathbf{x}^\nu \rightarrow \mathbf{x}^*$ , then

$$\mathbf{x}^* = \mathbf{h}(\mathbf{x}^*) \quad (6.8)$$

and  $\mathbf{x}^*$  is a solution of eq. (6.5).

In practice the iteration is stopped when the changes in  $\mathbf{x}^\nu$  become sufficiently small, i.e. when the norm of  $\Delta\mathbf{x}^\nu = \mathbf{x}^{\nu+1} - \mathbf{x}^\nu$  is less than a predetermined value  $\varepsilon$ .

To start the iteration a first guess of  $\mathbf{x}$  is needed. Usually, if no a priori knowledge of the solution is known, one selects all unknown voltage magnitudes and phase angles equal to the ones of the reference bus, usually around 1 p.u. and phase angle = 0. This initial solution is often called a *flat start*.

The difference between Gauss and Gauss-Seidel iteration can be explained by considering eq. (6.6) with all components written out explicitly<sup>1</sup>

$$\begin{aligned} x_2^{\nu+1} &= h_2(x_1, x_2^\nu, \dots, x_N^\nu) \\ x_3^{\nu+1} &= h_3(x_1, x_2^\nu, \dots, x_N^\nu) \\ &\vdots \\ x_N^{\nu+1} &= h_N(x_1, x_2^\nu, \dots, x_N^\nu) \end{aligned} \quad (6.9)$$

---

<sup>1</sup>In this particular formulation  $x_1$  is the value of the complex voltage of the slack bus and consequently known. For completeness we have included it as a variable in the equations above, but it is actually known

In carrying out the computation (normally by computer) we process the equations from top to bottom. We now observe that when we solve for  $x_3^{\nu+1}$  we already know  $x_2^{\nu+1}$ . Since  $x_2^{\nu+1}$  is presumably a better estimate than  $x_2^\nu$ , it seems reasonable to use the updated value. Similarly when we solve for  $x_4^{\nu+1}$  we can use the values of  $x_2^{\nu+1}$  and  $x_3^{\nu+1}$ . This is the line of reasoning called the Gauss-Seidel iteration:

$$\begin{aligned} x_2^{\nu+1} &= h_2(x_1, x_2^\nu, \dots, x_N^\nu) \\ x_3^{\nu+1} &= h_3(x_1, x_2^{\nu+1}, \dots, x_N^\nu) \\ &\vdots \\ x_N^{\nu+1} &= h_N(x_1, x_2^{\nu+1}, \dots, x_{N-1}^{\nu+1}, x_N^\nu) \end{aligned} \quad (6.10)$$

It is clear that the convergence of the Gauss-Seidel iteration is faster than the Gauss iteration scheme.

For PQ buses the complex power  $S_k$  is completely known and the calculation of the right hand side of eq. (6.3) is well defined. For PU buses however,  $Q$  is not defined but is determined so that the voltage magnitude is kept at the specified value. In this case we have to estimate the reactive power injection and an obvious choice is

$$Q_k^\nu = \Im \left[ E_k^\nu \sum_{m \in K} Y_{km}^* (E_m^*)^\nu \right] \quad (6.11)$$

In the Gauss-Seidel iteration scheme one should use the latest calculated values of  $E_m$ . It should be clear that also for PU buses the above iteration scheme gives a solution if it converges.

A problem with the Gauss and Gauss-Seidel iteration schemes is that convergence can be very slow, and sometimes even the iteration does not converge despite that a solution exists. Furthermore, no general results are known concerning the convergence characteristics and criteria. Therefore more efficient solution methods are needed, and one such method that is widely used in power flow computations is discussed in the subsequent sections.

## 6.2 Newton-Raphson Method

Before applying this method to the power flow problem we review the iteration scheme and some of its properties.

A system of nonlinear algebraic equations can be written as

$$\mathbf{f}(\mathbf{x}) = \mathbf{0} \quad (6.12)$$

where  $\mathbf{x}$  is an  $n$ -vector of unknowns and  $\mathbf{f}$  is an  $n$ -vector function of  $\mathbf{x}$ . Given an appropriate starting value  $\mathbf{x}^0$ , the Newton-Raphson method solves this

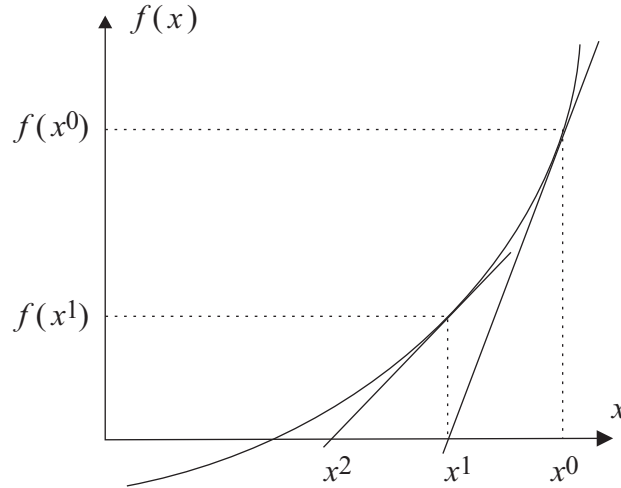


**Figure 6.1.** Newton-Raphson method in unidimensional case

vector equation by generating the following sequence:

$$\mathbf{J}(\mathbf{x}^\nu)\Delta\mathbf{x}^\nu = -\mathbf{f}(\mathbf{x}^\nu) \quad (6.13)$$

$$\mathbf{x}^{\nu+1} = \mathbf{x}^\nu + \Delta\mathbf{x}^\nu$$

where  $\mathbf{J}(\mathbf{x}^\nu) = \partial\mathbf{f}(\mathbf{x})/\partial\mathbf{x}$  is the Jacobian matrix with elements

$$J_{ij} = \frac{\partial f_i}{\partial x_j} \quad (6.14)$$

### 6.2.1 Unidimensional case

To get a better feeling for the method we first study the one-dimensional case, and eq. (6.12) becomes

$$f(x) = 0 \quad (6.15)$$

where  $x$  is the unknown and  $f(x)$  is a scalar function. Figure 6.1 illustrates a simple case in which there is a single solution to eq. (6.15). Under these circumstances, the following algorithm can be used to find the solution of eq. (6.15):

1. Set  $\nu = 0$  and choose an appropriate starting value  $x^0$ ;
2. Compute  $f(x^\nu)$ ;

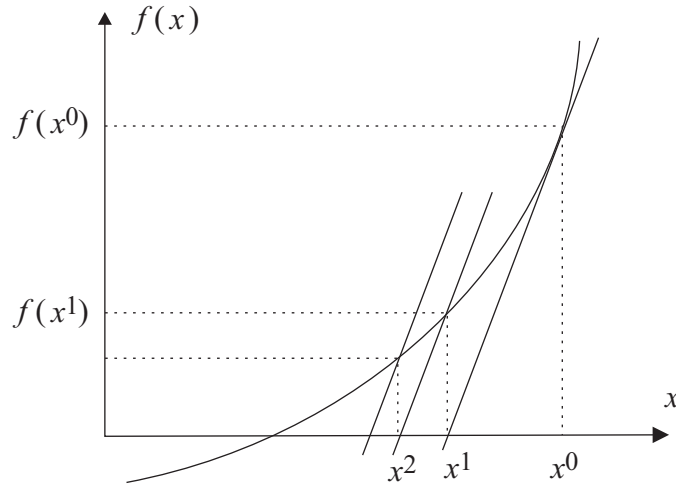


**Figure 6.2.** Dishonest Newton-Raphson method in unidimensional case

3. Compare  $f(x^\nu)$  with specified tolerance  $\varepsilon$ ;  
if  $|f(x^\nu)| \leq \varepsilon$ , then  $x = x^\nu$  is the solution to eq. (6.15);  
Otherwise,  $|f(x^\nu)| > \varepsilon$ , go to the next step;
4. Linearize  $f(x)$  at the current solution point  $[x^\nu, f(x^\nu)]$ , as shown in Figure 6.1. That is,  $f(x^\nu + \Delta x^\nu) \approx f(x^\nu) + f'(x^\nu)\Delta x^\nu$ , where  $f'(x^\nu)$  is calculated at  $x^\nu$
5. Solve  $f(x^\nu) + f'(x^\nu)\Delta x^\nu = 0$  for  $\Delta x^\nu$ , and update the solution estimate,  $x^{\nu+1} = x^\nu + \Delta x^\nu$ , where  $\Delta x^\nu = -f(x^\nu)/f'(x^\nu)$ ;
6. Update iteration counter  $\nu + 1 \rightarrow \nu$  and go to step 2.

The dishonest Newton-Raphson method is illustrated in Figure 6.2. In this case at Step 4 of the algorithm, a constant derivative is assigned and  $f'(x^\nu) = f'(x^0)$ . Although the number of iterations required for convergence usually increases, it is not necessary to recalculate the derivatives for each iteration and hence the computation burden at each iteration is lower. When only limited accuracy is needed, the overall performance of the dishonest version may be better than that of the full Newton-Raphson method.

### 6.2.2 Quadratic Convergence

Close to the solution point  $x^*$ , the Newton-Raphson method normally presents a property called quadratic convergence. This can be proved for the unidimensional case discussed above if it is assumed that  $x^*$  is a simple (not a multiple) root and that its first and second derivatives are continuous.

Hence,  $f(x^*) = 0$ , and for any  $x$  in a certain neighborhood of  $x^*$ ,  $f'(x) \neq 0$ . If  $\varepsilon_\nu$  denotes the error at the  $\nu$ -th iteration, i.e.

$$\varepsilon_\nu = x^* - x^{(\nu)} \quad (6.16)$$

the Taylor expansion about  $x^\nu$  yields

$$\begin{aligned} f(x^*) &= f(x^{(\nu)} + \varepsilon_\nu) \\ &= f(x^{(\nu)}) + f'(x^{(\nu)})\varepsilon_\nu + 1/2 f''(\bar{x})\varepsilon_\nu^2 \\ &= 0 \end{aligned} \quad (6.17)$$

where  $\bar{x} \in [x^{(\nu)}, x^*]$ . Dividing by  $f'(x^{(\nu)})$ , this expression can be written as

$$\frac{f(x^{(\nu)})}{f'(x^{(\nu)})} + \varepsilon_\nu + 1/2 \frac{f''(\bar{x})}{f'(x^{(\nu)})} \varepsilon_\nu^2 = 0 \quad (6.18)$$

Since,

$$\frac{f(x^{(\nu)})}{f'(x^{(\nu)})} + \varepsilon_\nu = \frac{f(x^{(\nu)})}{f'(x^{(\nu)})} + x^* - x^{(\nu)} = x^* - x^{(\nu+1)} = \varepsilon_{\nu+1} \quad (6.19)$$

the following relationship between  $\varepsilon_\nu$  and  $\varepsilon_{\nu+1}$  results:

$$\frac{\varepsilon_{\nu+1}}{\varepsilon_\nu^2} = -\frac{1}{2} \frac{f''(\bar{x})}{f'(x^{(\nu)})} \quad (6.20)$$

In the vicinity of the root, i.e. as  $x^\nu \rightarrow x^*$ ,  $\bar{x} \rightarrow x^*$ , and we thus have

$$|\varepsilon_{\nu+1}| = \frac{1}{2} \frac{|f''(x^*)|}{|f'(x^*)|} \varepsilon_\nu^2 \quad (6.21)$$

From eq. (6.21) it is clear that the convergence is quadratic with the assumptions stated above.

### 6.2.3 Multidimensional Case

Reconsider now the  $n$ -dimensional case

$$\mathbf{f}(\mathbf{x}) = \mathbf{0} \quad (6.22)$$

where

$$\mathbf{f}(\mathbf{x}) = (f_1(\mathbf{x}), f_2(\mathbf{x}), \dots, f_n(\mathbf{x}))^T \quad (6.23)$$

and

$$\mathbf{x} = (x_1, x_2, \dots, x_n)^T \quad (6.24)$$

Thus  $\mathbf{f}(\mathbf{x})$  and  $\mathbf{x}$  are  $n$ -dimensional (column) vectors.

The Newton-Raphson method applied to to solve eq. (6.22) follows basically the same steps as those applied to the unidimensional case above,

except that in Step 4, the Jacobian matrix  $\mathbf{J}(\mathbf{x}^\nu)$  is used, and the linearization of  $\mathbf{f}(\mathbf{x})$  at  $\mathbf{x}^\nu$  is given by the Taylor expansion

$$\mathbf{f}(\mathbf{x}^\nu + \Delta\mathbf{x}^\nu) \approx \mathbf{f}(\mathbf{x}^\nu) + \mathbf{J}(\mathbf{x}^\nu)\Delta\mathbf{x}^\nu \quad (6.25)$$

where the Jacobian matrix has the general form

$$\mathbf{J} = \frac{\partial \mathbf{f}}{\partial \mathbf{x}} = \begin{pmatrix} \frac{\partial f_1}{\partial x_1} & \frac{\partial f_1}{\partial x_2} & \cdots & \frac{\partial f_1}{\partial x_n} \\ \frac{\partial f_2}{\partial x_1} & \frac{\partial f_2}{\partial x_2} & \cdots & \frac{\partial f_2}{\partial x_n} \\ \vdots & \vdots & \ddots & \vdots \\ \frac{\partial f_n}{\partial x_1} & \frac{\partial f_n}{\partial x_2} & \cdots & \frac{\partial f_n}{\partial x_n} \end{pmatrix} \quad (6.26)$$

The correction vector  $\Delta\mathbf{x}$  is the solution to

$$\mathbf{f}(\mathbf{x}^\nu) + \mathbf{J}(\mathbf{x}^\nu)\Delta\mathbf{x}^\nu = 0 \quad (6.27)$$

Note that this is the linearized version of the original problem  $\mathbf{f}(\mathbf{x}^\nu + \Delta\mathbf{x}^\nu) = 0$ . The solution of eq. (6.27) involves thus the solution of a system of linear equations, which usually is done by Gauss elimination (LU factorization).

The Newton-Raphson algorithm for the  $n$ -dimensional case is thus as follows:

1. Set  $\nu = 0$  and choose an appropriate starting value  $\mathbf{x}^0$ ;
2. Compute  $\mathbf{f}(\mathbf{x}^\nu)$ ;
3. Test convergence:  
If  $|f_i(\mathbf{x}^\nu)| \leq \varepsilon$  for  $i = 1, 2, \dots, n$ , then  $\mathbf{x}^\nu$  is the solution  
Otherwise go to 4;
4. Compute the Jacobian matrix  $\mathbf{J}(\mathbf{x}^\nu)$ ;
5. Update the solution

$$\Delta\mathbf{x}^\nu = -\mathbf{J}^{-1}(\mathbf{x}^\nu)\mathbf{f}(\mathbf{x}^\nu) \quad (6.28)$$

$$\mathbf{x}^{\nu+1} = \mathbf{x}^\nu + \Delta\mathbf{x}^\nu$$

6. Update iteration counter  $\nu + 1 \rightarrow \nu$  and go to step 2.

### 6.3 Newton-Raphson applied to the Power Flow Equations

In this section we will now formulate the Newton-Raphson iteration of the power flow equations. Firstly, the state vector of unknown voltage angles and magnitudes is ordered such that

$$\mathbf{x} = \begin{pmatrix} \theta \\ \mathbf{U} \end{pmatrix} \quad (6.29)$$

and the nonlinear function  $\mathbf{f}$  is ordered so that the first components correspond to active power and the last ones to reactive power:

$$\mathbf{f}(\mathbf{x}) = \begin{pmatrix} \Delta \mathbf{P}(\mathbf{x}) \\ \Delta \mathbf{Q}(\mathbf{x}) \end{pmatrix} = \begin{pmatrix} \mathbf{P}(\mathbf{x}) - \mathbf{P}^{(s)} \\ \mathbf{Q}(\mathbf{x}) - \mathbf{Q}^{(s)} \end{pmatrix} \quad (6.30)$$

with

$$\mathbf{f}(\mathbf{x}) = \begin{pmatrix} P_2(\mathbf{x}) - P_2^{(s)} \\ \vdots \\ P_m(\mathbf{x}) - P_m^{(s)} \\ \text{-----} \\ Q_2(\mathbf{x}) - Q_2^{(s)} \\ \vdots \\ Q_n(\mathbf{x}) - Q_n^{(s)} \end{pmatrix} \quad (6.31)$$

In eq. (6.31) the functions  $P_k(\mathbf{x})$  are the active power flows out from bus  $k$  given by eq. (4.11) and the  $P_k^{(s)}$  are the known active power injections into bus  $k$  from generators and loads, and the functions  $Q_k(\mathbf{x})$  are the reactive power flows out from bus  $k$  given by eq. (4.12) and  $Q_k^{(s)}$  are the known reactive power injections into bus  $k$  from generators and loads. The first  $m - 1$  equations are formulated for PU and PQ buses, and the last  $n - 1$  equations can only be formulated for PQ buses. If there are  $N_{PU}$  PU buses and  $N_{PQ}$  PQ buses,  $m - 1 = N_{PU} + N_{PQ}$  and  $n - 1 = N_{PQ}$ . The load flow equations can now be written as

$$\mathbf{f}(\mathbf{x}) = \begin{pmatrix} \Delta \mathbf{P}(\mathbf{x}) \\ \Delta \mathbf{Q}(\mathbf{x}) \end{pmatrix} = 0 \quad (6.32)$$

and the functions  $\Delta \mathbf{P}(\mathbf{x})$  and  $\Delta \mathbf{Q}(\mathbf{x})$  are called active and reactive (power) mismatches. The updates to the solutions are determined from the equation

$$\mathbf{J}(\mathbf{x}^\nu) \begin{pmatrix} \Delta \theta^\nu \\ \Delta \mathbf{U}^\nu \end{pmatrix} + \begin{pmatrix} \Delta \mathbf{P}(\mathbf{x}^\nu) \\ \Delta \mathbf{Q}(\mathbf{x}^\nu) \end{pmatrix} = 0 \quad (6.33)$$

The Jacobian matrix  $\mathbf{J}$  can be written as

$$\mathbf{J} = \begin{pmatrix} \frac{\partial \Delta \mathbf{P}}{\partial \theta} & \frac{\partial \Delta \mathbf{P}}{\partial \mathbf{U}} \\ \frac{\partial \Delta \mathbf{Q}}{\partial \theta} & \frac{\partial \Delta \mathbf{Q}}{\partial \mathbf{U}} \end{pmatrix} \quad (6.34)$$

which is equal to

$$\mathbf{J} = \begin{pmatrix} \frac{\partial \mathbf{P}(\mathbf{x})}{\partial \theta} & \frac{\partial \mathbf{P}(\mathbf{x})}{\partial \mathbf{U}} \\ \frac{\partial \mathbf{Q}(\mathbf{x})}{\partial \theta} & \frac{\partial \mathbf{Q}(\mathbf{x})}{\partial \mathbf{U}} \end{pmatrix} \quad (6.35)$$

or simply

$$\mathbf{J} = \begin{pmatrix} \frac{\partial \mathbf{P}}{\partial \theta} & \frac{\partial \mathbf{P}}{\partial \mathbf{U}} \\ \frac{\partial \mathbf{Q}}{\partial \theta} & \frac{\partial \mathbf{Q}}{\partial \mathbf{U}} \end{pmatrix} \quad (6.36)$$

In eq. (6.34) the matrices  $\partial \mathbf{P} / \partial \theta$  and  $\partial \mathbf{Q} / \partial \mathbf{U}$  are always quadratic, and so is of course  $\mathbf{J}$ .

## 6.4 $P\theta - QU$ Decoupling

The ac power flow problem above involves four variables associated with each network node  $k$ :

- $U_k$ , the voltage magnitude
- $\theta_k$ , the voltage angle
- $P_k$ , the net active power (generation – load)
- $Q_k$ , the net reactive power (generation – load)

For transmission systems, a strong coupling is normally observed between  $P$  and  $\theta$ , as well as between  $Q$  and  $U$ . This property will in this section be employed to simplify and speed up the computations. In the next section we will derive a linear approximation called dc power flow (or dc load flow). This linear model relates the active power  $P$  to the bus voltage angle  $\theta$ .

Let us consider a  $\pi$ -model of a transmission line, where the series resistance<sup>2</sup> and the shunt admittance both are neglected and put to zero.

---

<sup>2</sup>For voltage levels above 400 (380) kV the  $X/R$ -ratio is typically greater than 10 so omission of the line resistance is a valid approximation. For voltage levels between 130 and 220 kV the  $X/R$ -ratio is typically around 5 and the line resistance can be neglected for approximate calculations.

In this case, the active and reactive power flows are given by the following simplified expressions of eqs. (3.3) and (3.4)

$$P_{km} = \frac{U_k U_m \sin \theta_{km}}{x_{km}} \quad (6.37)$$

$$Q_{km} = \frac{U_k^2 - U_k U_m \cos \theta_{km}}{x_{km}} \quad (6.38)$$

where  $x_{km}$  is the series reactance of the line.

The sensitivities between power flows  $P_{km}$  and  $Q_{km}$  and the state variables  $U$  and  $\theta$  are for this approximation given by

$$\frac{\partial P_{km}}{\partial \theta_k} = \frac{U_k U_m \cos \theta_{km}}{x_{km}} \quad \frac{\partial P_{km}}{\partial U_k} = \frac{U_m \sin \theta_{km}}{x_{km}} \quad (6.39)$$

$$\frac{\partial Q_{km}}{\partial \theta_k} = \frac{U_k U_m \sin \theta_{km}}{x_{km}} \quad \frac{\partial Q_{km}}{\partial U_k} = \frac{2U_k - U_m \cos \theta_{km}}{x_{km}} \quad (6.40)$$

When  $\theta_{km} = 0$ , perfect decoupling conditions are observed, i.e.

$$\frac{\partial P_{km}}{\partial \theta_k} = \frac{U_k U_m}{x_{km}} \quad \frac{\partial P_{km}}{\partial U_k} = 0 \quad (6.41)$$

$$\frac{\partial Q_{km}}{\partial \theta_k} = 0 \quad \frac{\partial Q_{km}}{\partial U_k} = \frac{2U_k - U_m}{x_{km}} \quad (6.42)$$

As illustrated in Figure 6.3, in the usual range of operations (relatively small voltage angles), a strong coupling between active power and voltage angle as well as between reactive power and voltage magnitudes exists, while a much weaker coupling between reactive power and voltage angle, and between voltage magnitude and active power exists. Notice, however, that for larger angles this is no longer true. In the neighbourhood of  $\theta_{km} = 90^\circ$ , there is strong coupling between  $P$  and  $U$  as well as between  $Q$  and  $\theta$ .

**Example 6.1.** *A 750 kV transmission line has 0.0175 p.u. series reactance (the series resistance and the shunt admittance are ignored in this example). The terminal bus voltage magnitudes are 0.984 and 0.962 p.u. and the angle difference is  $10^\circ$ . Calculate the sensitivities of the active and reactive power flows with respect to voltage magnitude and phase angle.*

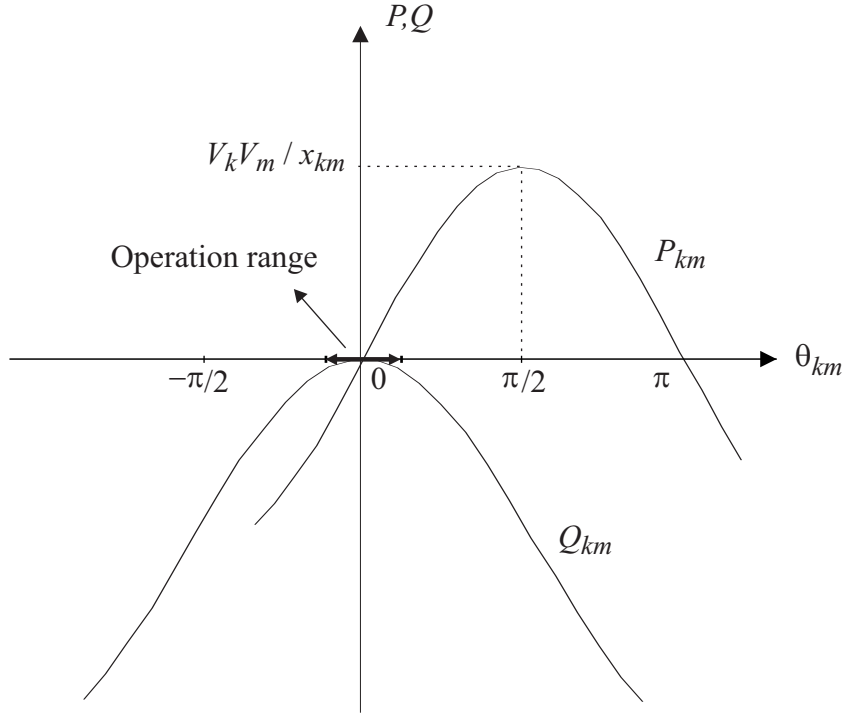


**Figure 6.3.**  $P - \theta$  and  $Q - \theta$  curves for a line with a series resistance and a shunt admittance of zero and considering terminal voltages  $U_k = U_m = 1.0$  p.u.

**Solution** The four sensitivities are calculated by using eqs. (6.39) and (6.40):

$$\frac{\partial P_{km}}{\partial \theta_k} = \frac{U_k U_m \cos \theta_{km}}{x_{km}} = \frac{0.984 \cdot 0.962 \cos 10^\circ}{0.0175} = 54.1$$

$$\frac{\partial P_{km}}{\partial U_k} = \frac{U_m \sin \theta_{km}}{x_{km}} = \frac{0.962 \sin 10^\circ}{0.0175} = 9.5$$

$$\frac{\partial Q_{km}}{\partial \theta_k} = \frac{U_k U_m \sin \theta_{km}}{x_{km}} = \frac{0.984 \cdot 0.962 \sin 10^\circ}{0.0175} = 9.4$$

$$\frac{\partial Q_{km}}{\partial U_k} = \frac{2U_k - U_m \cos \theta_{km}}{x_{km}} = \frac{2 \cdot 0.984 - 0.962 \cos 10^\circ}{0.0175} = 58.3$$

As seen the  $P - \theta$  and  $Q - U$  couplings are much greater than the other couplings. ♦

If the couplings  $Q-\theta$  and  $P-U$  are neglected the Newton-Raphson iteration scheme can be simplified. With this assumption the Jacobian Matrix can be written as

$$\mathbf{J}_{DEC} = \begin{pmatrix} \frac{\partial \mathbf{P}}{\partial \theta} & 0 \\ 0 & \frac{\partial \mathbf{Q}}{\partial \mathbf{U}} \end{pmatrix} \quad (6.43)$$

Thus there is no coupling between the updates of voltage magnitudes and angles and eq. (6.33) can be written as two uncoupled equations:

$$\frac{\partial \mathbf{P}}{\partial \theta} \Delta \theta^\nu + \Delta \mathbf{P}(\theta^\nu, \mathbf{U}^\nu) = 0 \quad (6.44)$$

$$\frac{\partial \mathbf{Q}}{\partial \mathbf{U}} \Delta \mathbf{U}^\nu + \Delta \mathbf{Q}(\theta^{\nu+1}, \mathbf{U}^\nu) = 0 \quad (6.45)$$

In this formulation two systems of linear equations have to be solved instead of one system. Of course, the total number of equations to be solved is the same, but since the needed number of operations to solve a system of linear equations increases more than linearly with the dimension, it takes less operations to solve eqs. (6.44) and (6.45) than eq. (6.33) with the complete Jacobian matrix,  $\mathbf{J}$ . It should be noted that if the iterations of eqs. (6.44) and (6.45) converge, it converges to a correct solution of the load flow equations. No approximations have been introduced in the functions  $\mathbf{P}(\mathbf{x})$  or  $\mathbf{Q}(\mathbf{x})$ , only in the way we calculate the updates. The convergence of the decoupled scheme is somewhat slower than the full scheme, but often the faster solution time for the updates compensates for slower convergence, giving as faster overall solution time. For not too heavily loaded systems a faster overall solution time is almost always obtained. The two equations (6.44) and (6.45) are solved sequentially, and then the updated unknowns of the first equation, eq. (6.44), can be used to calculate the mismatches of the second system of equations, eq. (6.45), resulting in an increased speed of convergence.

A number of approximations can be made to calculate the matrix elements of the the two sub-matrices of the Jacobian in eqs. (6.44) and (6.45). This will only influence the speed of convergence of the solution. If the method converges to a solution, this is the correct solution as long as the accurate expression for  $\Delta \mathbf{P}$  and  $\Delta \mathbf{Q}$  are used.

If approximations regarding the active and reactive power mismatches are used, the solution can be even faster, but then only an approximative solution will be obtained. This is further elaborated in the next section.

## 6.5 Approximative Solutions of the Power Flow Problem

In the previous section the exact expressions of the power flow equations were used. However, since the power flow equations are solved frequently in the operation and planning of electric power systems there is a need that the equations can be solved fast, and for this purpose the approximations introduced in this chapter have proved to be of great value. Often the approximations described here are used together with exact methods. Approximative methods could be used to identify the most critical cases, which are then further analysed with the full models. The fast, approximative methods can also be used to provide good initial guesses for a complete solution of the equations.

### 6.5.1 Linearization

In this subsection the linearized dc power flow equations will be derived.

#### Transmission Line

Consider again expressions for the active power flows ( $P_{km}$  and  $P_{mk}$ ) in a transmission line:

$$P_{km} = U_k^2 g_{km} - U_k U_m g_{km} \cos \theta_{km} - U_k U_m b_{km} \sin \theta_{km} \quad (6.46)$$

$$P_{mk} = U_m^2 g_{km} - U_k U_m g_{km} \cos \theta_{km} + U_k U_m b_{km} \sin \theta_{km} \quad (6.47)$$

These equations can be used to determine the real power losses in a transmission line

$$P_{km} + P_{mk} = g_{km}(U_k^2 + U_m^2 - 2U_k U_m \cos \theta_{km}) \quad (6.48)$$

If the terms corresponding to the active power losses are ignored in eqs. (6.46) and (6.47), the result is

$$P_{km} = -P_{mk} = -U_k U_m b_{km} \sin \theta_{km} \quad (6.49)$$

The reactive power flows in this case are given by

$$Q_{km} = -U_k^2 (b_{km} + b_{km}^{sh}) + U_k U_m b_{km} \cos \theta_{km} \quad (6.50)$$

$$Q_{mk} = -U_m^2 (b_{km} + b_{km}^{sh}) + U_k U_m b_{km} \cos \theta_{km} \quad (6.51)$$

The following additional approximations are often valid, particularly during light load conditions, i.e. small values of  $\theta_{km}$ :

$$U_k \approx U_m \approx 1 \text{ p.u.} \quad (6.52)$$

$$\sin \theta_{km} \approx \theta_{km} \quad (6.53)$$

And since

$$b_{km} = -1/x_{km} \quad (6.54)$$

we can simplify the expression for the active power flow  $P_{km}$  to

$$P_{km} = \theta_{km}/x_{km} = \frac{\theta_k - \theta_m}{x_{km}} \quad (6.55)$$

This equation is analogous to Ohm's law applied to a resistor carrying a dc current:

- $P_{km}$  is the dc current;
- $\theta_k$  and  $\theta_m$  are the dc voltages at the resistor terminals;
- $x_{km}$  is the resistance.

This is illustrated in Figure 6.4.

We also see that reactive power flows in eqs. (6.50) and (6.51) reduce to the part corresponding to the shunt element  $b_{km}^{sh}$  since  $\cos \theta_{km} \approx 1$  when  $\theta_{km}$  is small. The reactive flows occurring due to angle differences vanish thus and the reactive power flows can thus not be modelled with these approximations.

### Series Capacitor

For a given voltage angle spread, the active power flow in a transmission line decreases with the line reactance (and series reactance normally increases with line length). Series compensation aims at reducing the effective electric length of the line: a series capacitor connected in series with the line. If, for example, a 40% compensation corresponds to a capacitor with a reactance of 40% of the original line reactance, but with opposite sign, the resulting reactance of the compensated line becomes 60% of the original value. Thus

$$x_{km}^{comp} = x_{km} - x_{sc} \quad (6.56)$$

with obvious notation. In the dc power flow model the series capacitor can thus be regarded as a negative resistance inserted in series with the equivalent line resistance.

### In-Phase Transformer

The active power flows,  $P_{km}$  and  $P_{mk}$ , in an in-phase transformer are given by eq. (3.10)

$$P_{km} = (a_{km}U_k)^2 g_{km} - a_{km}U_k U_m g_{km} \cos \theta_{km} - a_{km}U_k U_m b_{km} \sin \theta_{km} \quad (6.57)$$

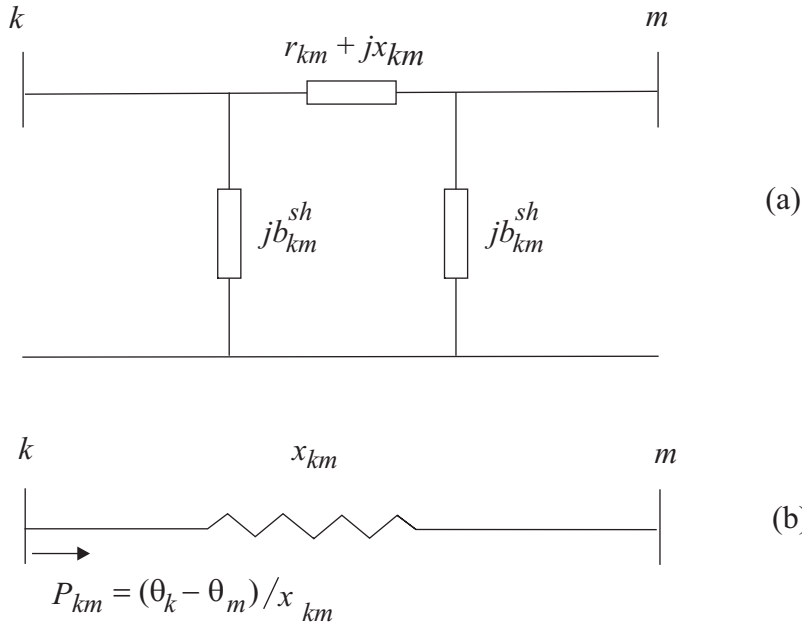


**Figure 6.4.** Transmission line. (a) Equivalent  $\pi$ -model. (b) DC power flow model.

Neglecting the terms associated with losses and introducing the same approximations used for transmission lines yields

$$P_{km} = \frac{\theta_{km}}{x_{km}/a_{km}} \quad (6.58)$$

where further approximating  $a_{km} \approx 1$ , i.e. the transformer tap ratio is close to the relation between the nominal voltages of the two sides, yields the same expression as for transmission lines

$$P_{km} = \frac{\theta_{km}}{x_{km}} \quad (6.59)$$

This is illustrated in Figure 6.5.

### Phase Shifter

Let us consider again the expression for the active power flow  $P_{km}$  in a phase-shifting transformer of the type represented in Figure 2.6 with  $a_{km} = 1$  (eq. (3.14)):

$$P_{km} = U_k^2 g_{km} - U_k U_m g_{km} \cos(\theta_{km} + \varphi_{km}) - U_k U_m b_{km} \sin(\theta_{km} + \varphi_{km})$$

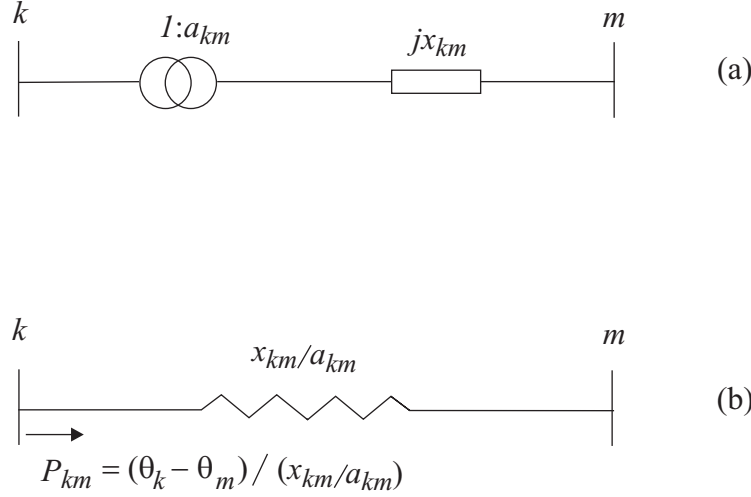


**Figure 6.5.** In-phase transformer. (a) Transformer comprising ideal transformer and series reactance. (b) DC power flow model.

As with transmission lines and in-phase transformers, if the terms associated with active power losses are ignored and  $U_k = U_m = 1$  p.u. and  $b_{km} = -x_{km}^{-1}$ , the result is

$$P_{km} = \frac{\sin(\theta_{km} + \varphi_{km})}{x_{km}} \quad (6.60)$$

and if  $(\theta_{km} + \varphi_{km}) \ll \pi/2$ , then linear approximation can be used, giving

$$P_{km} = \frac{(\theta_{km} + \varphi_{km})}{x_{km}} \quad (6.61)$$

Note that  $P_{km}$  has two components, the first depending on the terminal bus voltage angles,  $\theta_{km}/x_{km}$ , and the other depending only on the phase-shifting transformer angle,  $\varphi_{km}/x_{km}$ . If  $\varphi_{km}$  is considered to be a constant, eq. (6.61) can be represented by the linearized model shown in Figure 6.6, where the constant part of the active power flow,  $\varphi_{km}/x_{km}$ , appears as an extra load on the terminal bus  $k$  and an extra generation on the terminal bus  $m$  if  $\varphi_{km} > 0$ , or vice-versa if  $\varphi_{km} < 0$ .

### 6.5.2 Matrix Formulation of DC Power Flow Equations

In this section, the dc model developed above is expressed in the form  $\mathbf{I} = \mathbf{Y}\mathbf{E}$ . According to the dc model, the active power flow in a branch is given by

$$P_{km} = x_{km}^{-1} \theta_{km} \quad (6.62)$$

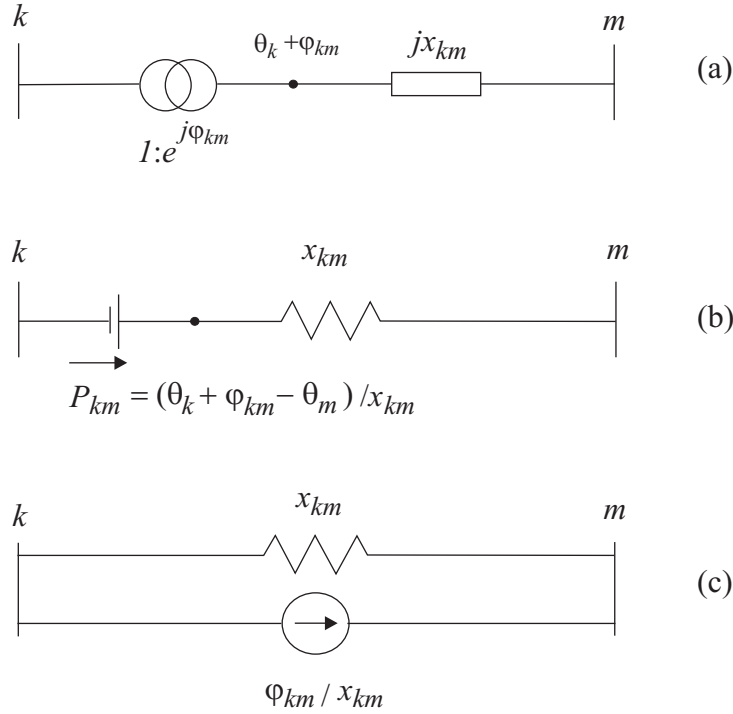


**Figure 6.6.** Phase-shifting transformer. (a) Phase-shifting transformer model (b) Thévenin dc power flow model. (c) Norton dc power flow model.

where  $x_{km}$  is the series reactance of the branch (parallel equivalent of all the circuits existing in the branch).

The active power injection at bus  $k$  is thus given by

$$P_k = \sum_{m \in \Omega_k} x_{km}^{-1} \theta_{km} = \left( \sum_{m \in \Omega_k} x_{km}^{-1} \right) \theta_k + \sum_{m \in \Omega_k} (-x_{km}^{-1} \theta_m) \quad (6.63)$$

for  $k = 1, 2, \dots, N$ , where  $N$  is the number of buses in the network. This can be put into matrix form as follows:

$$\mathbf{P} = \mathbf{B}' \boldsymbol{\theta} \quad (6.64)$$

where

- $\mathbf{P}$  is the vector of the net injections  $P_k$
- $\mathbf{B}'$  is the nodal admittance matrix with the following elements:

$$B'_{km} = -x_{km}^{-1}$$

$$B'_{kk} = \sum_{m \in \Omega_k} x_{km}^{-1}$$

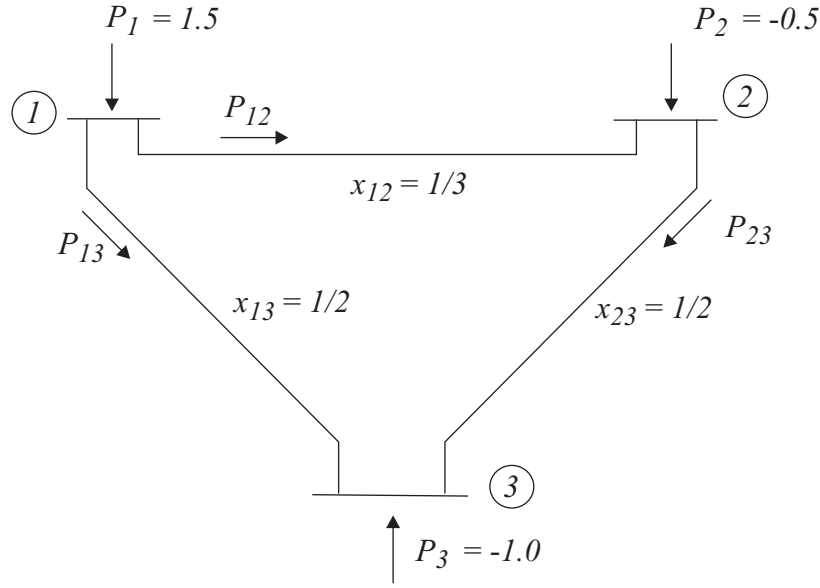


Figure 6.7. 3-bus network. (Active power in p.u.; branch reactances in p.u.)

- $\theta$  is the vector of voltage angles  $\theta_k$

If phase shifting transformers are present in the system eq. (6.64) will be extended by a term representing the power injections by the phase shifting transformers according to Fig. 6.5.1

$$\mathbf{P} = \mathbf{B}'\theta - \mathbf{P}_{\text{pst}} \quad (6.65)$$

where  $\mathbf{P}_{\text{pst}}$  are the injections from the phase shifting transformers defined as positive into the bus.

The matrix  $\mathbf{B}'$  in eq. (6.64) is singular, i.e. its determinant is equal to zero. This means that the system of equations in eq. (6.64) has no unique solution and that the rows of  $\mathbf{B}'$  are linearly dependent. To make the system solvable, one of the equations in the system is removed, and the bus associated with that row is chosen as the angle reference, i.e.  $\theta_{ref} = 0$ . Since the network losses are ignored in this approximation a slack node is not required to compensate for these a priori unknown losses, but of course still an angle reference is needed.

**Example 6.2.** Consider the network given in Figure 6.7 in which the reference angle is  $\theta_1 = 0$ . Use the dc power flow method to calculate the power flows in the lines.

**Solution** In this case, the elements of the matrix  $\mathbf{B}'$  are calculated as

$$\begin{aligned} B_{22} &= x_{21}^{-1} + x_{23}^{-1} = (1/3)^{-1} + (1/2)^{-1} = 5 \\ B_{23} &= -x_{23}^{-1} = -(1/2)^{-1} = -2 \\ B_{32} &= -x_{32}^{-1} = -(1/2)^{-1} = -2 \\ B_{33} &= x_{31}^{-1} + x_{32}^{-1} = (1/2)^{-1} + (1/2)^{-1} = 4 \end{aligned}$$

and thus

$$\mathbf{B}' = \begin{pmatrix} 5 & -2 \\ -2 & 4 \end{pmatrix}$$

and

$$(\mathbf{B}')^{-1} = \begin{pmatrix} 1/4 & 1/8 \\ 1/8 & 5/16 \end{pmatrix}$$

The nodal voltage angles (in radians) can now easily be calculated

$$\begin{aligned} \theta &= \begin{pmatrix} \theta_2 \\ \theta_3 \end{pmatrix} = (\mathbf{B}')^{-1} \mathbf{P} \\ &= \begin{pmatrix} 1/4 & 1/8 \\ 1/8 & 5/16 \end{pmatrix} \begin{pmatrix} -0.5 \\ -1.0 \end{pmatrix} = \begin{pmatrix} -0.250 \\ -0.375 \end{pmatrix} \end{aligned}$$

The power flows in the transmission lines are according to the dc power flow model

$$\begin{aligned} P_{12} &= x_{12}^{-1} \theta_{12} = 3 \cdot 0.25 = 0.75 \text{ p.u.} \\ P_{13} &= x_{13}^{-1} \theta_{13} = 2 \cdot 0.375 = 0.75 \text{ p.u.} \\ P_{23} &= x_{23}^{-1} \theta_{23} = 2 \cdot 0.125 = 0.25 \text{ p.u.} \end{aligned}$$

◆

The linearized model  $\mathbf{P} = \mathbf{B}'\theta$  can be interpreted as the model for a network of resistors fed by dc current sources where  $\mathbf{P}$  is the vector of nodal current injections,  $\theta$  is the nodal vector of dc voltages, and  $\mathbf{B}'$  is the nodal conductance matrix, as illustrated in Figure 6.8.

In the derivation of the DC power flow model we neglected the line resistances and consequently there are no losses occurring in the solutions obtained. However, we can calculate an estimate of the losses by taking the line currents obtained from the DC power flow,  $I_{km}^{DC}$  and compute the losses as  $R_{km}(I_{km}^{DC})^2$ ,  $R_{km}$  being the line resistance, for a given line. This gives quite often a fairly good approximation.

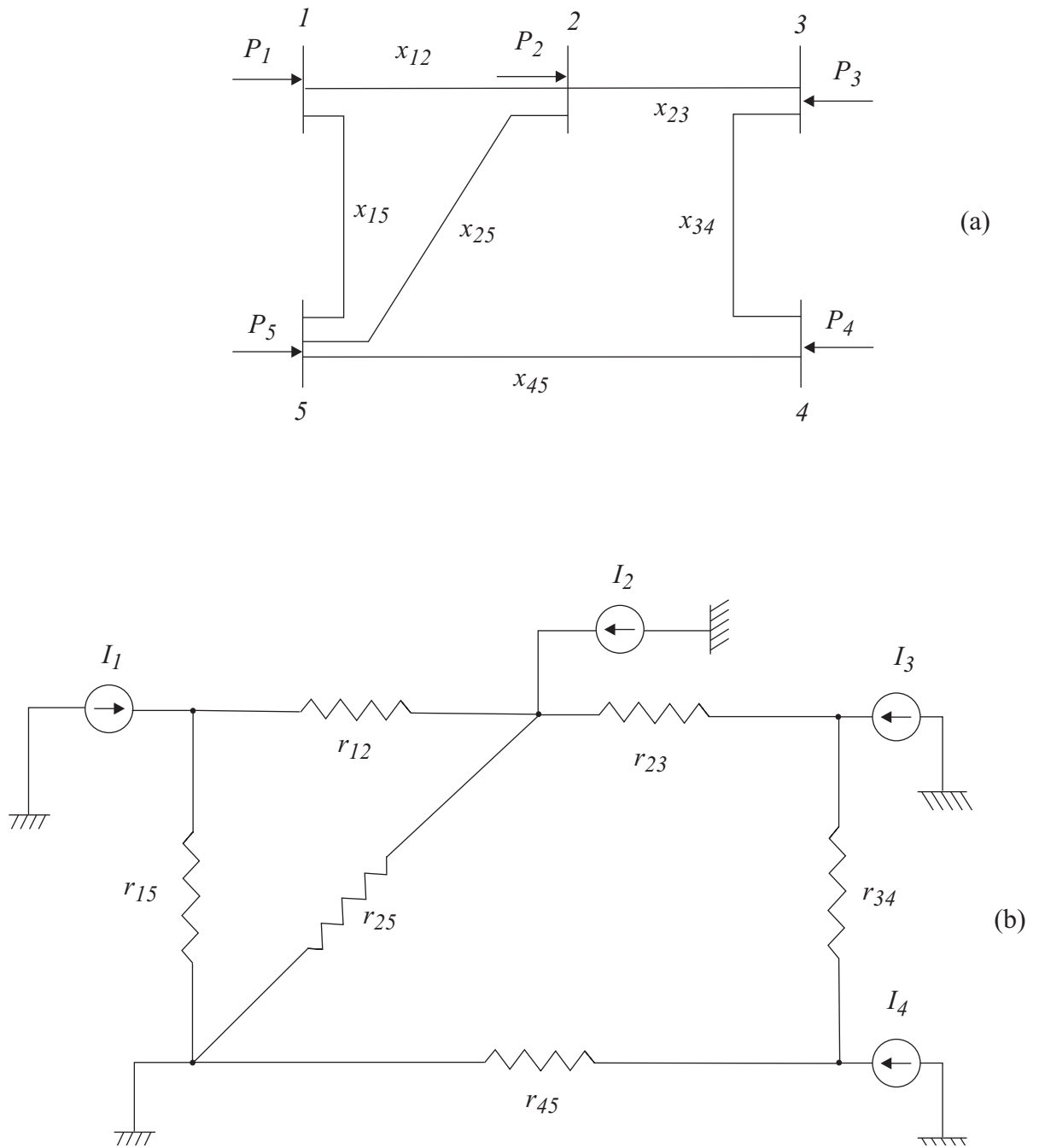


**Figure 6.8.** 6-bus network. (a) power network. (b) dc power flow model.

# 7

## Fault Analysis

*This chapter presents computation techniques for the currents that may occur in the network under symmetrical short circuit conditions. These short circuit currents determine the rating of circuit breakers that must be able to clear the fault in order to avoid permanent damage to the equipment.*

SO FAR we have dealt with steady state behavior of power systems under normal operating conditions. This chapter is devoted to abnormal system behavior under conditions of faults. Such conditions are caused in the system accidentally through insulation failure of equipment or flashover of lines initiated by a lightning stroke or through accidental faulty operation.

In high voltage networks, short circuits are the most frequent type of faults. Short circuits may be solid or may involve an arc impedance. Figure 7.1 illustrates different types of short circuits. The most frequent type of faults are single-phase earth faults, which typically constitute 50 - 80 % of all faults on transmission lines. Number of faults vary from region to region and depends on meteorological conditions, e.g. lightning intensity, and other factors. In Germany and Switzerland faults occur with a frequency of 2 - 5 faults per year and 100 km in the transmission systems.

Depending on the location, the type, the duration, and the system grounding short circuits may lead to

- electromagnetic interference with conductors in the vicinity (disturbance of communication lines),
- stability problems,
- mechanical and thermal stress (i.e. damage of equipment, personal danger)
- danger for personnel

The system must be protected against flow of heavy short circuit currents by disconnecting the faulty part of the system by means of circuit breakers operated by protective relaying. The safe disconnection can only be guaranteed if the current does not exceed the capability of the circuit breaker. Therefore, the short circuit currents in the network must be computed and

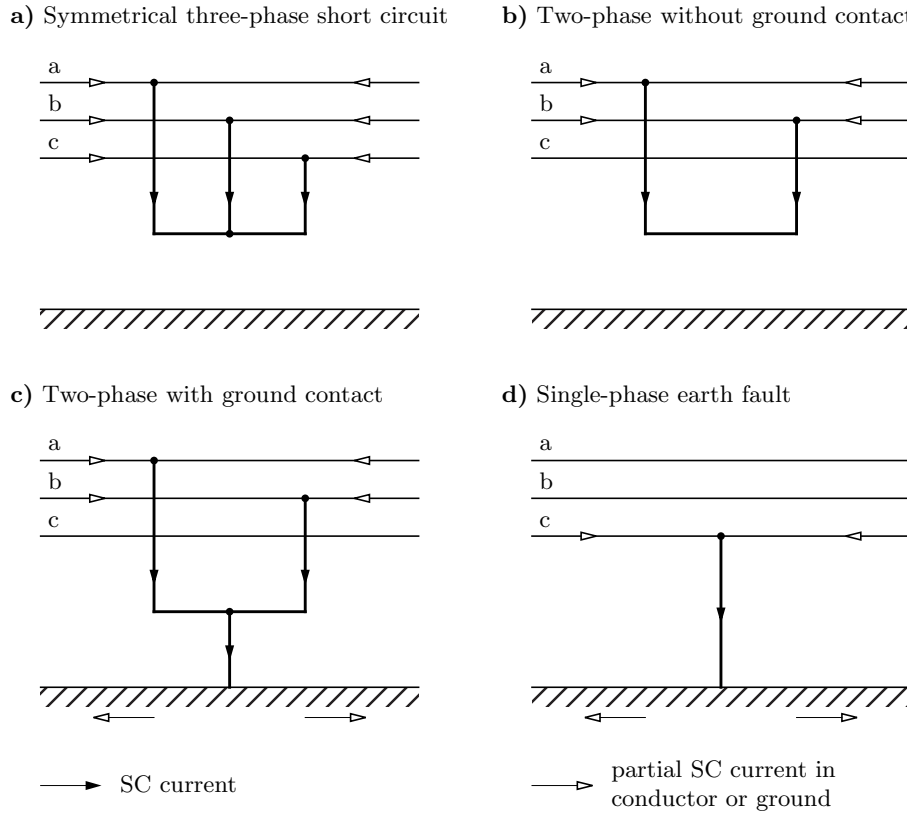


**Figure 7.1.** Examples for different types of short circuits.

compared with the ratings of the circuit breakers at regular intervals as part of the normal operation planning.

As illustrated in Figure 7.2, the short circuit currents at network nodes are generally increasing over the years due to

- more generators,
- new lines in existing networks,
- interconnection of isolated networks to an integrated one.

This is primarily a problem for the *expansion planning*, where the impacts of long-term changes on the short circuit currents have to be assessed. If the short circuit current exceeds the admissible limit at a network node, the circuit breakers have to be replaced by breakers with higher ratings. Alternatively, the impedance between feeder and fault location can be increased in order to reduce the short circuit current. This is commonly achieved by

- introducing a higher voltage level while splitting the existing lower voltage network (Figure 7.3),

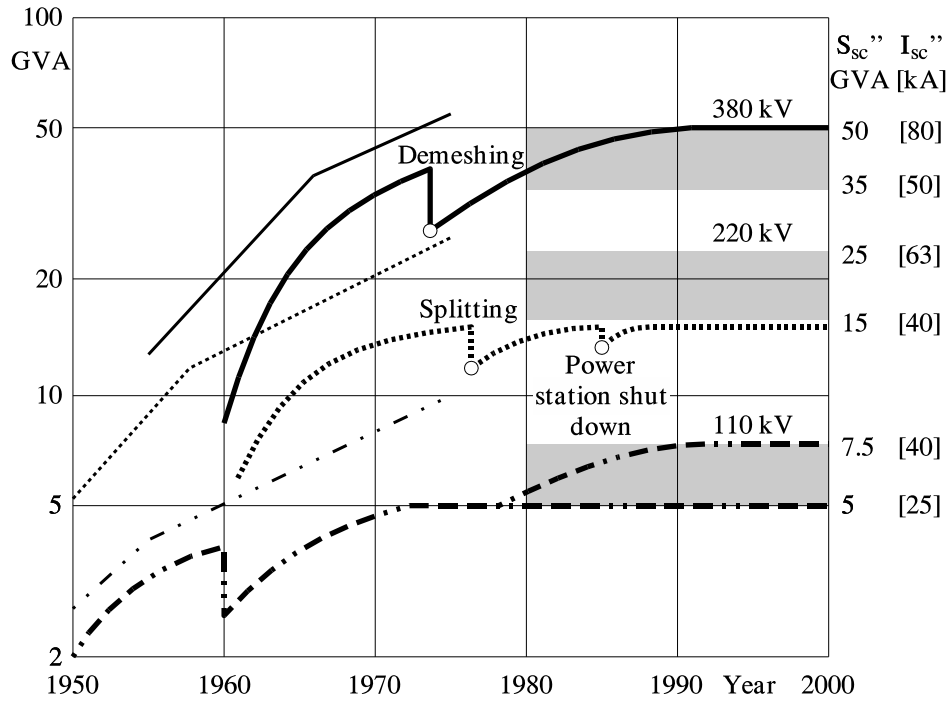


Figure 7.2. Development of short circuit currents over the years.

- use of multiple busbars (Figure 7.4),
- fast decoupling of busbars during faults (Figure 7.5).

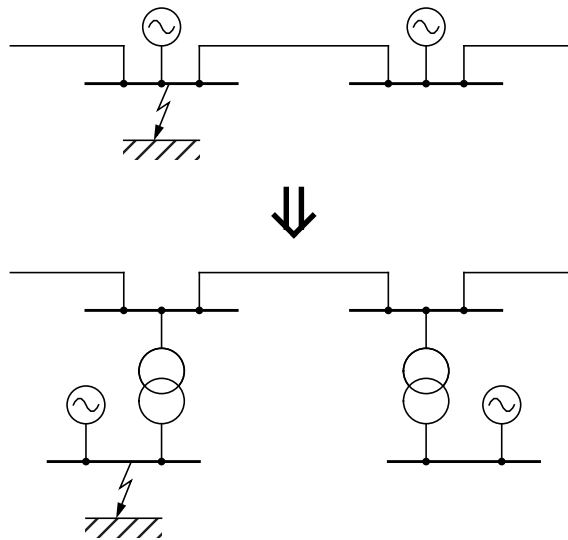
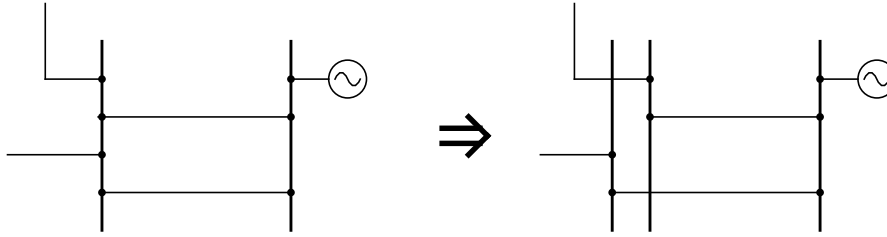
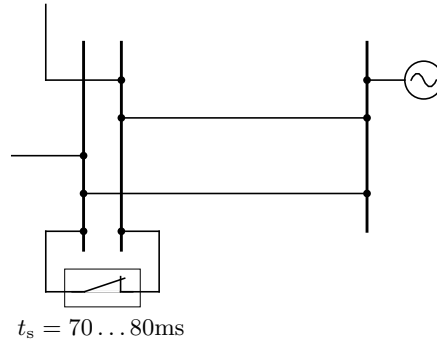


Figure 7.3. Introduction of a higher voltage level.



**Figure 7.4.** Multiple busbar operation.



**Figure 7.5.** Fast busbar decoupling.

Since changing the circuit breakers involves very high costs, the proposed means to reduce the short circuit currents are the generally preferred solution. However, this results in a more complex network structure. It also leads to more possibilities to reconfigure the network topology during operation. When a multiple busbar is introduced, for example, a line can be switched from one busbar to another.

Switching actions have a significant influence on the short circuit currents, but not all possible topologies can be studied during network planning. Therefore, calculating the short circuit currents has become more and more a problem for the *network operation planning*. Prior to each switching action all short circuit currents of the new topology must be calculated in order to decide if the switching action may be carried out. This requires computation algorithms that are sufficiently fast for real time applications.

The majority of system faults are not three-phase faults but faults involving one line to ground or occasionally two lines to ground. These are unsymmetrical faults requiring special computational methods like symmetrical components. Though symmetrical faults are rare, symmetrical short circuit analysis must be carried out, as this type of fault generally leads to the most severe fault current flow against which the system must be protected. Symmetrical fault analysis is, of course, simpler to carry out.

A power network comprises synchronous generators, transformers, lines, and loads. Though the operating conditions at the time of fault are impor-

tant, the loads can usually be neglected during short circuits, as voltages dip very low so that currents drawn by loads can be neglected in comparison with short circuit currents.

The synchronous generator during short circuit has a characteristic time-varying behavior. In the event of a short circuit, the flux per pole undergoes dynamic change with associated transients in damper and field windings. The reactance of the circuit model of the machine changes in the first few cycles from a low subtransient reactance to a higher transient value, finally settling at a still higher synchronous (steady state) value. Depending upon the arc interruption time of the circuit breakers, an appropriate reactance value is used for the circuit model of synchronous generators for the short circuit analysis.

In a modern large interconnected power system, heavy currents flowing during a short circuit must be interrupted much before the steady state conditions are established. Furthermore, from the considerations of mechanical forces that act on the circuit breaker components, the maximum current that a breaker has to carry momentarily must also be determined. For selecting a circuit breaker we must, therefore, determine the initial current that flows on occurrence of a short circuit and also the current in the transient that flows at the time of circuit interruption.

We distinguish between two different approaches to calculate the short circuits in a power system:

- Calculation of transient currents
- Calculation of stationary currents

First, we will focus on the calculation of transient currents since this will help us to understand the physical phenomena during short circuits. However, for large power systems, the computation of transient currents is not feasible. For this reason simplified techniques for short circuit current computation will be presented that are based on stationary models.

## 7.1 Transients on a transmission line

Let us consider the short circuit transient on a transmission line. Certain simplifying assumptions are made at this stage:

1. The line is fed from a constant voltage source.
2. Short circuit takes place when the line is unloaded.
3. Line capacitance is negligible and the line can be represented by a lumped RL series circuit.

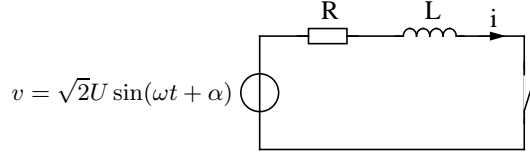


**Figure 7.6.** Transmission line model.

With the above assumptions the line can be represented by the circuit model of Figure 7.6. The short circuit is assumed to take place at  $t = 0$ . The parameter  $\alpha$  controls the instant on the voltage wave when short circuit occurs. It is known from circuit theory that the current after short circuit is composed of two parts, i.e.

$$i = i_s + i_t \quad (7.1)$$

where  $i_s$  represents the steady state alternating current

$$i_s = \frac{\sqrt{2}U}{|Z|} \sin(\omega t + \alpha - \theta) \quad (7.2)$$

and  $i_t$  represents the transient direct current

$$i_t = -i_s(0) e^{-(R/L)t} = \frac{\sqrt{2}U}{|Z|} \sin(\theta - \alpha) e^{-(R/L)t} \quad (7.3)$$

with

$$Z = \sqrt{R^2 + \omega^2 L^2} \angle \left( \theta = \tan^{-1} \frac{\omega L}{R} \right). \quad (7.4)$$

A plot of  $i = i_s + i_t$  is shown in Figure 7.7. In power system terminology, the sinusoidal steady state current is called the *symmetrical short circuit current* and the unidirectional transient component is called the *DC off-set current*, which causes the total short circuit current to be unsymmetrical till the transient decays.

It follows easily from Figure 7.7 that the *maximum momentary short circuit current*  $i_{\text{mm}}$  corresponds to the first peak. If the decay of transient current in this short time is neglected,

$$i_{\text{mm}} = \frac{\sqrt{2}U}{|Z|} \sin(\theta - \alpha) + \frac{\sqrt{2}U}{|Z|} \quad (7.5)$$

Since transmission line resistance is small,  $\theta \approx 90^\circ$ .

$$i_{\text{mm}} = \frac{\sqrt{2}U}{|Z|} \cos \alpha + \frac{\sqrt{2}U}{|Z|} \quad (7.6)$$

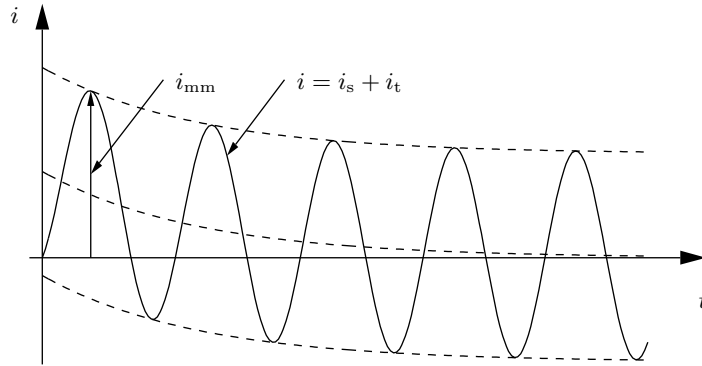


**Figure 7.7.** Waveform of a short circuit current on a transmission line.

This has the maximum possible value for  $\alpha = 0$ , i.e. short circuit occurring when the voltage wave is going through zero. Thus  $i_{mm}$  may be as high as twice the maximum of the symmetrical short circuit current:

$$i_{mm} \leq 2 \frac{\sqrt{2}U}{|Z|} \quad (7.7)$$

For the selection of circuit breakers, momentary short circuit current is taken corresponding to its maximum possible value.

The next question is ‘what is the current to be interrupted’? As has been pointed out earlier, modern circuit breakers are designed to interrupt the current in the first few cycles (five cycles or less). With reference to Figure 7.7 it means that when the current is interrupted, the DC off-set  $i_t$  has not yet died out and contributes thus to the current to be interrupted. Rather than computing the value of the DC off-set at the time of interruption (this would be highly complex in a network of even moderately large size), the symmetrical short circuit current alone is calculated. This current is then increased by an empirical multiplying factor to account for the DC off-set current.

## 7.2 Short circuit of a synchronous machine

Under steady state short circuit conditions, the armature reaction of a synchronous generator produces a demagnetizing flux. In terms of a circuit this effect is modelled as a reactance  $X_a$  in series with the induced electromagnetic field. This reactance when combined with the leakage reactance  $X_l$  of the machine is called *synchronous reactance*  $X_d$ . The index d denotes the direct axis. Since the armature reactance is small, it can be neglected. The steady state short circuit model of a synchronous machine is shown in Figure 7.8.

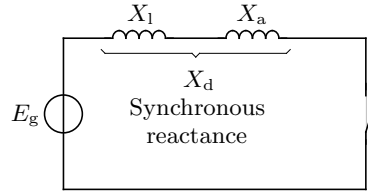


**Figure 7.8.** Steady state short circuit model of a synchronous machine.

Consider now the sudden short circuit of a synchronous generator that has initially been operating under open circuit conditions. The machine undergoes a transient in all the three phases finally ending up in the steady state condition described above. The circuit breaker must interrupt the current long before the steady state condition is reached. Immediately upon short circuit, the DC off-set currents appear in all three phases, each with a different magnitude since the point on the voltage wave at which short circuit occurs is different for each phase. These DC off-set currents are accounted for separately on an empirical basis. Therefore, for short circuit studies, we need to concentrate our attention on the symmetrical short circuit current only.

In the event of a short circuit, the symmetrical short circuit current is limited initially only by the leakage reactance of the machine. Since the air gap flux cannot change instantaneously, to counter the demagnetization of the armature short circuit current, currents appear in the field winding as well as in the damper winding in a direction to help the main flux. These currents decay in accordance with the winding time constants. The time constant of the damper winding which has low X/R-ratio is much less than the one of the field winding, which has high leakage inductance with low resistance. Thus, during the initial part of the short circuit, the damper and field windings have transformer currents induced in them. In the circuit model their reactances— $X_f$  of field winding and  $X_{dw}$  of damper winding—appear in parallel with  $X_a$  as shown in Figure 7.9.

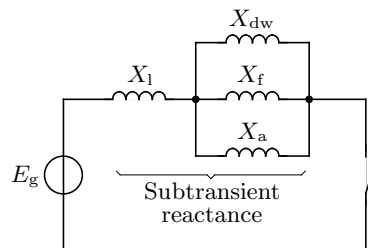


**Figure 7.9.** Approximate circuit model during subtransient period of short circuit.

As the damper winding currents are first to die out,  $X_{dw}$  effectively

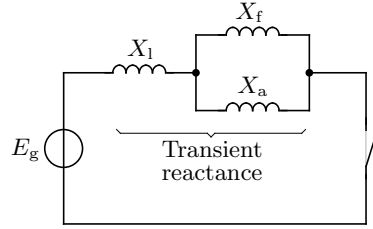


**Figure 7.10.** Approximate circuit model during transient period of short circuit.

becomes open circuited and at a later stage  $X_f$  becomes open circuited. The machine reactance thus changes from the parallel combination of  $X_a$ ,  $X_f$ , and  $X_{dw}$  during the initial period of the short circuit to  $X_a$  and  $X_f$  in parallel (Figure 7.10) during the middle period. The machine reactance finally becomes  $X_a$  in steady state (Figure 7.8). The reactance presented by the machine in the initial period of the short circuit, i.e.

$$X_d'' = X_l + \frac{1}{1/X_a + 1/X_f + 1/X_{dw}} \quad (7.8)$$

is called the *subtransient reactance* of the machine; while the reactance effective after the damper winding currents have died out, i.e.

$$X_d' = X_l + \frac{1}{1/X_a + 1/X_f} \quad (7.9)$$

is called the *transient reactance*. Of course, the reactance under steady state conditions is the *synchronous reactance*. Obviously  $X_d'' < X_d' < X_d$ . The machine thus offers a time-varying reactance which changes from  $X_d''$  to  $X_d'$  and finally to  $X_d$ .

If we examine the oscillogram of the short circuit current of a synchronous machine after the DC off-set has been removed, we will find the current wave shape as given in Figure 7.11. The short circuit current can be divided into three periods—the initial subtransient period when the current is large as the machine offers subtransient reactance, the middle transient period where the machine offers transient reactance, and finally the steady state period when the machine offers synchronous reactance. Hence we distinguish between

- the steady state current  $I_{sc}$ ,
- the transient current  $I_{sc}'$ , and
- the initial subtransient current  $I_{sc}''$ .

None of the three currents includes a DC component. The steady state and transient currents are obtained by extrapolating their envelopes backwards

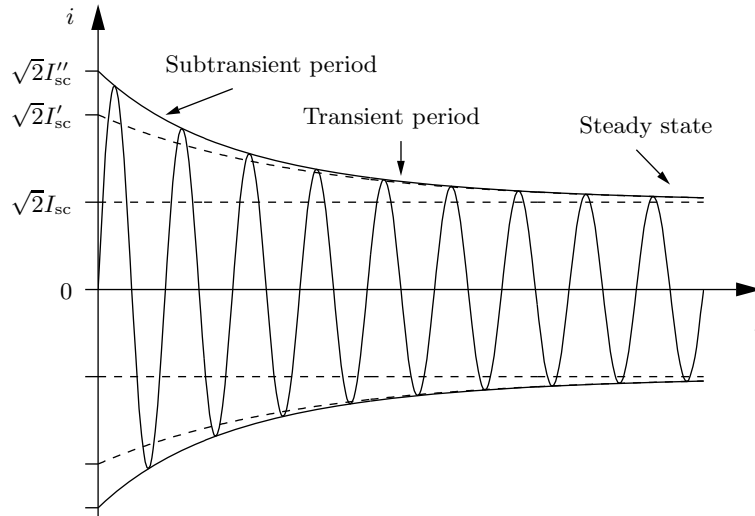


**Figure 7.11.** Symmetrical short circuit armature current in synchronous machine.

in time. Since we are normally interested in maximum short circuit current, most short circuit computations are based only on the subtransient current. In some systems a weighted average of the subtransient and the transient reactance is used.

## 7.3 Algorithms for short circuit studies

### 7.3.1 Generator model

In the power flow analysis we are modeling generators as constant power sources (PU characteristics) which leads to nonlinear power flow equations. However, for the short transient period during a short circuit this model is no longer valid since the power and the voltage regulators operate with much larger time constants. Here, the linear model outlined in Figure 7.12 is more appropriate. It is used for generators and infeeds, where  $E''$  represents the subtransient electro-magnetic field and  $X''_d$  represents the subtransient reactance of generators or the internal grid impedance of a feeder. This model may also be applied to large motor loads.

### 7.3.2 Simplifications

When computing short circuits in a power system further simplifications can be made. The following simplifications are also proposed in the German standard VDE 0102:

- All line capacitances are ignored.

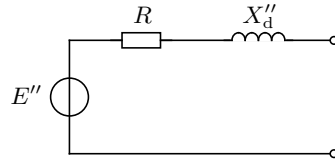


**Figure 7.12.** Linear generator model for short circuit computation.

- All non-motor shunt impedances are ignored; motor loads are treated the same way as generators.
- The voltage magnitude and phase angle of generators and infeeds are all set to the same value

$$E_i'' = c \cdot U_{\text{nom}} \quad (7.10)$$

where  $U_{\text{nom}}$  is the nominal voltage of the system in which the short circuit occurs. In high voltage systems ( $\geq 35$  kV)  $c = 1.1$  represents the difference between the effective voltage and the system voltage. If the minimum rather than the maximum initial AC short circuit current is to be calculated,  $c$  is set to  $c = 0.95$ .

- All tap changing transformers are in middle position.

These simplifications are indicated for studies regarding medium- and long-term network planning. In the planning stage, the calculations are based on estimated and hence inaccurate data. Therefore, the demands on the short circuit computation algorithm are lower than for real-time applications in the network operation, where accurate results are desired. Studies have shown that the shunt elements and loads have little influence on the short circuit currents (0.5% ... 4%) and may compensate each other. However, disregarding the actual generator pole voltages and the actual positions of tap changing transformers may sometimes lead to errors of up to 30%.

### 7.3.3 Solving the linear system equations

With the linear models of the network elements, a system of linear equations can be set up for a short circuit at any node  $i$ . Figure 7.13 illustrates the network model. The voltage sources of the generators (Figure 7.12) must be transformed into equivalent current sources. The admittance of the current source is considered in the respective element of the admittance matrix.

In order to calculate the short circuit current  $I_{\text{sc}}''$  at node  $i$  the equation

$$\mathbf{Y} \cdot \mathbf{U} = \mathbf{I} \quad (7.11)$$

must be solved, where

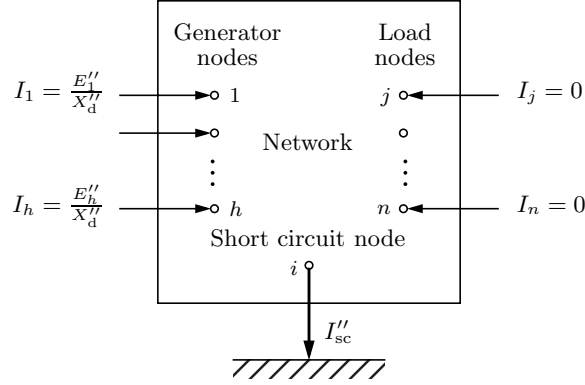


Figure 7.13. Network with short circuit at node  $i$ .

- $\mathbf{Y}$  is the nodal admittance matrix
- $\mathbf{U}$  is the nodal voltage vector

$$\mathbf{U} = \begin{cases} U_j & \text{if } j \neq i \\ 0 & \text{if } j = i \end{cases} \quad (7.12)$$

- $\mathbf{I}$  is the vector of injection currents

$$\mathbf{I} = \begin{cases} \frac{E_j''}{X_{dj}''} & \text{for generator nodes } j \neq i \\ 0 & \text{for load nodes } j \neq i \\ -I_{sc}'' & \text{for short circuit node without generation } j = i \\ -I_{sc}'' + \frac{E_j''}{X_{dj}''} & \text{for short circuit node with generation } j = i \end{cases} \quad (7.13)$$

All elements  $U_j$  of vector  $\mathbf{U}$  are unknown variables with the exception of voltage  $U_i = 0$  at the short circuit node  $i$ . On the contrary, all elements of vector  $\mathbf{I}$  are known except for the current  $I_i$  at the short circuit node  $i$ . To solve the system of equations (7.11), the  $i$ th row and the  $i$ th column are removed. The remaining admittance matrix is then factorized into triangular matrices. Backward substitution yields the unknown voltages. The unknown current  $I_i$  at the short circuit node  $i$  can be calculated from the voltages using the  $i$ th row of eq. (7.11).

If the short circuit currents  $I_{sci}''$  are calculated for all nodes  $i = 1, \dots, n$  the equation system has to be set up and solved for every short circuit node. Since always another row and another column are removed the matrix must be factorized each time anew. Therefore, with the proposed method the computation of all short circuit currents is considerably expensive.

### 7.3.4 The superposition technique

If two equal voltage sources in opposite direction are introduced into the short circuit path at node  $i$  according to Figure 7.14, neither currents nor voltages in the network are affected. Since the network consists only of linear elements the short circuit calculation is a linear problem. Therefore, the superposition principle can be applied, that means the computation of the short circuit current may be performed in two steps. These steps are illustrated in Figure 7.15 and Figure 7.16. The superposition, i.e. the addition of the results finally yields the desired values. The advantage of inserting two opposite voltage sources becomes clear if both steps are regarded separately.

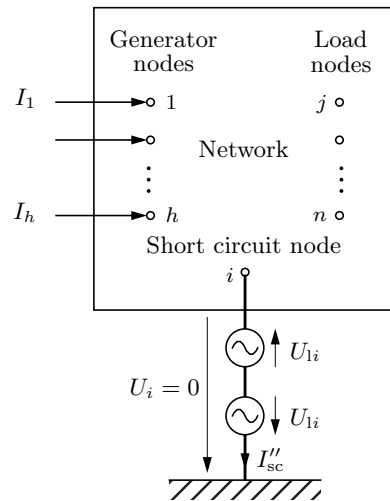


Figure 7.14. Network with short circuit at node  $i$ .

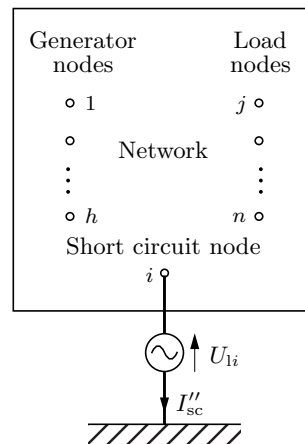
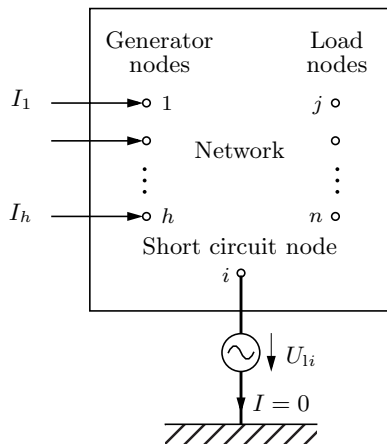


Figure 7.15. Superposition 1st step.

Figure 7.16. Superposition 2nd step.

### First step

Principally, the voltage  $U_{li}$  can be chosen arbitrarily. If it is chosen in such a way that  $I_{sc}''^{(1)} = 0$ , the first step corresponds to the computation of node voltages and branch currents in a power flow analysis. The power flow analysis yields the voltage  $U_{li}$ , i.e. the voltage at the short circuit node  $i$  before the fault occurs.

If the above simplifications are applied, the first step can be omitted. For all generators, infeeds and loads the voltage is then uniformly presumed

$$E_i'' = c \cdot U_{nom} . \quad (7.14)$$

As already mentioned, disregarding the actual generator voltages may lead to considerable errors. Therefore, this approximation is not always recommended. The first step, i.e. calculating the pre-fault voltages, is identical for all short circuit nodes  $i = 1, \dots, n$  and needs to be done only once. Thus, the additional effort for an exact calculation of the node voltages is comparatively small.

### Second step

In the second step the voltage  $U_{li}$  is inserted in reverse direction at the short circuit node  $i$ . All other sources like generators and infeeds are disregarded. This yields the equation system

$$\mathbf{Y} \cdot \mathbf{U}^{(2)} = \mathbf{I}^{(2)} \quad (7.15)$$

with

- Elements of vector  $\mathbf{U}^{(2)}$ :

$$\mathbf{U}^{(2)} = \begin{cases} U_j^{(2)} & \text{if } j \neq i \\ -U_{li} & \text{if } j = i \end{cases} \quad (7.16)$$

- Elements of vector  $\mathbf{I}^{(2)}$ :

$$\mathbf{I}^{(2)} = \begin{cases} 0 & \text{if } j \neq i \\ -I_{sc}'' & \text{if } j = i \end{cases} \quad (7.17)$$

Vector  $\mathbf{U}^{(2)}$  contains the node voltages  $U_j^{(2)}$ , all of which are unknown with the exception of  $U_i^{(2)} = -U_{li}$ . In vector  $\mathbf{I}^{(2)}$  the only non-zero current is  $I_i^{(2)}$ . Dividing the system of equations (7.15) by  $-I_{sc}''$  yields the modified system of equations (7.18) where  $\hat{\mathbf{U}}^{(2)}$  contains only unknown and  $\hat{\mathbf{I}}^{(2)}$  only given values.

$$\mathbf{Y} \cdot \hat{\mathbf{U}}^{(2)} = \hat{\mathbf{I}}^{(2)} \quad (7.18)$$

with

- Elements of vector  $\hat{\mathbf{U}}^{(2)}$ :

$$\hat{\mathbf{U}}^{(2)} = \begin{cases} -\frac{U_j^{(2)}}{I_{sc}''} & \text{if } j \neq i \\ \frac{U_{li}}{I_{sc}''} & \text{if } j = i \end{cases} \quad (7.19)$$

- Elements of vector  $\hat{\mathbf{I}}^{(2)}$ :

$$\hat{\mathbf{I}}^{(2)} = \begin{cases} 0 & \text{if } j \neq i \\ 1 & \text{if } j = i \end{cases} \quad (7.20)$$

The transformation from eq. (7.15) to eq. (7.18) leaves the admittance matrix  $\mathbf{Y}$  unchanged. As a consequence, the triangular factorization of the admittance matrix must be done only once, even if multiple short circuit cases are investigated. The superposition technique should therefore be preferred to the direct solution of the linear system of equations (7.11).

However, if we compute the solution of eq. (7.18) with the known technique, i.e. triangular factorization and forward-backward-substitution, a new forward-backward-substitution is required for every short circuit case. This disadvantage can be avoided with the Takahashi method.

### 7.3.5 The Takahashi method

The principle idea behind the Takahashi method is the solution of eq. (7.18) by means of inversion. This yields

$$\mathbf{Z} \cdot \hat{\mathbf{I}}^{(2)} = \hat{\mathbf{U}}^{(2)} \quad (7.21)$$

where

$$\mathbf{Z} = \mathbf{Y}^{-1} \quad (7.22)$$

is the impedance matrix of the system. The unknown initial short circuit current  $I_{sc}''$  at node  $i$  can be found in the  $i$ th element of vector  $\hat{\mathbf{U}}^{(2)}$

$$\hat{U}_i^{(2)} = \frac{U_{li}}{I_{sc}''} \quad (7.23)$$

resp.

$$I_{sc}'' = \frac{U_{li}}{\hat{U}_i^{(2)}}. \quad (7.24)$$

From eqs. (7.20) and (7.21) follows

$$\hat{U}_i^{(2)} = z_{ii} \quad (7.25)$$

where  $z_{ii}$  is an element on the main diagonal of matrix  $\mathbf{Z}$ . Inserting eq. (7.25) in eq. (7.19) finally yields:

$$I''_{sc} = \frac{U_{li}}{z_{ii}} \quad (7.26)$$

For the calculation of the short circuit current only the main diagonal element  $z_{ii}$  of the impedance matrix  $\mathbf{Z}$  is required. Knowing all main diagonal elements  $z_{ii}$  ( $i = 1, \dots, n$ ) is therefore sufficient to compute the short circuit currents  $I''_{sci}$  at all nodes  $i$ .

Often, also the partial short circuit currents  $I_{ji}$  are to be determined. These are the currents that flow from adjacent nodes  $j$  to the short circuit node  $i$ . With the simplification that all generator voltages are identical the partial short circuit currents are

$$\begin{aligned} I_{ji} &= \left( U_j^{(2)} - U_i^{(2)} \right) y_{ji} \\ &= \left( U_j^{(2)} - U_{li}^{(2)} \right) y_{ji} \end{aligned} \quad (7.27)$$

where  $y_{ji}$  is the admittance of the branch between  $j$  and  $i$ . If this simplification is not permitted the terms from the first step must be added here.

With eq. (7.21) follows:

$$\begin{aligned} I_{ji} &= \left( -z_{ji} I''_{sci} + z_{ii} I''_{sci} \right) y_{ji} \\ &= I''_{sci} (z_{ii} - z_{ji}) y_{ji} \end{aligned} \quad (7.28)$$

For the calculation of the partial short circuit currents from node  $j$  to the short circuit node  $i$  in addition to the main diagonal element  $z_{ii}$  all elements  $z_{ji}$  are required. Because node  $j$  is connected directly to node  $i$ , the element  $y_{ji}$  in the admittance matrix is non-zero. Although the impedance matrix  $\mathbf{Z}$  is not sparse like the admittance matrix  $\mathbf{Y}$  relatively few elements of  $\mathbf{Z}$  must be known to calculate the short circuit currents and the partial short circuit currents for all nodes. Apart from the main diagonal elements  $z_{ii}$  these are the elements  $z_{ji}$  that are non-zero in the corresponding admittance matrix.

In the Takahashi method only those elements of  $\mathbf{Z}$  are determined that have non-zero counterparts in the triangularly factorized admittance matrix. Except for the few fill-ins that emerge during factorization these are the elements of  $\mathbf{Z}$  essential for the short circuit computation. The method shall be demonstrated here:

Eq. (7.22) can be written as

$$\mathbf{Y} \cdot \mathbf{Z} = \mathbf{E} \quad (7.29)$$

where  $\mathbf{E}$  is the identity matrix.  $\mathbf{Y}$  is factorized into triangular matrices and

eq. (7.29) can be transformed in the following way:

$$\begin{aligned}
\mathbf{L} \cdot \mathbf{D} \cdot \mathbf{R} \cdot \mathbf{Z} &= \mathbf{E} & | \cdot \mathbf{L}^{-1} & \quad (7.30) \\
\mathbf{D} \cdot \mathbf{R} \cdot \mathbf{Z} &= \mathbf{L}^{-1} & | \cdot \mathbf{D}^{-1} & \\
\mathbf{R} \cdot \mathbf{Z} &= \mathbf{D}^{-1} \cdot \mathbf{L}^{-1} & | + \mathbf{Z} - \mathbf{R} \cdot \mathbf{Z} & \\
\mathbf{Z} &= \mathbf{D}^{-1} \cdot \mathbf{L}^{-1} + \mathbf{Z} - \mathbf{R} \cdot \mathbf{Z} & & \\
\mathbf{Z} &= \mathbf{D}^{-1} \cdot \mathbf{L}^{-1} + (\mathbf{E} - \mathbf{R}) \mathbf{Z} & (7.31) &
\end{aligned}$$

The inverse of diagonal matrix  $\mathbf{D}$  is again a diagonal matrix. Each element on the main diagonal contains the reciprocal value of the element before the inversion:

$$\mathbf{D}^{-1} = \begin{bmatrix} d_{11} & & & \mathbf{0} \\ & d_{22} & & \\ & & \ddots & \\ \mathbf{0} & & & d_{nn} \end{bmatrix}^{-1} = \begin{bmatrix} \frac{1}{d_{11}} & & & \mathbf{0} \\ & \frac{1}{d_{22}} & & \\ & & \ddots & \\ \mathbf{0} & & & \frac{1}{d_{nn}} \end{bmatrix} \quad (7.32)$$

The inverse of the lower triangular matrix  $\mathbf{L}$  is a triangular matrix with the same structure. Since all elements on the main diagonal of  $\mathbf{L}$  are 1, the determinant is also 1. Thus, the main diagonal remains unchanged after inversion. The values of the remaining elements are of no interest due to the nesting of the system of equations (7.31).

$$\mathbf{L}^{-1} = \begin{bmatrix} 1 & & & \mathbf{0} \\ \cdot & 1 & & \\ \cdot & \cdot & \ddots & \\ \cdot & \cdot & \cdot & 1 \end{bmatrix}^{-1} = \begin{bmatrix} 1 & & & \mathbf{0} \\ \cdot & 1 & & \\ \cdot & \cdot & \ddots & \\ \cdot & \cdot & \cdot & 1 \end{bmatrix} \quad (7.33)$$

The product of the diagonal matrix  $\mathbf{D}^{-1}$  with the triangular matrix  $\mathbf{L}^{-1}$  is a triangular matrix with modified main diagonal. Therefore, eq. (7.31) has the following form:

$$\begin{bmatrix} z_{11} & z_{12} & \cdots & z_{1n} \\ z_{21} & z_{22} & \cdots & z_{2n} \\ \vdots & & & \vdots \\ \vdots & & & \vdots \\ z_{n1} & z_{n2} & \cdots & z_{nn} \end{bmatrix} = \begin{bmatrix} \frac{1}{d_{11}} & & & \mathbf{0} \\ \cdot & \frac{1}{d_{22}} & & \\ \cdot & \cdot & \ddots & \\ \cdot & \cdot & \cdot & \ddots \\ \cdot & \cdot & \cdot & \cdot & \frac{1}{d_{nn}} \end{bmatrix} - \begin{bmatrix} 0 & r_{12} & \cdots & r_{1n} \\ 0 & 0 & \cdots & r_{2n} \\ \vdots & \vdots & & \vdots \\ 0 & 0 & \cdots & r_{(n-1)n} \\ 0 & 0 & \cdots & 0 \end{bmatrix} \cdot \begin{bmatrix} z_{11} & z_{12} & \cdots & z_{1n} \\ z_{21} & z_{22} & \cdots & z_{2n} \\ \vdots & & & \vdots \\ \vdots & & & \vdots \\ z_{n1} & z_{n2} & \cdots & z_{nn} \end{bmatrix} \quad (7.34)$$

With the system of equations (7.34) all elements of the impedance matrix  $\mathbf{Z}$  can be determined recursively. We start with the main diagonal element  $z_{nn}$  on the  $n$ th row and continue with the row  $(n - 1)$ . For each row, first the secondary diagonal elements  $z_{ji}$  and then the main diagonal element  $z_{ii}$  are calculated.

Here we take advantage of the fact that the admittance matrix  $\mathbf{Y}$  and also their inverse—the impedance matrix  $\mathbf{Z}$ —are symmetrical. This is due to the simplifying assumption that all tap changing transformers are in middle position.

$$z_{ij} \Big|_{i < j} = z_{ji} = \begin{cases} \text{not calculated if } r_{ij} = 0 \\ - \sum_{l=i+1}^n r_{il} z_{lj} \end{cases} \quad (7.35)$$

$$z_{ii} = \frac{1}{d_{ii}} - \sum_{l=i+1}^n r_{il} z_{lj} \quad (7.36)$$

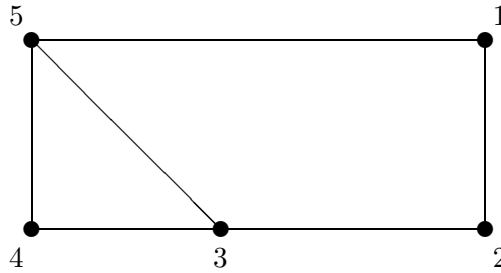


Figure 7.17. Sample network.

**Example 7.1.** *The whole procedure shall be demonstrated in single steps on the sample network given in Figure 7.17. With the arbitrarily chosen node numbering the admittance matrix  $\mathbf{Y}$  has the following structure.*

$$\mathbf{Y} = \begin{bmatrix} y_{11} & y_{12} & 0 & 0 & y_{15} \\ y_{21} & y_{22} & y_{23} & 0 & 0 \\ 0 & y_{32} & y_{33} & y_{34} & y_{35} \\ 0 & 0 & y_{43} & y_{44} & y_{45} \\ y_{51} & 0 & y_{53} & y_{54} & y_{55} \end{bmatrix} \quad (7.37)$$

**Solution** During the triangular factorization of  $\mathbf{Y}$  a fill-in element  $c_{25}$  is generated in the upper triangular matrix. The recursive solution of the

system of equations (7.34) is then

$$z_{55} = \frac{1}{d_{55}} \quad (7.38)$$

$$z_{45} = z_{54} = -r_{45} z_{55} \quad (7.39)$$

$$z_{44} = \frac{1}{d_{44}} - r_{45} z_{54} \quad (7.40)$$

$$z_{35} = -r_{34} z_{45} - r_{35} z_{55} \quad (7.41)$$

$$z_{34} = -r_{34} z_{44} - r_{35} z_{54} \quad (7.42)$$

$$z_{33} = \frac{1}{d_{33}} - r_{34} z_{43} - r_{35} z_{53} \quad (7.43)$$

$$z_{25} = -r_{23} z_{35} - r_{25} z_{55} \quad (7.44)$$

$$z_{23} = -r_{23} z_{33} - r_{25} z_{53} \quad (7.45)$$

$$z_{22} = \frac{1}{d_{22}} - r_{23} z_{32} - r_{25} z_{52} \quad (7.46)$$

$$z_{15} = -r_{12} z_{25} - r_{15} z_{55} \quad (7.47)$$

$$z_{12} = -r_{12} z_{22} - r_{15} z_{52} \quad (7.48)$$

$$z_{11} = \frac{1}{d_{11}} - r_{12} z_{21} - r_{15} z_{51} . \quad (7.49)$$

Figure 7.18 illustrates this sequence. ♦

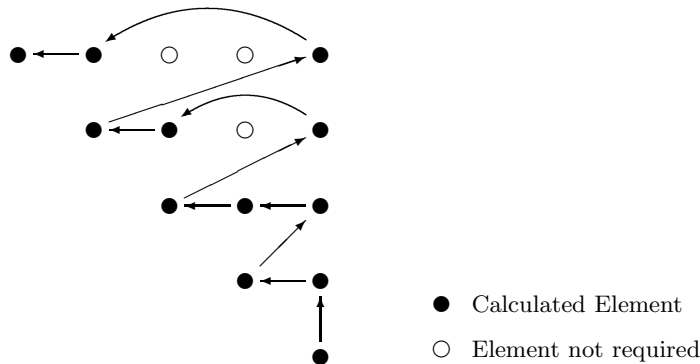


**Figure 7.18.** Solution sequence with Takahashi method.

Until now we have assumed that the admittance matrix  $\mathbf{Y}$  is symmetric. This assumption is valid only if all tap changing transformers are in middle position. However, the Takahashi method can also be applied to unsymmetric matrices. In this more general case we get instead of eq. (7.31) two similar matrix equations. With one of these equations the secondary diagonal elements above the main diagonal are calculated, with the other

equation the elements below the main diagonal. The elements on the main diagonal can be calculated with either equation.

Unsymmetric matrices require about double the effort of symmetric matrices. Since neglecting the actual tap positions can lead to errors of 30 %, considering the actual tap positions is indicated for network operation applications, that require short circuit computations with high accuracy.

### **Concluding remarks**

The Takahashi method is an algorithm especially designed for the demands of short circuit computations. Having the same accuracy it needs only a fraction of the computation time of conventional methods. This advantage is important in real-time applications.

However, with the Takahashi method only the initial short circuit currents can be calculated. This includes the partial short circuit currents  $I_{ji}$  that flow from the adjacent nodes to the short circuit node  $i$ . It is not possible to determine the short current shares delivered from individual generators or infeeds. Thus the breaking current at the generators can not be determined with the Takahashi method but requires Gauss elimination.

## Part II

# Power System Dynamics and Stability



# 8

## Classification and Definitions of Power System Stability

*This chapter contains a brief overview of some of the basic concepts in power system dynamics. A classification of different dynamic phenomena is given and the requirements on modelling are discussed. Stability is a fundamental concept and a definition of stability in power systems is introduced. Instabilities in power systems can be classified according to their physical origins, and this classification is reviewed. Finally, a list of further reading in the subject is given.*

IN AN ELECTRIC POWER SYSTEM a great variety of different dynamics occurs. These dynamic phenomena have different physical origin and they occur in different time scales. A system is in a dynamic state if the time derivative of any system quantity is non zero, and to describe a dynamic system mathematically differential or difference equations must be employed. As an example, the electric consumer loads in a power system vary spontaneously all the time, and consequently one could state that the power system is never in steady state in a strict mathematical sense. Such a point of view is however unpractical in most cases, and one must, as when it comes to most large and complex systems, study and analyse more or less simplified models of the system. To do relevant and adequate simplifications is beneficial for the analysis, and contributes also to achieving results that are easy to understand and easy to interpret. In addition, when deriving simplified models one is forced to identify the most important processes and phenomena in the studied systems, which provides insight and deeper understanding. Thus, as an example, the assumption that the loads are constant and that the electric power output from the generators are constant are relevant approximations for many studies of a power system, and the power system is under these assumptions described by a solution to the power flow equations. In the following we will refer to this state as the steady state of the power system.<sup>1</sup>

---

<sup>1</sup>In order to emphasise that this state is an approximation or idealisation, it is sometimes referred to as *quasi* steady state. More generally, a quasi steady state is a state that strictly is a dynamic state, but could with sufficient accuracy be described by algebraic

## 8.1 Dynamics in Power Systems

There are a lot of different dynamical phenomena with different characteristics in a power system. The phenomena could be local, in which case they only involve a minor part of the system or a single component. But they can also involve interactions between different parts of the system that might be geographically far from each other. In many cases these system-wide interactions are initiated by a local disturbance causing e.g. an earth fault with subsequent change in network topology. In this compendium interactions and phenomena that involve many power system components, e.g. generators and loads, or parts of the system are dealt with. These interactions have in common that they can cause system instabilities that can lead to black outs in large parts of the system, i.e. to interruptions of power supply for many consumers.

Dynamics can also be initiated by actions of different controllers or by switchings of lines or other components by system operators. Such “disturbances” should be regarded as normal and should consequently not endanger the stability of the system.

### 8.1.1 Classification of Dynamics

Dynamic phenomena in power systems are usually classified as

1. Electro-magnetic transients (100 Hz – MHz)
2. Electro-mechanical swings (rotor swings in synchronous machines) (0.1 – 3 Hz)
3. Non-electric dynamics, e.g. mechanical phenomena and thermodynamics (up to tens of Hz)

Approximate values of typical frequencies are given in brackets.

One single initial event in the power system can give rise to dynamics in all the three groups above. A lightning stroke in a power line can induce so high over-voltages that the insulation fails, causing an earth fault. The earth fault can cause rotor swings in synchronous machines with high amplitudes. This can trigger protections to disconnect generators, so that an unbalance between produced and consumed power in the system arises. The frequency in the system drops and generators participating in the frequency control compensate this by increasing their power outputs. Thus the initial lightning stroke has initiated dynamics in all the three groups above.

Another way to classify dynamic phenomena is given in Figure 8.1. This classification is based on the time scale of the phenomenon and the (mathematical) models used in analysis.

---

equations. One such example is fault current calculations, which often is done by using algebraic models even if it is a true dynamic phenomenon, see Figure 8.1.

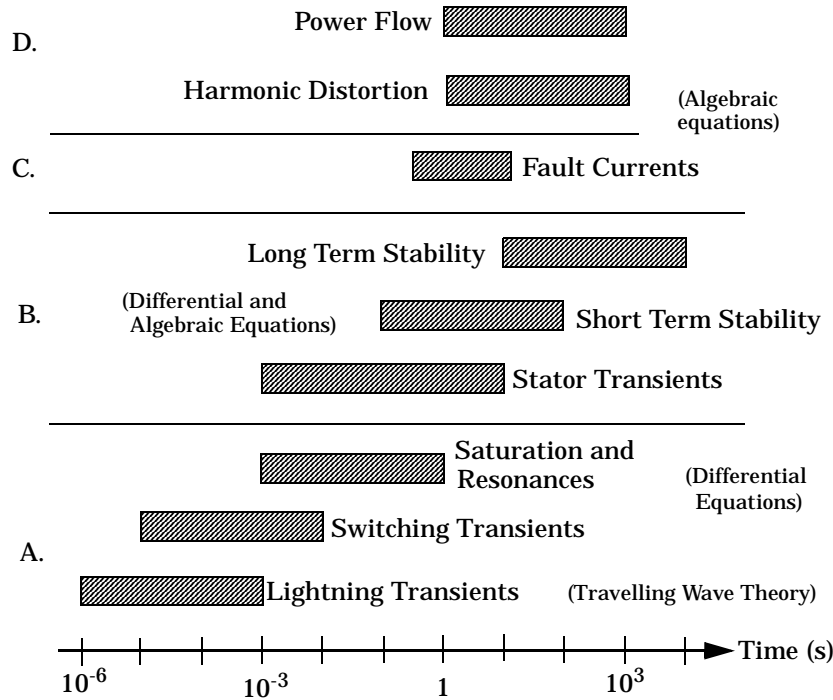


**Figure 8.1.** Dynamic phenomena in a power system. In the figure approximate time scales are given and types of mathematical models used. The different groups are called: A. Electro-magnetic transients. B. Synchronous machine dynamics. C. Quasi steady state phenomena D. Steady state phenomena.

### 8.1.2 Modelling

It is of course almost impossible to develop models that can describe all dynamics in a power system and still being of practical use. Often one has to utilise a model that captures correctly the specific dynamic phenomenon or interaction that is the aim of the particular investigation. Depending on the purpose of the study the appropriate model of a given power system component could vary significantly. It is obvious that if the aim is to study relatively slow power oscillations between generators in the system, completely different models are required as compared with if one wants to analyse the influence of lightning impulses in the windings of the synchronous machine.

Even if it were theoretically possible to develop a complete model of all the dynamics in the power system, it is questionable if such a model would be particularly useful. Firstly, such a model would require an enormous amount of parameter data to be uniquely specified. Secondly, the results obtained from such a model would be very hard to analyse and interpret. Critical review and understanding of obtained results is a necessary prerequisite

for sound engineering. When making simulations and computations, which all are done with the help of computers nowadays in system sciences, it is important to have an expectation of what are reasonable outputs. Thus trivial errors due to wrong input data files, mistakes in modelling, etc. can be eliminated to a large extent. The human factor is of utmost importance in computer-based analysis and simulation.

Models can in principle be erroneous in two different ways. Firstly, it can have the wrong structure. It can be too simple overlooking important interactions and processes or modelling them incorrectly. This is of course very serious and might give rise to detrimental consequences. But it is also very serious if wrong parameter data is used in a model of the correct structure. This latter shortcoming occurs not seldom in technical systems, which might look surprising at first sight. Since technical systems are man made, one should in principle have access to all design parameters defining the system. But it turns out that many parameters, e.g. the gain in the controller, could easily be changed after the system has been commissioned and such changes are not always reported to system analysts. It is obvious that the consequences could be very serious. In technical systems there are of course parameters that are “genuinely” unknown, e.g. the ground resistivity under a power line. In a large system like a power system, thousands of parameters are needed to define the system completely. It is a very difficult, but also very important, task to maintain and keep the data bases where all these parameter values are stored and updated. This is now a special activity usually referred to as data engineering.

In this compendium models needed for the problems to be analysed are developed. Due to space limitations more detailed and elaborate derivation cannot be presented, but the reader is advised to consult other sources, e.g. books in electrical machines or the books listed at the end of this chapter.

## **8.2 Power System Stability**

### **8.2.1 Definition of Stability**

A dynamic phenomenon in a power system is, as said above, initiated by a disturbance in the system. Such a disturbance could as an example be that a line impedance is changed due to an external cause. The behaviour of the system after this disturbance depends of course on a how “large” this disturbance is. A small disturbance results usually in small transients in the system that are quickly damped out, while a larger disturbance will excite larger oscillations. We all have an intuitive feeling for what is meant with stability in this context. Stability is associated with that the system oscillations decay and that the operation of the power systems can continue without any major impacts for any of the consumers. But, and this is very important, as the power system is a nonlinear system (this will be

elaborated on later) system stability depends on the kind and magnitude of the disturbance.<sup>2</sup> This distinguishes nonlinear systems from linear systems that can be classified as stable or unstable independent of the disturbance, i.e. stability is a property of the linear system as such. As will be shown later, stability of a power system is strongly coupled to both the magnitude and character of the disturbance as well as to the initial operating point.

Over the years many different definitions of power system stability have been proposed. The most recent one, which will be adopted in these lecture notes, was the result of a joint IEEE/CIGRE working group activity. In the report in reference 7 of section 8.3, the following definition is given:

**Definition 8.1.** *Power system stability is the ability of an electric power system, for a given initial operating condition, to regain a state of operating equilibrium after being subjected to a physical disturbance, with most system variables bounded so that practically the entire system remains intact.*

The following two comments elaborate on some important aspects of this definition.

**Comment 8.1.** *It is not necessary that the system regains the same steady state operating equilibrium as prior to the disturbance. This would be the case when e.g. the disturbance has caused any power system component (line, generator, etc.) to trip. Voltages and power flows will not be the same after the disturbance in such a case. Most disturbances that are considered in stability analyses incur a change in system topology or structure.*

**Comment 8.2.** *It is important that the final steady state operating equilibrium after the fault is steady state acceptable. Otherwise protections or control actions could introduce new disturbances that might influence the stability of the system. Acceptable operating conditions must be clearly defined for the power system under study.*

As mentioned above there are also other definitions of power system stability in the literature. They are not all identical, but could differ in some details, but most of them are in line with the definition proposed above. Power system dynamics can be modelled by systems of differential and algebraic equations, and the mathematics of those are studied in the theory of dynamic systems. It is therefore desirable that the stability definitions introduced in a more mathematically stringent way are compatible with the more practically oriented definition above. In the report where the above definition is proposed and motivated, these aspects are further discussed.

---

<sup>2</sup>To give an example of what is meant with magnitude in this context one could consider a three phase to earth fault on a power line that is cleared by disconnecting the line. The magnitude of this disturbance increases with the fault clearing time. If the fault clearing time is sufficiently small, the system will remain stable, while a longer fault clearing might cause system instability. Similarly, a high impedance fault gives a smaller disturbance than a solid fault.

### 8.2.2 Classification of Power System Stability

To achieve a better overview and structure of stability analyses of power systems, it is of great help to classify possible power system stability. The classification to be introduced here is based on the physical mechanism being the main driving force in the development of the associated instability. It could be either the active or the reactive power that is the important quantity.

A common characteristic of the instabilities to be discussed here is that they have their origin in too large an imbalance of active or reactive power in the system, locally or globally. This imbalance can then develop in different ways and cause unstable behaviour depending on system characteristics. Exactly what is meant with imbalance will be elaborated in the following.

#### Rotor Angular or Synchronous Stability

The total active electrical power fed into the power system by the generators is always equal to the active power consumed by the loads including the losses in the system. On the other hand, there is not always a similar balance between the loads and the power fed into the generators by the prime movers, e.g. the hydro and steam turbines. If such an imbalance develops, the rotating parts of the generators and other rotating machines will act as energy buffer, and the kinetic energy stored in these will decrease or increase as a result of the imbalance. *Rotor angle stability* refers to the ability of synchronous machines of a power system to remain in synchronism after a disturbance.

If the disturbance is local and substantial, e.g. an earth fault close to a generator, the generator can fall out of step since it has been accelerated during the fault. As quite big currents will flow in the generator windings in such a case, it must be disconnected to avoid that it is damaged. Typical time scale for such an instability to develop is a second to a couple of seconds. This kind of instability is called *transient instability* and instability appears usually in form of aperiodic angular separation due to lack of synchronizing torque. This form of instability is also referred to as *large-disturbance rotor angle instability*.

*Small-disturbance (or small-signal) rotor angle stability* is concerned with the ability of the power system to maintain synchronism under small disturbances. These disturbances are considered to be sufficiently small that linearization of the system equations is permissible for purposes of analysis. Usually small-disturbance rotor angle stability is associated with insufficient damping of oscillations.

### Frequency Stability

A third variety of active power imbalance, which is different from the ones above, is when the imbalance is not local but global. In the preceding cases, the sum of active power infeed was enough but there was an imbalance locally. But if the total power fed into the system by the prime movers is less than what is consumed by the loads, including losses, this imbalance will influence the frequency of the whole system. As explained above the kinetic energy stored in rotating parts of the synchronous machines, and other rotating electrical machines, will compensate for the imbalance resulting in a frequency deviation. If the imbalance is not too large the generators participating in the frequency control will regulate the active power input from their prime movers, and bring back the frequency deviation to acceptable values. If the imbalance is too large, the frequency deviation will be significant with possible serious consequences. Particularly thermal power plants are sensitive to large frequency drops of long durations, since detrimental oscillations could be excited in the turbines. As a last resort the generators are disconnected, making the situation even more serious. This type of instability is called *frequency instability* and the time scale could be from a few seconds up to several minutes. Since the involved mechanisms could be quite different, one often distinguishes between *short-term* and *long-term* frequency instability. In the latter, the control and protection characteristics of turbines, boilers, and reactors play important roles.

### Voltage Stability

When it comes to reactive power balance the situation is not as clear and simple as concerning active power. There is always a balance between “produced” and “consumed” reactive power in every node of a network. This is in fact a direct consequence of Kirchoff’s first current law. When one talks about imbalance in this context we mean that the injected reactive power is such, normally too small, that the voltage in the node cannot be kept to acceptable values. (At low load the injected reactive power could be high resulting in a too high voltage, possibly higher than the equipment might be designed for. This is of course not desirable but it could usually be controlled in such a way that no instabilities develop.) When we talk about imbalance in this case we thus mean that the injected reactive power differs from the desired injected reactive power, needed to keep the desired voltage. If this imbalance gets too high, the voltages exceed the acceptable range.

Reactive power is a more local quantity than active power since it cannot be transported as easily in power system where normally  $X \gg R$ . This explains why voltage problems often are local, and often only occur in part of the system. When the imbalances (voltage problems) develop into insta-

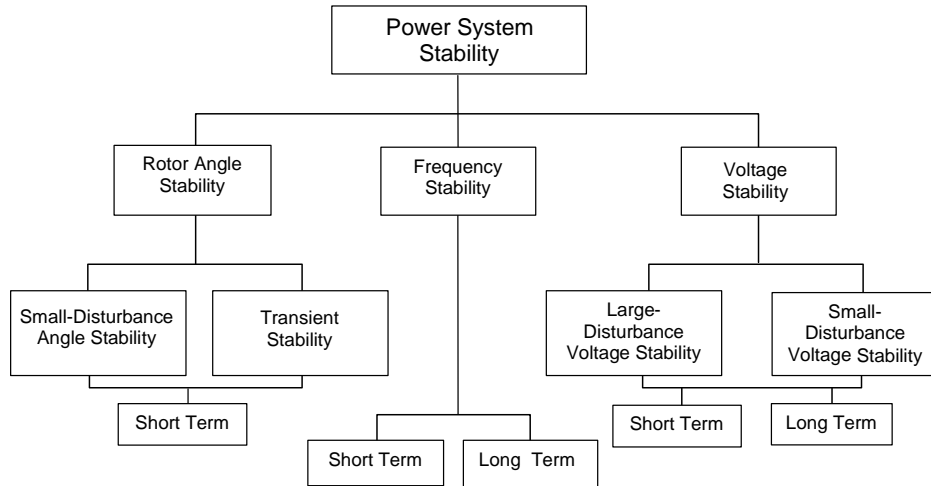


**Figure 8.2.** Classification of power system stability.

bilities these are called *voltage instabilities* or *voltage collapses*. In the latter case the instability develops into very low voltages in the system. In principle too high voltages can also occur at a voltage instability. Low voltages arise at high load conditions, while high voltages are associated with low load conditions. Depending on the time scale the voltage instabilities are classified as *short-term*, a couple of seconds, or *long-term*, tens of seconds to minutes. The short-term voltage instability involves dynamics of fast acting components such as induction motors, electronically controlled loads, and HVDC converters, while the long-term voltage instability involves slower acting equipment such as tap-changing transformers, thermostatically controlled loads, and generator current limiters. As for rotor angle stability one distinguishes between *large-disturbance* and *small-disturbance* voltage stability.

The classification of power system instabilities is summarised as in Figure 8.2.

### Connection between Instabilities and System Components

As explained above the generators, i.e. the synchronous machines, are very important in angular instabilities, and it is sometimes said that these are the driving force in this instability. A more detailed analysis shows that the loads are very often the driving force when it comes to voltage instability, which consequently sometimes is called *load instability*.

### Instabilities in Real Systems

The classification above is based on simplified and ideal conditions in the system. In a real system these assumptions might not be valid. In real systems it is not seldom a combination of active and reactive power imbalances that trigger an instability. However, in many cases it is possible to identify which is the dominating processes in the beginning of the instability. During the course of the dynamics new consequential imbalances might occur, resulting in a combined angular and voltage instability in the final phase. There are examples of black outs in power systems that have started as slow voltage instabilities, which through low voltages have reduced the power transfer capability resulting in rotor angular instabilities causing the final collapse of the system. On the other hand, rotor angular instabilities can cause generators to trip, which most systems are designed to cope with, but it can effect the reactive power balance in such a way that voltage instabilities can develop.

The purpose of a classification is to define a structure for a complicated problem and thereby better understanding it. Furthermore it often helps to identify important and critical quantities, processes and components in the system. Classifications of this kind should not be driven too far. Most important is always that useful and adequate results are obtained from realistic models of the power system.

## 8.3 Literature on Power System Dynamics and Stability

These lecture notes should be seen as an introduction to power system dynamics and stability. For those who want to get deeper knowledge in the subject there are a number of books that can be recommended. They have all their strong and weaker sides, and one has often to consult several books to get a complete view of a problem. Below are only references listed that are fairly modern and focus on power system dynamics and stability.

1. *Power System Stability and Control* by Prabha Kundur. (McGraw-Hill Inc., 1994, ISBN 0-07-035958-X, 1176 pages)

This is the most complete modern book on the subject and is already a classic textbook. It covers most subtopics and its approach is rather practical, but it contains a fair amount of theory also. The book contains a lot of references to other books and published papers.

2. *Power System Dynamics and Stability* by Jan Machowski, Janusz W. Bialek and James R. Bumby. (John Wiley & Sons Ltd, 1997, ISBN 0-471-97174-X, 461 pages)

This book does not contain as many applications as the previous one.

On the other hand, it contains rather detailed motivations and derivations of many of the basic assumptions in power system analysis. A large part of the book is devoted to control and supervision of power systems.

3. *Power Systems Dynamics. Stability and Control* by K. R. Padiyar. (John Wiley & Sons Ltd, 1996, ISBN 0-471-19002-0, 629 pages)  
The book gives a good overview with many solved problems. The focus is on angular stability, while voltage stability is on briefly dealt with.
4. *Power System Dynamics and Stability* by Peter W. Sauer and M. A. Pai. (Prentice Hall, 1998, ISBN 0-13-678830-0, 357 pages) The mathematical level in this book is higher than the previous ones and to fully appreciate it knowledge in the theory of nonlinear systems is needed. Only angular stability is included.
5. *Power System Voltage Stability* by Carson W. Taylor. (McGraw-Hill Inc., 1994, ISBN 0-07-063184-0, 273 pages) This book deals only with voltage stability. The approach is rather practical. Many examples from voltage instabilities in real systems are reviewed and analysed.
6. *Voltage Stability of Electric Power Systems* by Thierry Van Cutsem and Costas Vournas. (Kluwer Academic Publishers, 1998, ISBN 0-7923-8139-4, 378 pages) Voltage stability is the subject of this book also. However the approach is more mathematical than in the previous one, and to fully appreciate it, knowledge about nonlinear systems is required.
7. *Definition and Classification of Power System Stability* IEEE/CIGRE Joint Task Force on Stability Terms and Definitions, 2002.

# 9

## Synchronous Machine Models

*This chapter starts with a short discussion that motivates why synchronous machines are important when electro-mechanical oscillations are studied. A brief overview of the operating principles and design of the synchronous machine is given. This forms the basis of simplified models that are derived – first for stationary, then for dynamic operation. Even if the dynamic model is very simple and neglects a number of features, it captures the most important properties to model electro-mechanical oscillations in power systems.*

**S**YNCHRONOUS MACHINES, i.e. practically all generators together with synchronous motors and synchronous compensators, are the most important power system components in the analysis of electro-mechanical oscillations in power systems. The oscillations are manifested in that the rotors of the synchronous machines do not rotate with constant angular velocity corresponding to system frequency, but superimposed are low frequency oscillations, typically 0.1 – 4 Hz. It is important that these superimposed oscillations are not too large, because then the stability of the power system can be endangered. A correct description of these oscillations often requires detailed models of many different system components, but to get an understanding of and insight into the basic physical phenomena and processes that determine the stability it is often sufficient to employ the simple model that will be derived and motivated in this chapter. This simplified model of the synchronous machine together with a simple model of the power transmission system provide a description that will be used in chapter 11.

As the name electro-mechanical oscillations suggests, both electrical and mechanical phenomena are involved, i.e. both currents in and voltages across different windings in the machines but also the mechanical motion of the rotor. Therefore, models of both electrical and mechanical parts of the synchronous machine are needed.

### 9.1 Design and Operating Principle

In the synchronous machine a magnetized rotor creates a rotating magnetic field in the air gap. If the rotor field is ideally sinusoidal and if the rotor rotates at constant speed, this will induce ideally sinusoidal voltages in the

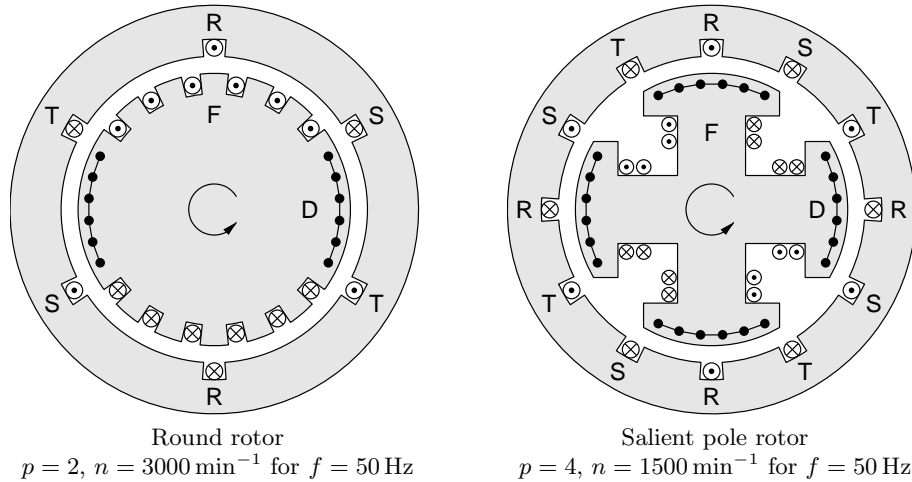


**Figure 9.1.** Cross-sections through different rotor types.

stator windings.

If the machine terminals are connected, the currents flowing in the stator windings create a second rotating magnetic field which causes a torque on the rotor. In a synchronous motor, this torque drives a mechanical load; in a synchronous generator, the magnetic torque opposes the mechanical driving torque of the prime mover (e.g. a turbine). Under balanced, steady-state conditions the magnetic torque is equal to the mechanical torque, and so the rotor continues to rotate at constant speed.

### 9.1.1 Rotor Types

The magnetic rotor field is generated by a *field winding*  $F$  on the rotor which is fed with an adjustable direct current. In addition, the rotor has a short-circuited *damper winding*  $D$  at the surface. This winding serves to dampen electrical and mechanical oscillations and to shield the field winding from inverse rotating fields in case of asymmetries or harmonics in the stator currents. (In rotors without an explicitly realized damper winding, eddy currents in the rotor iron can have a similar effect.)

Depending on the application of the generator, two different types of rotors are used that are shown in Figure 9.1.

**Round Rotor** Round rotors are used with high-speed turbines such as steam or gas turbines. For this reason, generators with round rotors are also called *turbo generators*. They can have ratings as high as 1800 MVA per unit. Due to the large centrifugal forces, the rotor consists of a long, narrow, solid steel cylinder.

The field windings are mounted in slots that are mill-cut into about 2/3 of the perimeter. Because of the discrete distribution of the windings on the

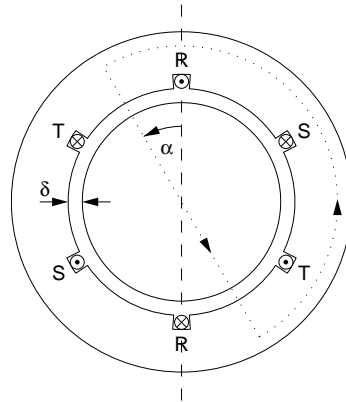


**Figure 9.2.** Simplified arrangement of a stator with a solid, unwound rotor.

rotor surface, the magnetic flux density in the air gap always has a stair-step form. Through proper distribution of the windings these stair-steps can be made *approximately sinusoidal!*

**Salient Pole Rotor** Salient pole rotors are used with low-speed hydro turbines with rated powers of up to 800 MVA per unit. In order to obtain the appropriate electrical power frequency in spite of the low rotor speed, salient pole rotors typically have multiple pole pairs. For run-of-river power stations the number of poles can be as high as  $p = 200!$  Such rotors have very large diameters (several meters) and short lengths.

The field windings are mounted on the individual poles. By properly designing the geometric form of the poles, the magnetic flux density in the air gap at the stator surface can also be made *approximately sinusoidal!*

### 9.1.2 Stator Field

The magnetic stator field is generated by an alternating three-phase current flowing in the stator windings. The variation of this field in space and time can best be studied using the simplified arrangement shown in Figure 9.2. In this arrangement, the stator has only one pole pair and the slots are assumed to be infinitely narrow. The rotor is replaced by a solid, unwound cylinder. The stator field is derived here for a stator with one single pole pair. The transfer to the case of a stator with  $p$  poles is left as an exercise to the reader.

The magnetic field strength in the iron is neglected and the induction in the air gap is assumed to be radial. Due to the  $\pi$ -symmetry of the set-up

Ampère's law gives for the dotted path shown in Figure 9.2

$$\Theta(\alpha) = \iint_{A(\alpha)} \vec{i} \, d\vec{a} = \frac{1}{\mu_0} \oint_{S(\alpha)} \vec{B} \, d\vec{s} = \frac{B(\alpha)}{\mu_0} \cdot 2 \cdot \delta \quad (9.1)$$

where  $A(\alpha)$  is the area enclosed by the path,  $\delta$  is the width of the air gap,  $B(\alpha)$  is the flux density in the air gap at the angle  $\alpha$ , and  $\Theta(\alpha)$  is the total flux linkage (or number of ampere windings) enclosed by the path.

**One single-phase winding** If only phase R is fed by an alternating current, the total enclosed flux linkage is either  $+w \cdot i_R(t)$  or  $-w \cdot i_R(t)$ , depending on whether the path encloses the upper slot ( $0 < \alpha < \pi$ ) or the lower one ( $\pi < \alpha < 2\pi$ ).  $w$  is the number of windings in one slot.

The left side of Figure 9.3 shows the flux linkage of a single-phase winding plotted against the angle  $\alpha$  for different instants of time. Since  $B(\alpha)$  is directly proportional to  $\Theta(\alpha)$  as shown in eq. (9.1), the magnetic field in the air gap is a rectangular, *standing wave* with a *variable amplitude*.

**Three-phase windings** If the three phases R, S and T are fed by an alternating three-phase current, the integration path in Figure 9.2 always encloses three slots that carry windings with different momentary currents. The resulting total flux as a function of the angle  $\alpha$  is thus a superposition of three rectangular curves that are shifted by  $2/3 \cdot \pi$  and have different amplitudes.

This is shown on the right side of Figure 9.3. It is evident that the fundamental component of the total flux is a *traveling wave* with a *constant amplitude* which moves with the angular velocity  $\omega$ . This angular velocity of the stator field is the same as the angular frequency of the alternating currents. In a real stator, the windings are of course not concentrated in infinitely narrow slots. Instead, they are distributed among several slots of finite extent – possibly with a different number of windings in different slots. Through proper design the magnetic field in the air gap can be made approximately sinusoidal.

It should be noted that this simplified treatment of the stator field is only applicable for generators with round rotors where the air gap has a constant width. In the case of a salient pole rotor, the width of the air gap is variable, and therefore the magnetic stator field depends not only on the momentary winding currents but also on the momentary rotational angle of the rotor. In some cases, the differences between round rotor and salient pole rotor can be neglected (as will be done frequently in the remainder of this chapter). However, it should be kept in mind that this is a simplification which needs to be justified from case to case.

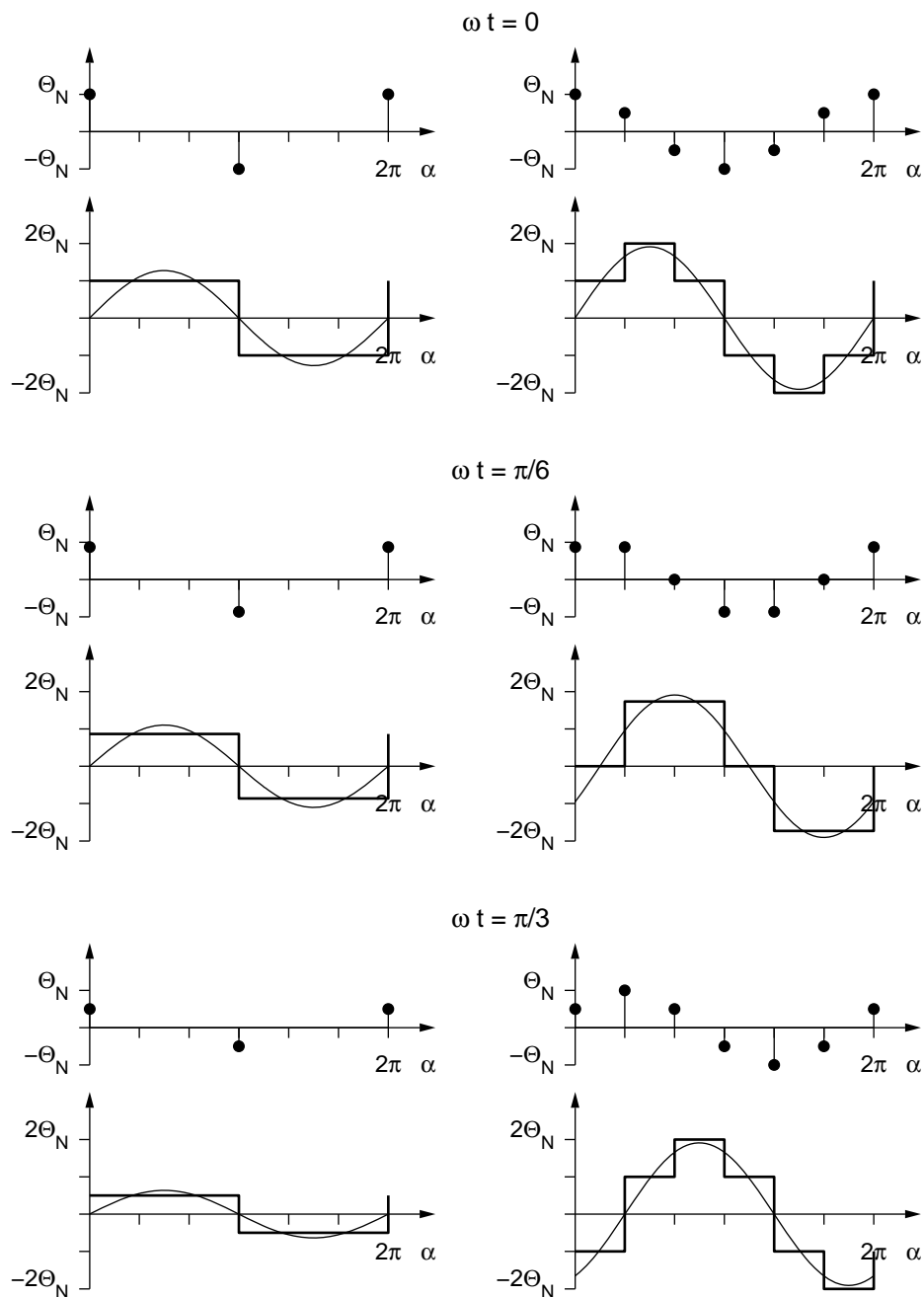


**Figure 9.3.** Magnetic field in the air gap of a stator with a solid, unwound rotor at different instants of time. Left: one single-phase stator winding; right: three-phase stator windings. The top plots show the ampere windings in the individual slots; the bottom plots show the total linkage.

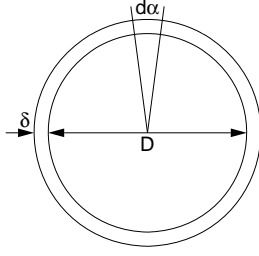


**Figure 9.4.** Geometric quantities used to calculate the magnetic energy stored in the air gap. The width of the air gap is assumed to be much smaller than the rotor diameter:  $\delta \ll D$ . Rotor and stator have the length  $l$ .

### 9.1.3 Magnetic Torque

The magnetic fields generated by the stator and rotor currents are superposed to a total field

$$B = B_s + B_r \quad (9.2)$$

with

$$\begin{aligned} B_s &= \hat{B}_s \sin\left(\frac{p}{2}(\alpha + \omega t)\right) \\ B_r &= \hat{B}_r \sin\left(\frac{p}{2}(\alpha + \omega t + \theta)\right) \end{aligned} \quad (9.3)$$

Both fields are assumed to be ideally sinusoidal and to rotate with the same angular velocity  $\omega$ ; the rotor field (together with the rotor itself) leads the stator field by the angle  $\theta$ .  $p$  is the number of poles.

Using the geometry shown in Figure 9.4, the energy stored in the magnetic field of the air gap is given by

$$W_m = \int_V \frac{B^2(\alpha, t, \theta)}{2\mu_0} dV = \frac{1}{2\mu_0} \int_0^{2\pi} B^2(\alpha, t, \theta) \cdot l\delta \frac{D}{2} d\alpha \quad (9.4)$$

The torque on the rotor is obtained by calculating the derivative of the energy with respect to the displacement angle  $\theta$  between the rotor and the stator field

$$M = \frac{\partial W_m}{\partial \theta} = \frac{l\delta D}{4\mu_0} \int_0^{2\pi} \frac{\partial B^2(\alpha, t, \theta)}{\partial \theta} d\alpha \quad (9.5)$$

Using several trigonometric identities together with the fact that only  $B_r$  depends on  $\theta$ , this can be simplified to

$$M = M_{\max} \cdot \sin\left(-\frac{p}{2}\theta\right) \quad (9.6)$$

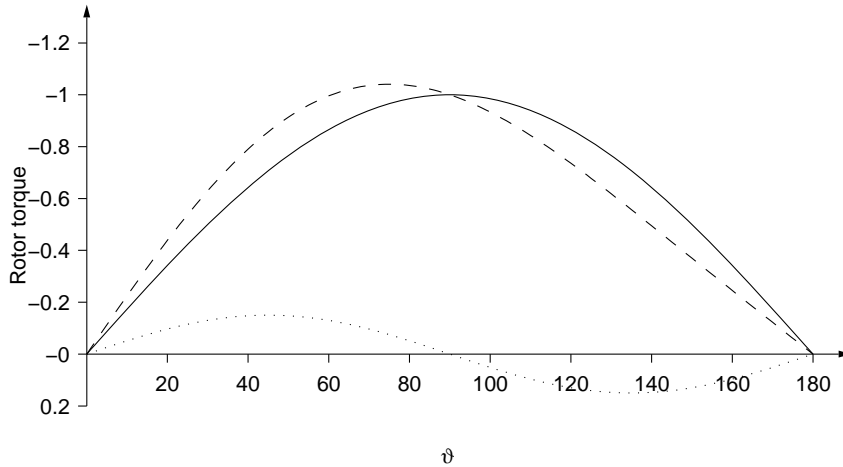


**Figure 9.5.** Rotor torques in function of the rotor angle  $\theta$ . Solid line: round rotor torque; dotted line: reluctance torque; dashed line: salient pole rotor torque.

where

$$M_{\max} = \frac{l\delta D\pi}{4\mu_0} \hat{B}_s \hat{B}_r \quad (9.7)$$

is the maximum torque that the machine can exert on the rotor. If the mechanical torque from the turbine exceeds this limit, the generator will fall out of step. If no protective measures are taken to reduce the turbine power, the rotor will accelerate until the centrifugal forces eventually destroy the generator! This is particularly dangerous in the case of turbo generators, that have a high speed to begin with.

As noted before, the stator field can only be regarded as sinusoidal for a turbo generator. In the salient pole generator, the inhomogeneous air gap gives rise to a *reluctance torque*  $M_r \sim \sin(p\theta)$  which is added to the torque given in eq. (9.6). This is shown in Figure 9.5 for  $p = 2$ .

## 9.2 Stationary Operation

### 9.2.1 Stationary Single Phase Equivalent Circuit

If the rotor rotates at constant speed the rotor field will induce sinusoidal voltages in the stator windings that are shifted by  $120^\circ$  with respect to each other. The frequency of the voltages is equal to the rotor frequency (multiplied by the number of pole pairs). The magnitude of the voltages depends on both the rotor speed and the magnitude of the rotor field; it can therefore be controlled via the rotor field current. Due to the symmetry of the voltages, the generator can be represented by the single phase equivalent circuit shown in Figure 9.6. In this circuit the induced voltages are modeled

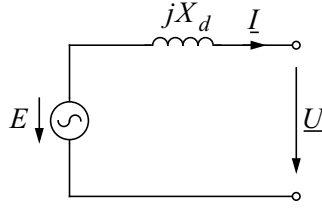


**Figure 9.6.** Stationary single phase equivalent circuit.

by the voltage source  $\underline{E}$ ;  $\underline{I}$  is the stator current, and  $\underline{U}$  is the terminal voltage of the generator.

With the losses neglected, the total impedance of the generator as seen from the stator can be modeled with a single lumped inductance  $X_d$ . This is strictly only valid for the turbo generator with its homogeneous air gap. In the salient pole generator, the same effects that give rise to the reluctance torque mentioned earlier also cause the active part of the stator current (with respect to the induced voltage  $\underline{E}$ ), to “see” a smaller reactance  $X_q$  than the reactive part, for which the reactance  $X_d$  is effective. This is illustrated in Figure 9.7. Typical values for  $X_d$  and  $X_q$  are listed in Table 9.1. For our purposes in this lecture we will neglect these differences (but keep in mind that they exist).

If the terminal voltage  $\underline{U}$  is assumed to lie on the real axis, the phasor equation is

$$\underline{E} = \underline{U} + jX_d\underline{I} \quad (9.8)$$

or – in polar form –

$$E \cdot (\cos \theta + j \sin \theta) = U + X_d I \cdot (j \cos \varphi + \sin \varphi) \quad (9.9)$$

where  $\theta$  is the angle between  $\underline{E}$  and the real axis counted *counter-clockwise*, and  $\varphi$  the angle between  $\underline{I}$  and the real axis counted *clockwise*. Looking only at the imaginary part gives

$$\frac{E}{X_d} \cdot \sin \theta = I \cdot \cos \varphi \quad (9.10)$$

The active power of the machine (which is directly proportional to the mechanical torque) is given by

$$P = UI \cos \varphi \quad (9.11)$$

Using eq. (9.10) this can be written as

$$P = \frac{UE}{X_d} \sin \theta \quad (9.12)$$

A comparison with eq. (9.6) reveals that – for a machine with a single pole pair – the *mechanical* angle between the magnetic fields of rotor and stator is identical to the *electrical* angle between the phasors of the induced voltage  $\underline{E}$  and the terminal voltage  $\underline{U}$ .

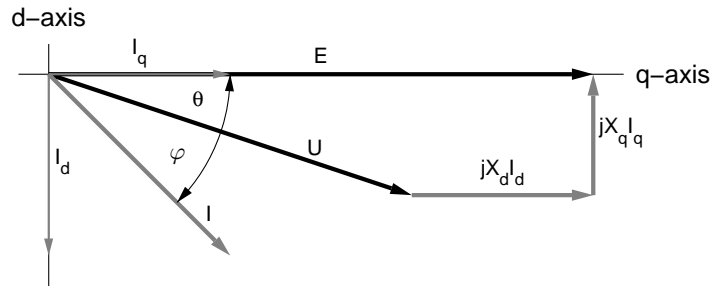


Figure 9.7. Phasor diagram of voltages and currents of the salient pole machine.

	Round Rotor	Salient Pole Rotor
$X_d$ (p.u.)	1.0 – 2.3	0.6 – 1.5
$X_q$ (p.u.)	1.0 – 2.3	0.4 – 1.0

Table 9.1. Typical values of reactances for synchronous machines.

### 9.2.2 Phasor diagram

Figure 9.8 illustrates the relation between the three phasors for different modes of operation. They can be categorized as described below. It is assumed that the terminal voltage phasor,  $\underline{U}$ , is the reference phasor, i.e. parallel with the real axis. The angle between the induced voltage phasor and the terminal voltage phasor is  $\theta$ , and the angle between the terminal voltage phasor and the stator current phasor is  $\varphi$ . It should be noted that the statements concerning leading and lagging currents are based on the current reference definition of Figure 9.7.

**Generator operation (right column):**  $|\varphi| < 90^\circ$ ,  $\theta > 0$

The machine delivers active power. The stator current phasor lies in the right half-plane; the induced voltage phasor leads the terminal voltage phasor.

**Motor operation (left column):**  $|\varphi| > 90^\circ$ ,  $\theta < 0$

The machine consumes active power. The stator current phasor lies in the left half-plane; the induced voltage phasor lags the terminal voltage phasor.

**Overexcitation (top row):**  $|\underline{E}| \cdot \cos \theta > |\underline{U}|$

The machine delivers reactive power (i.e. it acts like a capacitor). The stator current phasor lags the terminal voltage phasor; the real part of the induced voltage phasor is larger than the terminal voltage.

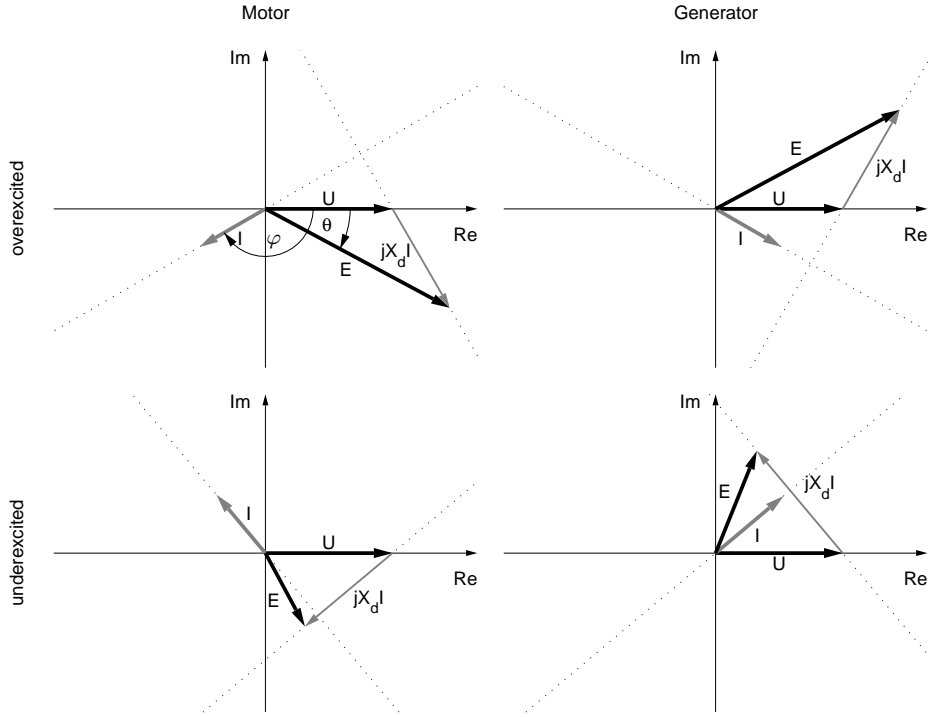


**Figure 9.8.** Phasor diagrams for different modes of operation of a synchronous machine.

**Underexcitation (bottom row):**  $|\underline{E}| \cdot \cos \theta < |\underline{U}|$

The machine consumes reactive power (i.e. it acts like an inductor).

The stator current phasor leads the terminal voltage phasor; the real part of the induced voltage phasor is smaller than the terminal voltage.

As a special case consider a synchronous machine where the rotor is running idle. In steady state the mechanical torque is zero and therefore the machine neither consumes nor delivers active power ( $\theta = 0$ ). Nevertheless, depending on the excitation it can either consume (underexcitation) or deliver (overexcitation) reactive power, i.e.  $\varphi = \pm 90^\circ$ . Such a set-up is called *synchronous compensator* and is used for variable reactive power compensation.

### 9.2.3 Operational Limits

Solving eq. (9.8) for  $\underline{I}$  gives

$$\underline{I} = -\frac{U}{jX_d} + \frac{\underline{E}}{jX_d} \quad (9.13)$$

If the terminal voltage  $U$  is considered constant, the stator current is determined by two parameters. According to eq. (9.11), the real part of

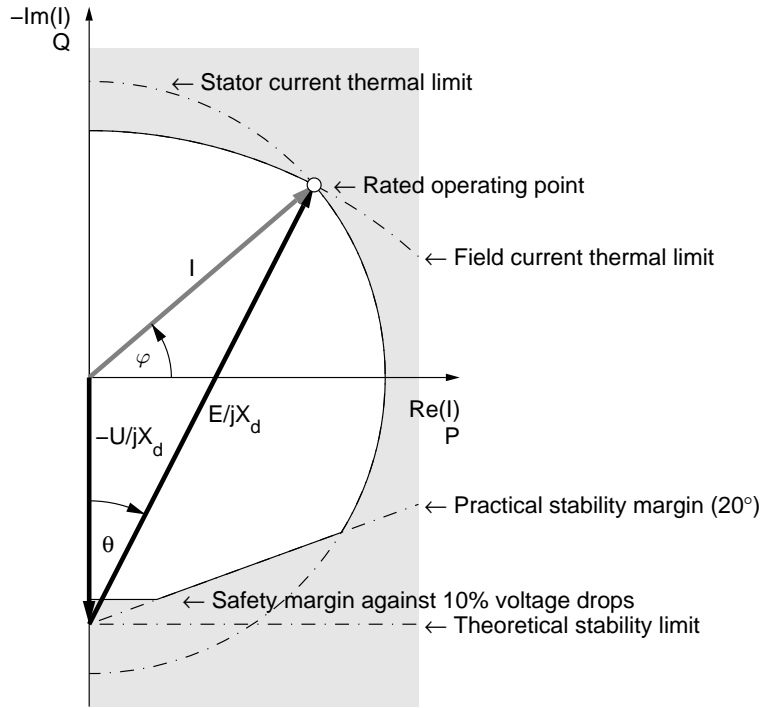


**Figure 9.9.** Operational limits of the synchronous generator.

the stator current is given by the turbine power. The imaginary part can then be controlled by adjusting the magnitude of the induced voltage via the rotor field current.

Eq. (9.13) is illustrated in Figure 9.9 in the P-Q plane. The limits of the operating area can be constructed as follows.

**Stator current thermal limit:**  $|\underline{I}| < I_{\max}$

The stator current limit is a circle around the origin with radius  $I_{\max}$ .

**Field current thermal limit:**  $|\underline{E}| = f(I_f) \Rightarrow \frac{|\underline{E}|}{X_d} < \frac{f(I_{f,\max})}{X_d}$

The field current limit is a circle around  $-\frac{U}{jX_d}$ .

**Rotor angle stability limit:**

The *theoretical* rotor angle stability limit is determined by  $\theta < 90^\circ$ . It is a parallel of the real axis that passes through  $-\frac{U}{jX_d}$ . In *practice*, a safety margin of  $20^\circ$  is kept to this limit.

**Safety margin against voltage drops:**

If the generator delivers little or no active power and operates close to the stability limit (underexcitation), even small voltage drops at the machine terminals could cause the rotor angle to exceed  $90^\circ$ . To allow

for 10 % voltage drops, the operating point must stay above a parallel of the real axis passing through  $-0.9 \cdot \frac{U}{jX_d}$ .

Depending on the design of the generator, there may be other limiting factors (e.g. for turbo generators the *stator end region heating limit* mentioned in section 2.5).

## 9.3 Dynamic Operation

### 9.3.1 Transient Single Phase Equivalent Circuit

During network transients, the reactance of the synchronous generator is not constant. For symmetrical transients, as discussed in section 7.2 on short circuits of synchronous machines, the machine reactance itself undergoes transient changes as the machine passes through the sub-transient, transient, and steady-state stages. In the fault analysis in chapter 7, only the first few cycles after a fault were of interest. The generator was therefore modeled with the sub-transient reactance  $X_d''$ .

Compared to the time scale of short-circuit overcurrents, electro-mechanical oscillations are much slower (0.1 – 4 Hz as mentioned in the introduction to this chapter). For the study of these phenomena, the sub-transient phase is therefore neglected and the generator is modeled with the transient reactance  $X_d'$ . Similarly, during transients, the magnitude of the induced voltage drops to the value  $E'$  which can be calculated as follows

$$E' = \frac{X_d'}{X_d} \cdot E^0 + \frac{X_d - X_d'}{X_d} \cdot U^0 \cdot \cos \theta^0 \quad (9.14)$$

or

$$E' = E^0 - (X_d - X_d') \cdot I^0 \cdot \sin \varphi^0 \quad (9.15)$$

where the superscript <sup>0</sup> denotes the steady-state quantities prior to the transient.

Thus, the phasor equation valid during network transients is

$$\underline{E}' = U + jX_d' \underline{I} \quad (9.16)$$

### 9.3.2 Simplified Mechanical Model

As stated above the rotor of a synchronous machine rotates with synchronous speed in steady state. If the electrical frequency of the system is  $\omega_e$ , the mechanical angular velocity  $\omega_m$  of the rotor is given by

$$\omega_m = \frac{\omega_e}{p/2} \quad (9.17)$$

where  $p$  is the number of poles of the machine.

Type of Synchronous Machine	Inertia Constant $H$ (s)
Thermal Power	
• Steam Turbine	4 – 9
• Gas Turbine	7 – 10
Hydro Power	
• Slow ( $< 200 \text{ min}^{-1}$ )	2 – 3
• Fast ( $\geq 200 \text{ min}^{-1}$ )	2 – 4
Synchronous Compensators	1 – 1.5
Synchronous Motors	$\approx 2$

**Table 9.2.** Typical values of  $H$  for different types of synchronous machines.

An important parameter in the analysis of rotor oscillations is the total moment of inertia of the synchronous machine  $J$ . This is the sum of all moments of inertia of all rotating parts of the synchronous machine, i.e. the sum of the moments of inertia of the rotor, turbines, shafts and other devices on the shaft system, e.g. generator feeding the field winding. As for electrical quantities it is practical to express  $J$  in a suitable p.u. base and therefore the inertia constant of the synchronous machine  $H$  is defined as

$$H = \frac{0.5J\omega_{mo}^2}{S} \quad (9.18)$$

where  $S$  is the MVA rating of the machine. In eq. (9.18) the numerator is an expression for the total kinetic energy stored in the synchronous machine in steady state and the unit for  $H$  is thus seconds. (If there is a gear box in the system, it is of course difficult to define *one* mechanical angular velocity. In such a case  $H$  is calculated as the ratio between total stored kinetic energy and the MVA rating of the machine.) The inertia constant states how much time it would take to bring the machine from synchronous speed to standstill if rated power is extracted from it while no mechanical power is fed into it. The value of the inertia constant will vary within a much smaller range than the value of  $J$  for different machines. Table 9.2 shows typical values of  $H$  for different types of synchronous machines. It can be concluded that the value is higher for thermal units as compared with hydro units. Typically 30 – 60% of the total moment of inertia comes from the turbines and shafts for thermal units, while the corresponding value for hydro units is 5 – 15%. For synchronous motors the inertia constant depends to a high degree of what kind of load that is connected.



# 10

## The Swing Equation

*This chapter contains a derivation and a discussion of the swing equation, which is the basic mathematical relation describing how the rotor of a synchronous machine will move (swing) when there is an unbalance between mechanical power fed into the machine and the electrical power extracted from it. Even if the basic physical relations are very simple, a number of simplifications must be done to make the equation useful in practice.*

THE SWING EQUATION is of fundamental importance in the study of power oscillations in power systems. Electro-mechanical oscillations is an important phenomenon that must be considered in the analysis of most power systems, particularly those containing long transmission lines, as e.g. the Swedish system. In normal steady state operation all synchronous machines in the system rotate with the same electrical angular velocity, but as a consequence of disturbances one or more generators could be accelerated or decelerated and there is risk that they can fall out of step, i.e. lose synchronism. This could have a large impact on system stability and generators losing synchronism must be disconnected otherwise they could be severely damaged. A short description of power system protections is given in Appendix B.

### 10.1 Derivation of the Swing Equation

The synchronous machine models developed in the previous chapter will form the basis for the derivation of the swing equation describing the electro-

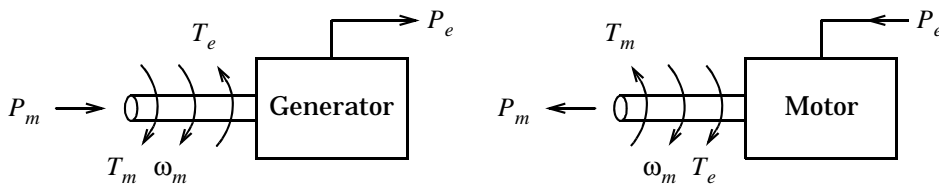


**Figure 10.1.** Schematic description of powers and torques in synchronous machines.

mechanical oscillations in a power system. Schematically the different torques and powers of a synchronous machine can be depicted as in Figure 10.1. Index  $m$  denotes in the following a mechanical quantity, and index  $e$  denotes an electrical quantity. The differential equation describing the rotor dynamics is

$$J \frac{d^2 \theta_m}{dt^2} = T_m - T_e \quad (10.1)$$

The quantities in eq. (10.1) are:

$J$ : The total moment of inertia of the synchronous machine ( $\text{kg}\cdot\text{m}^2$ )

$\theta_m$ : The mechanical angle of the rotor (rad)

$T_m$ : Mechanical torque from turbine or load ( $\text{N}\cdot\text{m}$ ). Positive  $T_m$  corresponds to mechanical power fed into the machine, i.e. normal generator operation in steady state.

$T_e$ : Electrical torque on the rotor ( $\text{N}\cdot\text{m}$ ). Positive  $T_e$  in normal generator operation.

If eq. (10.1) is multiplied with the mechanical angular velocity  $\omega_m$  one gets

$$\omega_m J \frac{d^2 \theta_m}{dt^2} = P_m - P_e \quad (10.2)$$

where

$P_m = T_m \omega_m =$  mechanical power acting on the rotor (W)

$P_e = T_e \omega_m =$  electrical power acting on the rotor (W)

If the angular acceleration should be expressed in electrical angle instead, eq. (9.17) is used to give

$$\frac{2}{p} \omega_m J \frac{d^2 \theta_e}{dt^2} = P_m - P_e \quad (10.3)$$

where the left hand side can be re-arranged:

$$2 \frac{2}{p \omega_m} \left( \frac{1}{2} \omega_m^2 J \right) \frac{d^2 \theta_e}{dt^2} = P_m - P_e \quad (10.4)$$

If eq. (10.4) is divided by the rating of the machine  $S$ , and eq. (9.17) is utilised again, the result is

$$\frac{2}{\omega_e} \frac{(\frac{1}{2} \omega_m^2 J)}{S} \frac{d^2 \theta_e}{dt^2} = \frac{P_m - P_e}{S} \quad (10.5)$$

Observations and experiences from real power systems show that during disturbances, the angular velocity of the rotor will not deviate significantly from the nominal values, i.e. from  $\omega_{m0}$  and  $\omega_{e0}$ , respectively. This implies that eq. (10.5) together with the definition eq. (9.18) can be written as

$$\frac{2H}{\omega_{e0}} \frac{d^2 \theta_e}{dt^2} = P_m^{pu} - P_e^{pu} \quad (10.6)$$

where superscript  $^{pu}$  indicates that the mechanical and electrical powers should be expressed in p.u. of the rating of the synchronous machine. It is of course possible to use another base power than the rating of the machine in eq. (10.6), but this must then be made consistently regarding the definition of  $H$  and when calculating the power values in the right hand side. If another base power than the rating is used, the physical interpretation of  $H$  made in section 9.3.2 will not be valid anymore. Furthermore the typical values of  $H$  in Table 9.2 do not apply. In the following it will be assumed, if not otherwise explicitly stated, that electrical angles and electrical angular velocities are considered, and consequently the index  $_e$  in the left hand side of eq. (10.6) can be omitted. It is also assumed that powers are expressed on the same base power as  $H$ , and the superscript  $^{pu}$  can also be omitted in eq. (10.6). We are thus going to use the following form of the swing equation:

$$\frac{2H}{\omega_0} \frac{d^2\theta}{dt^2} = P_m - P_e \quad (10.7)$$

## 10.2 Analysis of the Swing Equation

Before applying the swing equation to a specific system, it could be of value to briefly discuss the different terms of eq. (10.7) and their influence. This will give an insight into the fundamental relations governing the dynamics during rotor oscillations.

The difference between mechanical power fed into the machine and the electrical output power will cause a motion of the rotor relative to a rotation with constant angular velocity  $\omega_0$ .<sup>1</sup> Therefore it is of interest to discuss in some detail how  $P_e$  and  $P_m$  will vary during a rotor swing.

The mechanical power  $P_m$  is in most cases provided by a hydro, steam or gas turbine. This power is determined by the gate opening of the turbine, and the time constant for changing the mechanical power is in most cases several seconds. There are different reasons why the mechanical power should be changed. For each generator there is a dispatch plan made for each hour. This plan is determined by the expected load in the power system. These plans are often the result of extensive optimisations of the resources available with due consideration to load, prices, cost, etc. The mechanical input powers are changed in accordance with these dispatch plans. But it is not possible to exactly forecast the power consumption in the system. Furthermore, generators could suddenly be disconnected due to faults, resulting in a shortage of power in the system. These unbalances will cause a

---

<sup>1</sup>In the following it is assumed that the synchronous machine is a generator. The same discussion could be applied to a synchronous motor, but then the signs of the electrical and mechanical powers must be changed. But since the dynamics of the system is dominated by the generators, it is natural to use these as the basis for type discussion. However, there is no principal difference in the dynamics between a synchronous motor and generator.

frequency deviation in the system. This frequency deviation can be used as an input signal to selected generators, which will change their mechanical input power and thereby their electrical output so that the frequency deviation is brought down to acceptable levels, typically  $\pm 0.1$  Hz in interconnected systems. The frequency controller could be rather fast, but since it takes several seconds to change the mechanical power  $P_m$  it will take some time for the frequency control to act. Generally it can be said that  $P_m = P_m(\dot{\theta})$  for those generators that are equipped with frequency controllers, but if time scales up to some seconds are considered it is a fair approximation to say that  $P_m = \text{constant}$ , at least for studies and discussion of more principal nature.

In section 9.2 an expression for the active power of a synchronous machine connected to an infinite bus was derived, eq. (9.12). As can be seen, the power depends on the angle  $\theta$ , and the rotor angle occurs thus on both sides of the swing equation. This applies for a synchronous machine connected to an infinite bus, but it can be shown to be the case also for more complex systems with more synchronous machines. In this latter case, the electrical power of a given machine will not only depend on the value of its own rotor angle, but also on the rotor angles of other machines. The result is thus a system of coupled differential equations.

A more detailed analysis of the electrical power shows that it depends not only on  $\theta$  but also on  $\dot{\theta}$ , that is on the relative angular velocity as compared with a synchronously rotating system. This contribution, which only occurs during transients, is due to currents induced in the rotor circuits, and it tends to damp out the oscillations. A voltage controller might also give a contribution to the electrical power depending on  $\dot{\theta}$ .

With fairly good accuracy the electrical power can be written as

$$P_e = P_e(\theta, \dot{\theta}) = P_s(\theta) + P_d(\dot{\theta}) \quad (10.8)$$

with  $P_s$  being the synchronising power and  $P_d$  being the damping power. This is further explained in section 11.4.

### 10.3 Swing Equation as System of First Order Differential Equations

The swing equation (10.7) is an ODE of the second order.<sup>2</sup> ODEs of higher orders can be written as a system of first order ODEs, which in many cases is practical. Particularly for multi-machine systems this turns out to be an attractive approach. In most cases it is not possible to solve the swing equation analytically, but one has to use numerical integration in solving it. Numerical integration usually requires that the ODE is in the form of ODEs of first order.

---

<sup>2</sup>The abbreviation ODE for Ordinary Differential Equation is here introduced.

By introducing  $\omega = \dot{\theta}$  eq. (10.7) can be written as

$$\begin{bmatrix} \dot{\theta} \\ \dot{\omega} \end{bmatrix} = \begin{bmatrix} \omega \\ \frac{\omega_0}{2H}(P_m - P_e) \end{bmatrix} \quad (10.9)$$

This form of the swing equation will also be used in the following. The quantities  $\theta$  and  $\omega$  in eq. (10.9) are named state variables, or just states, and eq. (10.9) describes the system in state form or standard form. The vector  $[\theta \ \omega]^T$  is the state vector of the system.

Some clarifications will be made concerning the angular velocity  $\omega$  introduced in eq. (10.9) above. This angular velocity denotes the frequency with which the rotor oscillates relative to a system rotating with the synchronous and constant angular velocity  $\omega_0$ . The absolute angle of the rotor  $\theta_{abs}$  relative to a reference system at time  $t$  is given by

$$\theta_{abs} = \omega_0 t + \theta + \theta_0 \quad (10.10)$$

where  $\theta_0$  is the angle of the rotor at  $t = 0$ . Differentiation of eq. (10.10) with respect to time gives

$$\dot{\theta}_{abs} = \omega_0 + \dot{\theta} \quad (10.11)$$

from which it can be concluded that the absolute angular velocity of the rotor  $\omega_{abs}$  is given by

$$\omega_{abs} = \dot{\theta}_{abs} \quad (10.12)$$

and the angular velocity relative the synchronously rotating system  $\omega$  is given by

$$\omega = \dot{\theta} \quad (10.13)$$

It is this latter relative angular velocity that is of interest when rotor oscillations are studied, while the absolute angular velocity is of interest when studying frequency stability.



# 11

## Power Swings in a Simple System

*In this chapter the models and equations derived earlier are applied to the simple system of a synchronous machine connected to an infinite bus. Despite the simplicity of the system, useful and general information can be gained from this analysis. Through qualitative discussions the features of the equilibrium points of the system can be determined. Time domain simulations of the system show the principal behaviour of stable and unstable solutions. The equal area criterion is derived. This is a very powerful method for determining the stability of a system. Another powerful tool is provided by small signal analysis, or linear analysis, which gives valuable information about the local behaviour of the system. The chapter is concluded by a discussion of different ways of improving the angular stability of a power system.*

A COMPLETE STABILITY analysis of a power system is an extensive and complicated task. However, it turns out that many of the most important phenomena and mechanisms can be found in very simple systems, where they can be seen very clearly. In large and complicated systems it is often hard to distinguish the fundamental and decisive phenomena from the more irrelevant ones. It is therefore of importance to study simple systems to get an insight into and understanding of the basics, that can be used in the analysis of more complex systems. This chapter focuses on power oscillations in the simple system of Figure 11.1. This system can be a model of a synchronous machine or group of synchronous machines connected to a larger system through one or more power lines. The reactance  $X_e$  in Figure 11.1 is an equivalent reactance including transformers and parallel lines. Even if this system is simple, a number of simplifications are required to get simple solutions to the system.

The reader is encouraged to solve problems from the problem set to get a better understanding of the issues discussed here.

### 11.1 The Swing Equation and its Solutions

The solutions to the swing equations of the simple system in Figure 11.1 will be analysed and discussed in this sub-section. Despite its simplicity, a

number of important conclusions concerning the angular stability in large systems can be drawn from this example. Earlier a number of simplifications and assumptions have been made, more or less explicitly, and for the sake of completeness and clarity they are summarised here:

1. The synchronous machine is modelled as a constant electro-magnetic field behind the transient reactance  $X'_d$ . The angle of the electro-magnetic field is assumed to coincide with the rotor angle.
2. Resistances in lines, transformers, and synchronous machines are neglected.
3. Voltages and currents are assumed to be perfectly symmetrical, i.e. pure positive sequence.
4. The angular velocity is close to the nominal one.
5. Static models for lines are used.
6. The mechanical power  $P_m$ , i.e. the power from the prime mover, is constant during the transient under study.

Furthermore, it is assumed that the damping power of the system can be written as

$$P_d = D\dot{\theta} \quad (11.1)$$

An electrical equivalent to Figure 11.1 is shown in Figure 11.2. Together with the assumptions above the swing equation can now be formulated as

$$\frac{2H}{\omega_0} \frac{d^2\theta}{dt^2} = P_m - P_e \quad (11.2)$$

with

$$P_e = \frac{E'_q U_N}{X'_d + X_e} \sin \theta + D\dot{\theta} \quad (11.3)$$

and

$$P_m = P_{m0} = \text{constant} \quad (11.4)$$

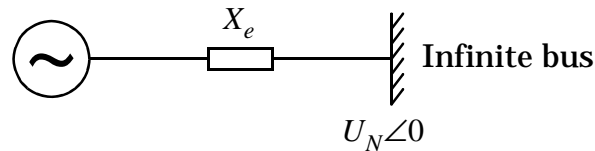


**Figure 11.1.** Synchronous machine connected to infinite bus.

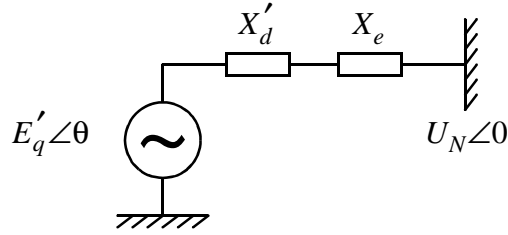


**Figure 11.2.** Equivalent electric circuit of a synchronous machine connected to an infinite bus.

Now we introduce

$$P_{e,max} = \frac{E'_q U_N}{X'_d + X_e} \quad (11.5)$$

and eq. (11.2) can be written as

$$\frac{2H}{\omega_0} \frac{d^2\theta}{dt^2} = P_{m0} - P_{e,max} \sin \theta - D\dot{\theta} \quad (11.6)$$

which is the complete swing equation of the simplified system with the introduced assumptions.

### 11.1.1 Qualitative Analysis

In order to make a qualitative analysis of the solutions to eq. (11.6) a further simplification will be made, i.e. the damping is neglected and  $D$  is thus set to zero :

$$\frac{2H}{\omega_0} \frac{d^2\theta}{dt^2} = P_{m0} - P_{e,max} \sin \theta \quad (11.7)$$

Of fundamental importance to a non-linear system are its equilibrium points, i.e. the points in state space where all time derivatives vanish. For the equilibrium points the right hand side of eq. (11.7) is thus zero resulting in the following equation for  $\theta_0$

$$P_{m0} = P_{e,max} \sin \theta_0 \quad (11.8)$$

Figure 11.3 shows how  $P_e$  and  $P_m$  vary with rotor angle  $\theta$ , and the following conclusions about the equilibrium points can be drawn from this figure:

1. If  $P_{m0} < P_{e,max}$  there are *two* equilibrium points, i.e.  $\theta_0$  and  $\pi - \theta_0$  for  $0 \leq \theta \leq \pi$ .
2. If  $P_{m0} = P_{e,max}$  there is exactly *one* equilibrium point  $\theta_0 = \pi/2$  for  $0 \leq \theta \leq \pi$ .
3. If  $P_{m0} > P_{e,max}$  there is *no* equilibrium point.

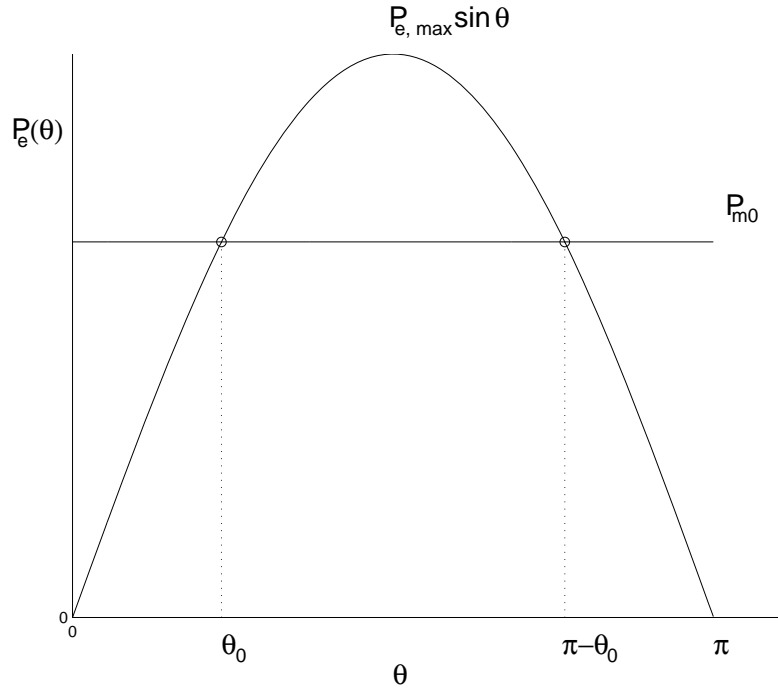


**Figure 11.3.** Diagram showing the variation of electric and mechanical power for the system in eq. (11.7).

(The angle  $\theta_0$  is given by  $\theta_0 = \arcsin(P_{m0}/P_{e,max})$ .)

It is clear that if  $P_{m0} > P_{e,max}$  the system is unstable and further analysis is superfluous. In this case the rotor will be accelerated until the protections trip the generator and turbine. A necessary condition for stability is that at least one equilibrium point exists.

In the case of  $P_{m0} < P_{e,max}$  the equilibrium point  $\theta = \theta_0$  is stable for (sufficiently) small disturbances, which implies that if the system is moved away from  $\theta_0$  the dynamics of the system tends to bring it back to  $\theta_0$ . This is verified by the following qualitative reasoning:

If the rotor has been accelerated so that  $\theta > \theta_0$ , the right hand side of eq. (11.7) will be negative and the system is decelerated and starts to move back to  $\theta_0$  (provided  $\omega$  is sufficiently small). Correspondingly, a deviation  $\theta < \theta_0$  will give an acceleration so that  $\theta$  is brought back to  $\theta_0$ . (As seen from Figure 11.3 these arguments are valid only for sufficiently small deviations from  $\theta_0$  and  $\omega = 0$ .) It is seen that if  $\theta > \pi - \theta_0$  and if  $\omega \geq 0$  then the system will never return to  $\theta = \theta_0$ .

For a state vector  $[\theta \ \omega]^T$  in the two dimensional state space, or phase space as it is sometimes referred to, that initially is close to  $[\theta \ \omega]^T = [\theta_0 \ 0]^T$ , will be close to this point for all  $t > 0$ . As in a real system there is posi-

tive (hopefully) damping, so the solution will converge (asymptotically) to  $[\theta_0 \ 0]^T$ . The region that has been described above as close to  $[\theta_0 \ 0]^T$  is called the region of attraction of this equilibrium point, and the curve that separates this region from points that will not converge to  $[\theta_0 \ 0]^T$ , is called the separatrix. This curve separates the stable and unstable solutions from each other.

A similar discussion concerning the equilibrium point  $\theta = \pi - \theta_0$  shows that this point is unstable.

A stability criterion for the system in Figure 11.3 can now be formulated:

### Stability Criterion

*The system in Figure 11.3 is stable, i.e. the synchronous machine will not fall out of step, if it is after a disturbance in the region of attraction of the equilibrium point  $[\theta_0 \ 0]^T$ .*<sup>1</sup>

The criterion above implies that the system must have decelerated so that  $\omega = 0$  before the point  $\theta = \pi - \theta_0$  is reached, otherwise the generator will fall out of step. The discussion above has disclosed a number of important features of the system without that any equation has been solved. The solutions to eq. (11.7) are not easy to obtain analytically. It is seen that eq. (11.7) is the same as the equation describing a mathematical pendulum, and the exact solutions are given by elliptic integrals. Usually a mathematical pendulum is studied by its linearised equations, but one cannot get all information regarding stability from these equations. The linearised equations can however give other kinds of useful information, and we will come back to that in section 11.4.

In the next section the behaviour of the stable and unstable solutions will be discussed.

### 11.1.2 Stable and Unstable Solutions

In order to verify the conclusions drawn from the qualitative discussion above simulated solutions to eq. (11.7), i.e. for the system in Figure 11.1, will be shown for a few cases.

The disturbance considered here is a three phase to earth fault on one of the lines close to the generator. That the fault is close to the generator implies that the electric power during the fault is zero. The faulty line is disconnected by the distance protections, see Appendix B.2, causing that the reactance  $X_e$  is changed when the fault is cleared. By varying the

---

<sup>1</sup>It is clear that  $\theta = \theta_0$  is the only possible stable equilibrium point.  $P(\theta)$  is periodic with the period  $2\pi$ , but if the system has moved so that  $\theta$  is close to another “stable” equilibrium point,  $\omega$  will be so large that it is outside the region of attraction of this equilibrium point.

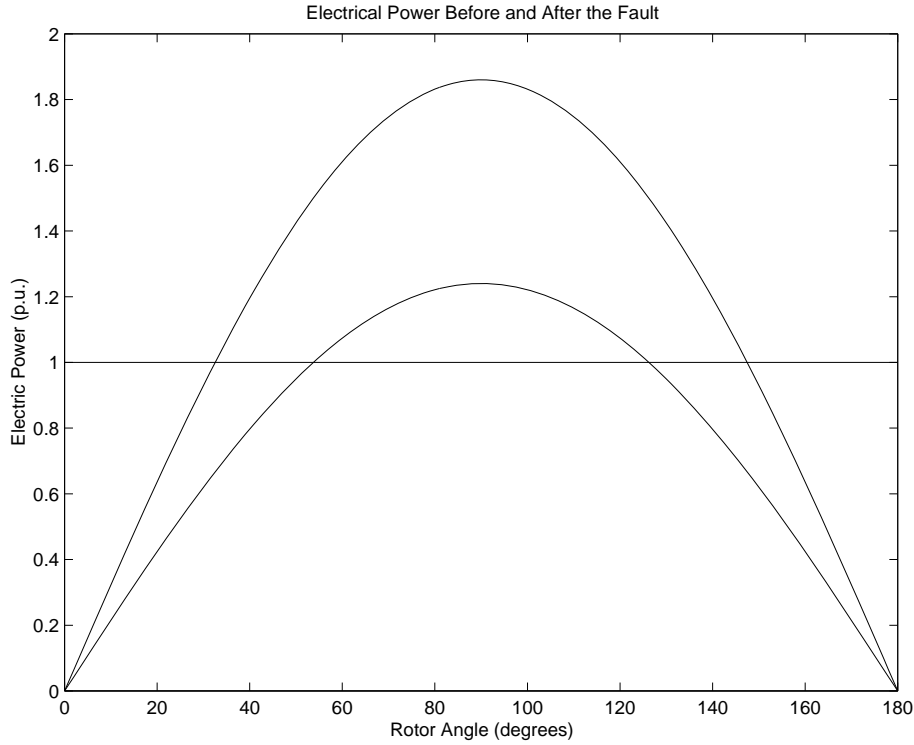


**Figure 11.4.** The electric power before the fault,  $P_e = 1.86 \sin \theta$ , after the fault,  $P_e = 1.26 \sin \theta$ , and the mechanical power,  $P_m = 1$ , as function of the rotor angle,  $\theta$ .

fault clearing time different types of solutions to the swing equation can be obtained.

The system is thus described by the following equation

$$\frac{2H}{\omega_0} \frac{d^2\theta}{dt^2} = P_{m0} - P_{e,max} \sin \theta - D\dot{\theta} \quad (11.9)$$

The electric power is as follows: Pre-fault  $P_{e,max} = 1.86$  p.u., post fault  $P_{e,max} = 1.26$  p.u. and during the fault  $P_e = 0$ . Power curves before and after fault are shown in Figure 11.4 where also the constant power from the turbine  $P_m = 1$  p.u. is drawn. Before the fault  $\theta = 32.5^\circ$ , which corresponds to the left intersection between  $P_e = 1.86 \sin \theta$  and  $P_m = 1$ . During the fault the rotor will accelerate since  $P_e = 0$  and consequently  $P_m - P_e > 0$ . When the fault is cleared the electric power will follow the curve  $P_e = 1.24 \sin \theta$ . If the system is stable it will settle down to the point  $\theta = 53.5^\circ$  which is the left intersection between  $P_e = 1.24 \sin \theta$  and  $P_m = 1$ . When the rotor angle is between  $53.5^\circ$  and  $180 - 53.5 = 126.5^\circ$ , which corresponds to the right intersection between  $P_e = 1.24 \sin \theta$  and  $P_m = 1$ , then  $P_m - P_e < 0$

and the rotor will decelerate. Should the rotor move beyond this point, then  $P_m - P_e > 0$  and the rotor will accelerate and the system becomes unstable. It is often said that the generator falls out of step or loses synchronism.

The longer the duration of the fault, the more the rotor will be accelerated and the larger the rotor angle. If the duration of the fault is too long there is a risk that the rotor swing is so large that it passes the right equilibrium point and the synchronous machine loses synchronism. To verify and demonstrate this the system has been simulated for fault clearing times equal to 4, 6, 6.5, and 8 cycles.<sup>2</sup> Results from these simulations are shown in Figures 11.5 to 11.8 where both the swing curves and the phase portraits of the system are shown. The phase portrait, or phase trajectory, is the trajectory of the system in the  $(\omega, \theta)$ -plane during the transient. The damping  $D$  is set to 0.02. The value of the damping determines how fast a stable solution will converge to its equilibrium point, and this value has minor influence on the first swing directly after the fault.<sup>3</sup>

With a fault clearing time of 4 cycles the system is clearly stable, see Figure 11.5. The maximal rotor angle is  $\approx 90^\circ$  which gives an ample margin to the critical value of  $126.5^\circ$ . The system will eventually converge to the point  $\theta = 53.5^\circ$ .

If the fault clearing time is increased to 6 cycles, see Figure 11.6, the stability margin is much smaller. The rotor swings out to  $\approx 120^\circ$  and it is very close to the critical point where it will start to accelerate. If the fault clearing time is increased to 6.5 cycles the curves of Figure 11.7 are obtained, and here the system is unstable. The generator cannot be decelerated enough before it reaches the critical point, but it passes this point and is further accelerated and loses synchronism. This type of instability is called *first swing instability*. The phase portrait in this case shows that rotor is close to be decelerated before reaching the critical point, but it never reaches a zero value of  $\omega$ . The previous fault clearing time, i.e. 6 cycles, is called *critical fault clearing time*.

The last case shows a simulation with the fault clearing time equal to 8 cycles, see Figure 11.8. In this case the rotor is accelerated for such a long time that it passes the critical point very soon. The deceleration period could hardly be seen in the swing curve. The phase portrait shows also that

---

<sup>2</sup>Fault clearing times are often given in cycles of the power frequency. The reason for this is that part of the clearing time comes from the time needed for the breakers to clear the fault. Since the fault current can only be intercepted at a zero crossing, it is natural to measure the breaker time in cycles. Modern high voltage breakers can break a fault current in 2 – 3 cycles. Should still faster breaker times be required, special breakers could be installed, but these are more expensive than standard breakers. Protections are also described in Appendix B.

<sup>3</sup>This is the case for realistic values of  $D$ . If the damping is very large, and positive, this will increase the stability significantly in the system. The value used here is typical in a system where no special equipment has been installed to increase the damping, e.g. *Power System Stabilisers* on the voltage regulators.

the deceleration just after fault clearing is clearly insufficient to stabilise the system.

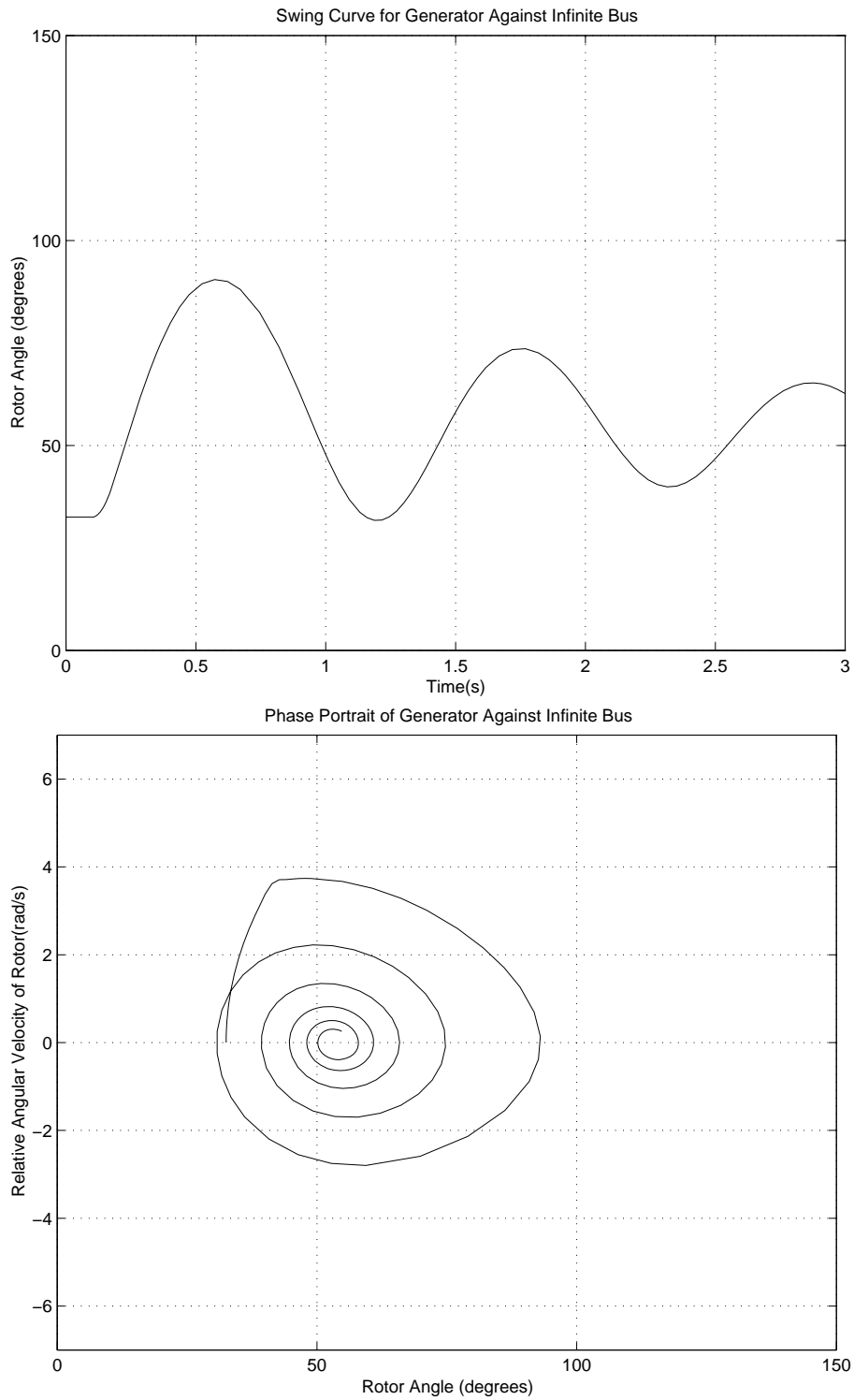


**Figure 11.5.** Swing curve and phase portrait for generator swinging against an infinite bus. Fault clearing time = 4 cycles. Critical fault clearing time = 6 cycles.

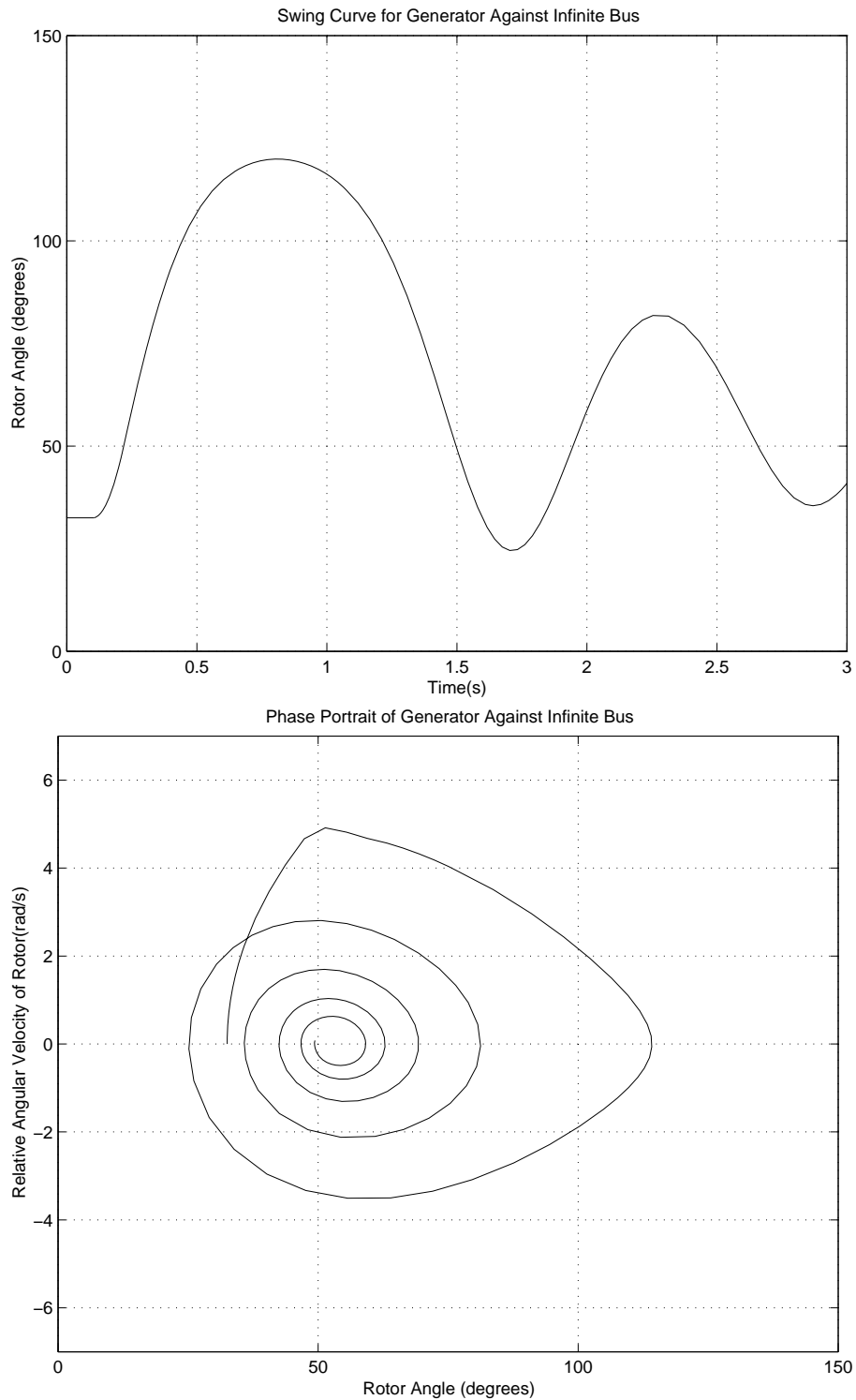


**Figure 11.6.** Swing curve and phase portrait for generator swinging against an infinite bus. Fault clearing time = 6 cycles. Critical fault clearing time = 6 cycles.

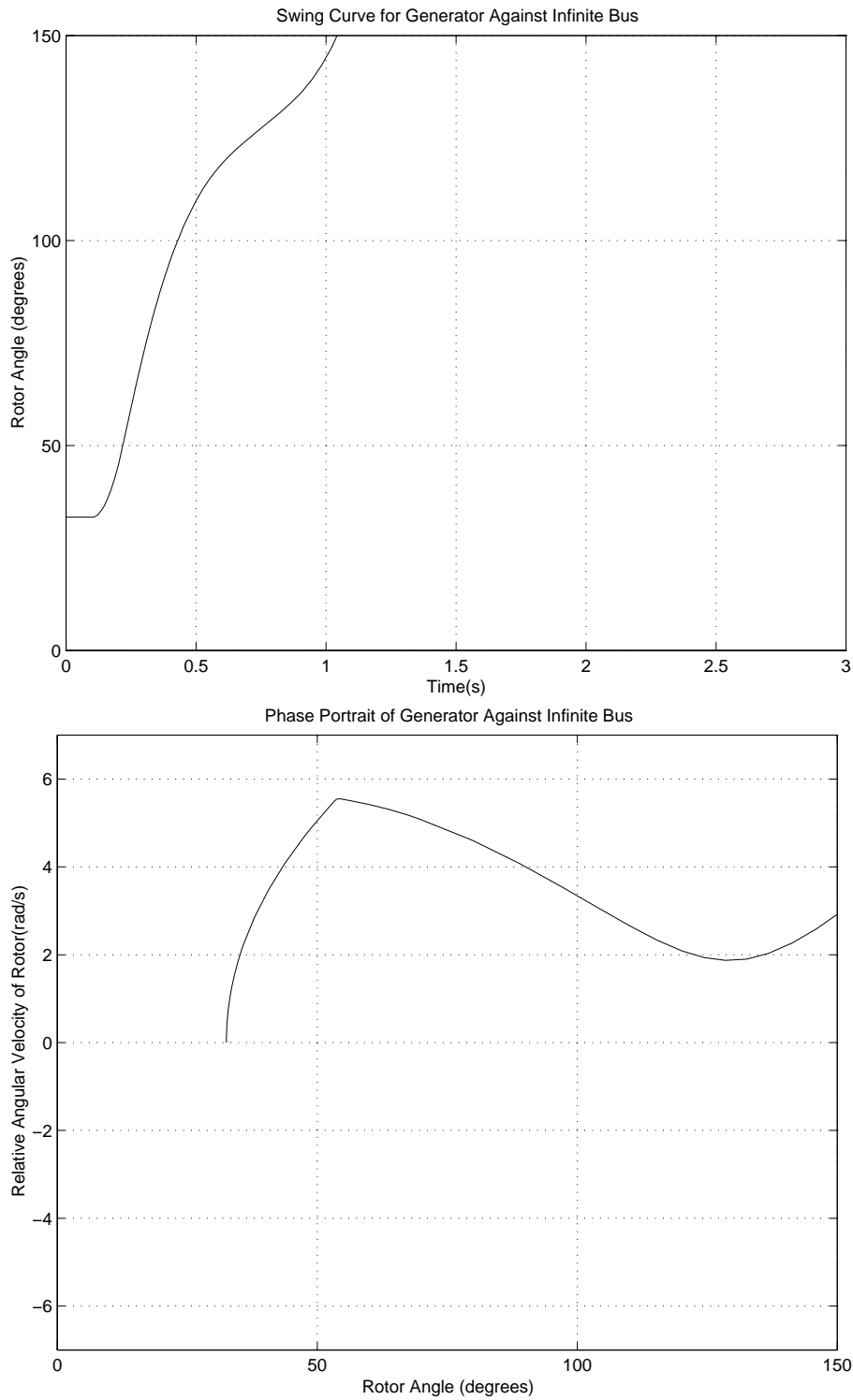


**Figure 11.7.** Swing curve and phase portrait for generator swinging against an infinite bus. Fault clearing time = 6.5 cycles. Critical fault clearing time = 6 cycles.

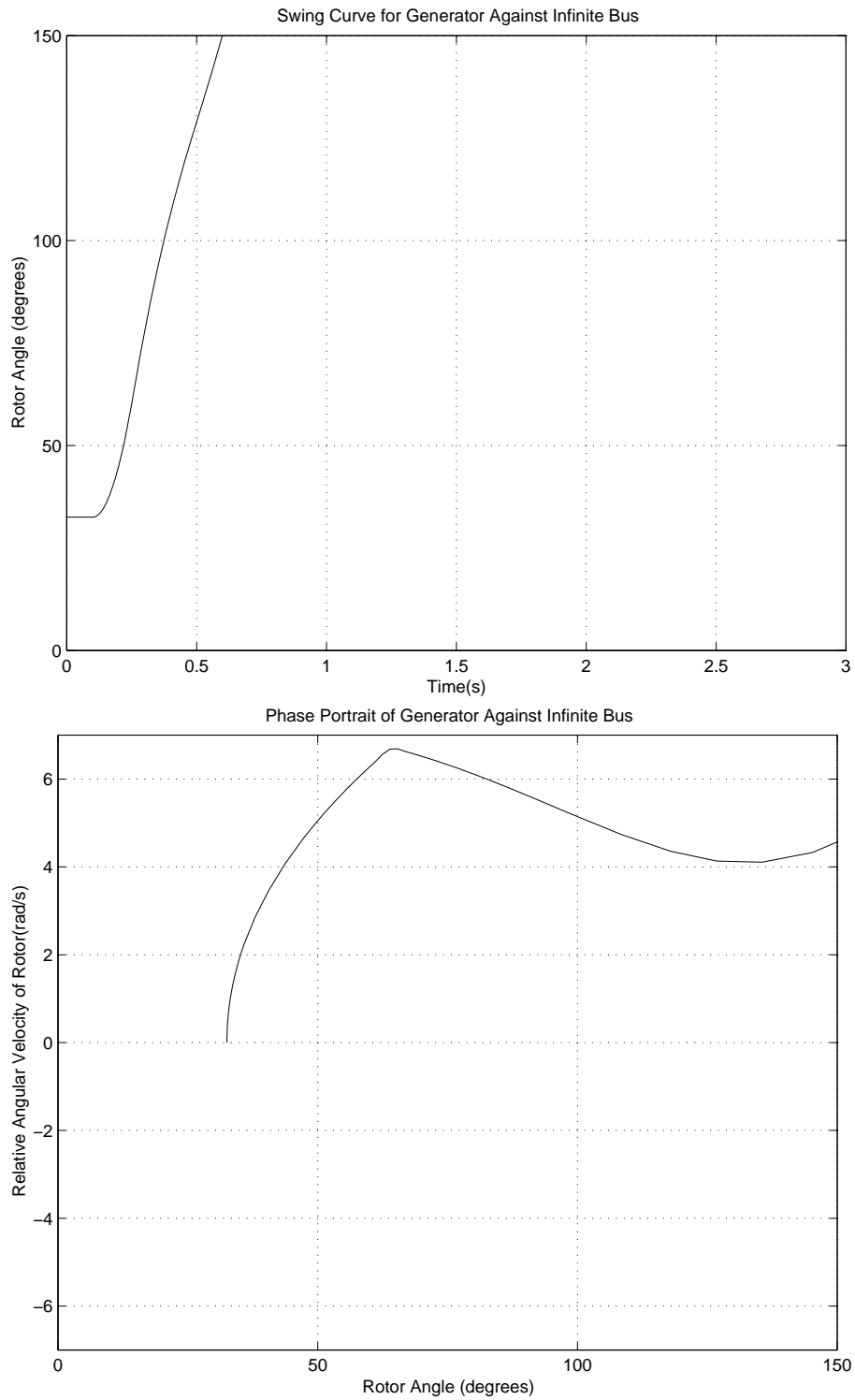


**Figure 11.8.** Swing curve and phase portrait for generator swinging against an infinite bus. Fault clearing time = 8 cycles. Critical fault clearing time = 6 cycles.

## 11.2 Equal Area Criterion

It was concluded above that even for quite simple systems, like the one in Figure 11.1 it was hard to get analytical solutions to the system equations. But quite often the exact behaviour of the solutions is not of interest, but most important is to determine if the system is stable or not after a given contingency. By using the equal area criterion that will be derived in this section, it is possible with rather simple calculations to investigate the stability of the system in Figure 11.1 for different disturbances. The equal area criterion can be extended to more complicated systems, so that preliminary stability analyses could be done very fast.

The swing equation of the system in Figure 11.1 can be written as

$$\frac{d^2\theta}{dt^2} = \frac{\omega_0}{2H}(P_m - P_{e,max} \sin \theta) \quad (11.10)$$

or

$$\frac{d^2\theta}{dt^2} = \frac{\omega_0}{2H}P_a \quad (11.11)$$

with the accelerating power  $P_a$  defined by

$$P_a = P_m - P_{e,max} \sin \theta \quad (11.12)$$

As the interest here is focused on the dynamics during the first swing, the damping can be neglected, i.e.  $D = 0$ . From the Figures 11.5 to 11.8 it can be concluded that a necessary, but not sufficient, condition for stability is that there exists a moment in time  $t_m$  during the swing such that  $\dot{\theta}(t_m) = 0$ . The corresponding angle is  $\theta_m$ . Some formal manipulations with eq. (11.11) together with the condition  $\dot{\theta}(t_m) = 0$  will provide a stability criterion. If eq. (11.11) is multiplied with  $\dot{\theta}$  one gets

$$\dot{\theta} \frac{d^2\theta}{dt^2} = \frac{\omega_0}{2H}P_a \dot{\theta} \quad (11.13)$$

which can be written as

$$\frac{1}{2} \frac{d}{dt} \left( \frac{d\theta}{dt} \right)^2 = \frac{d}{dt} \left( \frac{\omega_0}{2H} \int_{\theta_i}^{\theta} P_a d\theta' \right) \quad (11.14)$$

that can be integrated to give

$$\frac{d\theta}{dt} = \sqrt{\frac{\omega_0}{H} \int_{\theta_i}^{\theta} P_a d\theta' + C} \quad (11.15)$$

with  $C$  being a constant of integration, which is 0, since  $\dot{\theta} = 0$  when  $\theta = \theta_i$ . ( $\theta_i$  is the pre-fault rotor angle.) Thus a necessary condition for stability is that there is an angle  $\theta_m$  such that

$$\frac{\omega_0}{H} \int_{\theta_i}^{\theta_m} P_a d\theta' = 0 \quad (11.16)$$

or

$$\int_{\theta_i}^{\theta_m} P_a d\theta' = 0 \quad (11.17)$$

The stability criterion can thus be formulated as:

*The system is stable if there exists an angle  $\theta_m$  such that the area below the accelerating power  $P_a$  in the  $\theta$ - $P(\theta)$  diagram between  $\theta_i$  and  $\theta_m$  vanishes.*

In most cases of practical interest the dynamics could be divided into two different phases: A first phase when the rotor is accelerated, and a second phase when it is decelerated. Assume that the rotor is accelerated up to  $\theta = \theta_c$  and that it is decelerated when  $\theta_c \leq \theta \leq \theta_m$ . Then two different areas in the  $\theta$ - $P(\theta)$  plane can be defined as

$$A_a = \int_{\theta_i}^{\theta_c} (P_m - P_e(\theta')) d\theta' \quad (11.18)$$

$$A_r = \int_{\theta_c}^{\theta_m} (P_e(\theta') - P_m) d\theta' \quad (11.19)$$

Indices  $a$  and  $r$  denote here accelerating and decelerating (retarding) areas, respectively. The angle  $\theta_c$  is most conveniently chosen as the angle when the fault is cleared. The stability criterion can now be formulated as

*The system is stable if there exists an angle  $\theta_m$  such that the areas  $A_a$  and  $A_r$  are equal, i.e.  $A_a = A_r$ .*

This latter formulation gave rise to the name *equal area criterion* for this stability criterion. This is illustrated in Figure 11.9. Note that  $P_e$  is reduced to zero during the fault, hence the shape of the area  $A_a$ .

The advantage of the equal area criterion is that the stability of a system can be investigated without any excessive computational efforts. But the price paid is that the time  $t$  was eliminated from the equations. Since the time does not appear explicitly in the equations, actions to improve the stability must be formulated in the angle space, which is usually not so practical. It is of course of more interest to have these actions formulated in terms of times, e.g. critical fault clearing times. By the equal area criterion critical fault clearing angles could be formulated, and these must then be transformed to critical fault clearing times. Sometimes this can be done easily, sometimes it is not straightforward.

In the second formulation of the equal area criterion, an angle  $\theta_c$  was introduced. This angle defines for which values that  $P_a$  should be calculated as positive and negative, respectively. The choice of  $\theta_c$  has no influence on the result from the equal area criterion, which is obvious from the first formulation. When applying the equal area criterion in a practical case it is

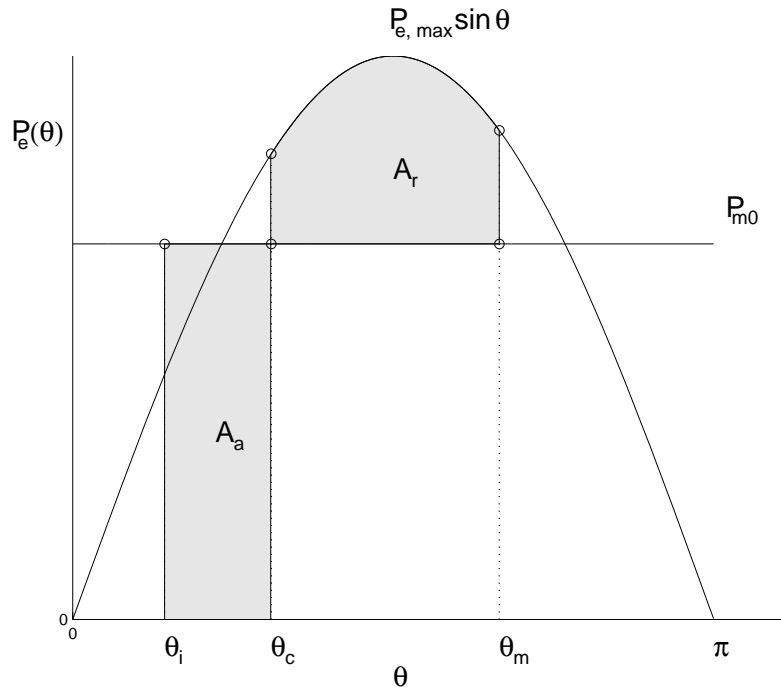


**Figure 11.9.** Application of the equal area criterion after a disturbance.

natural to choose  $\theta_c$  as the angle when the fault is cleared. At this angle the topology of the system is often changed, and thus the expression for  $P_e(\theta)$ , resulting in different expressions for  $P_e$  in the computation of  $A_a$  and  $A_r$ .

Different stability related problems can be solved by using the equal area criterion. One common application is the calculation of how fast a fault must be cleared to ensure stability of the system. The maximum fault clearing time for which the system remains stable is called critical fault clearing time, as mentioned above, and the corresponding angle is called critical fault clearing angle. The equal area criterion can also be used to calculate the maximum power that can be transmitted for a given fault scenario. A third application is to determine if a system is stable or not for given data and disturbances. It is strongly recommended that problems from the problem set are solved to get an understanding of the application of the equal area criterion.

### 11.3 Lyapunov Stability Criterion

The theory of the Russian mathematician A. Lyapunov (1857 -1918) offers powerful tools for stability analysis of dynamical systems. In this theory the following theorem, first formulated in 1899, forms the basis.

**Theorem.** Consider the dynamical system  $\dot{x} = f(x)$ , where  $x_0$  is an equilibrium point. If in a region around the point  $x_0$  there exists a real valued and continuously differentiable function  $\mathcal{V}$  such that

1.  $\mathcal{V}(x) > 0$  and  $\mathcal{V}(x_0) = 0$ ,
2.  $\dot{\mathcal{V}}(x) = \text{grad}(\mathcal{V}(x)) \cdot f(x) \leq 0$ ,

then  $x_0$  is a stable equilibrium point. If  $\dot{\mathcal{V}}(x) < 0$ , then  $x_0$  is asymptotically stable.

The existence of the function  $\mathcal{V}$  is also a necessary condition for stability. A problem with Lyapunov's theorem is that it does not give any information on how to find the function  $\mathcal{V}$ . It is obvious from the theorem that  $\mathcal{V}$  can be regarded as a form of energy, and the theorem says that if the system is stable, it will stay in the region around  $x = x_0$  where  $\mathcal{V}$  is positive definite provided the "energy" introduced to the system by a disturbance is sufficiently small.

For the system studied above the following function can be shown to fulfill the requirements of Lyapunov's theorem

$$\mathcal{V}(\omega, \theta) = \frac{H}{\omega_0} \omega^2 + P_{m0}(\theta_0 - \theta) + P_{e,max}(\cos \theta_0 - \cos \theta) = \mathcal{V}_k + \mathcal{V}_p \quad (11.20)$$

with

$$\mathcal{V}_k = \frac{H}{\omega_0} \omega^2 \quad (11.21)$$

and

$$\mathcal{V}_p = P_{m0}(\theta_0 - \theta) + P_{e,max}(\cos \theta_0 - \cos \theta) \quad (11.22)$$

$\mathcal{V}_k$  can here be interpreted as kinetic energy and  $\mathcal{V}_p$  as potential energy.

It is straightforward to show that  $\dot{\mathcal{V}} = -D\omega^2$  by using eq. (11.6), and consequently the second requirement of the above theorem is fulfilled if  $D \geq 0$ . It is clear that  $\mathcal{V}$  is positive definite in  $\omega$ . In Figure 11.10 the potential energy,  $\mathcal{V}_p$  is shown for a system with  $P_{m0} = 0.3$  and  $P_{e,max} = 1$  and it can be seen that it is positive definite in a neighbourhood of the equilibrium point  $\theta_0 = \arcsin(P_{m0}/P_{e,max})$ . Thus, if the energy injected into the system during the fault will be less than the potential energy at the local maximum of  $\mathcal{V}_p$ , the system will be stable. It can be shown that the above Lyapunov function,  $\mathcal{V}$ , gives the same stability criterion as the equal area criterion.

## 11.4 Small Signal Analysis

The equal area criterion offers a tool to make stability analyses of the system in Figure 11.1 by rather simple computations. For this system it is also possible to do other types of analyses that do not require any more extensive

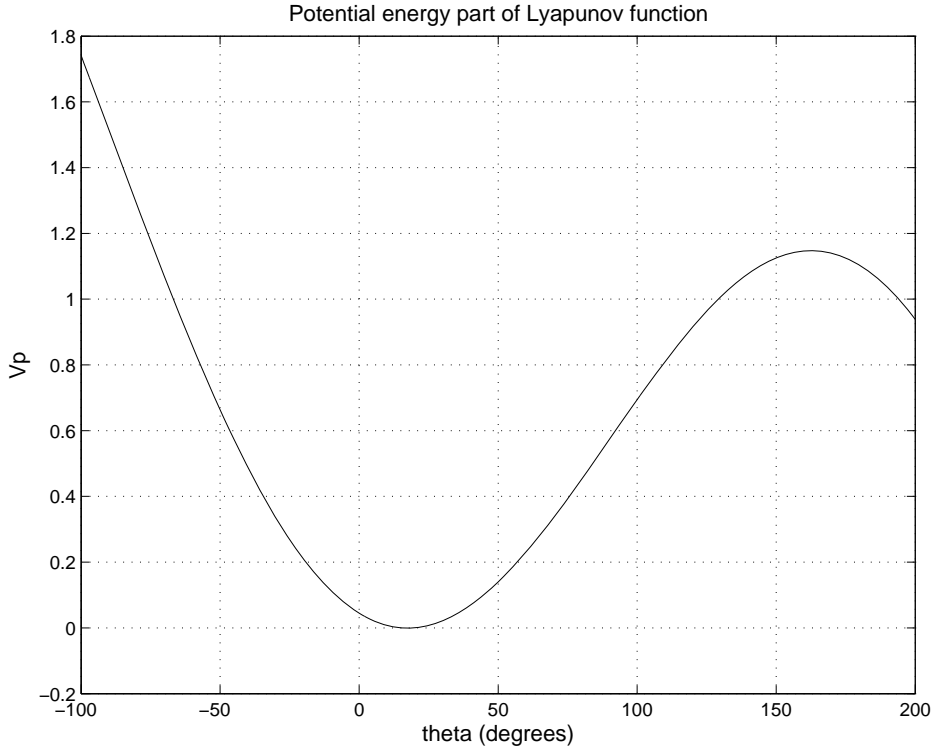


**Figure 11.10.** The function  $\mathcal{V}_p$  of eq. (11.22).

computations. One method often used to analyse non-linear systems is to linearise the system and study this latter system. Linear analysis is usually not so computationally demanding, and there exist many different tools for linear analysis. If the non-linearities of the system are “small”, it is clear that the linear system is a good approximation of the non-linear one. But it can be shown that for non-linear systems in general, provided the system equations are locally differentiable, the linear system would give valuable information about the non-linear system, e.g. regarding its stability. Small signal, or linear, analysis will now be applied to the system in Figure 11.1.

The system in Figure 11.1 is described by

$$\begin{bmatrix} \dot{x}_1 \\ \dot{x}_2 \end{bmatrix} = \begin{bmatrix} x_2 \\ \frac{\omega_0}{2H} (P_{m0} - P_{e,max} \sin x_1 - Dx_2) \end{bmatrix} \quad (11.23)$$

with

$$[x_1 \ x_2]^T = [\theta \ \omega]^T \quad (11.24)$$

It is now assumed that the system is in an equilibrium point

$$[x_{10} \ x_{20}]^T = [\theta_0 \ 0]^T \quad (11.25)$$

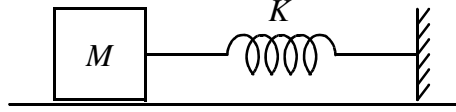


**Figure 11.11.** Mass and spring in analogy with the system in Figure 11.1.

The linearised system describes the behaviour of small oscillations around the equilibrium point eq. (11.25). A first order Taylor expansion of eq. (11.23) about the equilibrium point gives

$$\begin{bmatrix} \Delta \dot{x}_1 \\ \Delta \dot{x}_2 \end{bmatrix} = \begin{bmatrix} 0 & 1 \\ -\frac{\omega_0}{2H} P_{e,max} \cos x_{10} & -\frac{\omega_0}{2H} D \end{bmatrix} \begin{bmatrix} \Delta x_1 \\ \Delta x_2 \end{bmatrix} \quad (11.26)$$

From eq. (11.26) the frequency of small oscillations around the equilibrium point can be calculated and they are given by the eigenvalues of the  $2 \times 2$  matrix, the Jacobian matrix, in the right hand side of eq. (11.26).

First it is assumed that there is no damping in the system, i.e.  $D = 0$ . The eigenvalues of eq. (11.26) are then purely imaginary, which corresponds to (undamped) oscillations if  $0 \leq \theta_0 \leq \pi/2$ ,

$$\lambda = \pm \sqrt{-\frac{\omega_0}{2H} P_{e,max} \cos \theta_0} \quad (11.27)$$

and the frequency of oscillation is given by

$$\omega_p = \sqrt{\frac{\omega_0}{2H} P_{e,max} \cos \theta_0} \quad (11.28)$$

Eq. (11.28) is similar to the equation describing the motion for a mass connected to a wall with a spring according to Figure 11.11. The frequency of oscillation for this system is given by

$$\omega_{KM} = \sqrt{\frac{K}{M}} \quad (11.29)$$

By comparing eq. (11.28) with eq. (11.29) it is seen that the spring constant  $K$  in the mechanical system corresponds to  $P_{e,max} \cos \theta_0$ , which sometimes is called the stiffness of the electrical system or its synchronising power. Furthermore,  $M$  corresponds to  $2H/\omega_0$ .

From eq. (11.27) it is also seen that if  $\pi/2 < \theta_0 < \pi$ , the eigenvalues will be real, and one of them will be positive corresponding to an unstable mode. This was earlier also concluded by the qualitative discussion in section 11.1.1, and this is now verified by the mathematical analysis done here.

It was pointed out earlier that the damping is not significant for large disturbances in the system. For large disturbances it is the ability of the system to stay within the region of attraction of the equilibrium point that is important. This is depending on the stiffness of the system. The damping is more important for how the system settles down to the equilibrium point when it has survived the first swing. The linearised system could thus be used for studies of the damping in power systems. For the simple system studied here the eigenvalues with  $D \neq 0$  become

$$\lambda = -\frac{D'}{2} \pm j\sqrt{(\omega_p)^2 - \left(\frac{D'}{2}\right)^2} \quad (11.30)$$

with  $\omega_p$  given by eq. (11.28) and

$$D' = \frac{\omega_0}{2H}D \quad (11.31)$$

As the damping in a power system usually is quite small, eq. (11.30) can be approximated by

$$\lambda \approx -\frac{D'}{2} \pm j\omega_p \quad (11.32)$$

The frequency of oscillations can also be approximated in this case with good accuracy by eq. (11.28), and it is thus determined mainly by the stiffness of the system and the inertia constant of the machine.

## 11.5 Methods to Improve System Stability

It is obvious that it is desirable that a power system can withstand as many disturbances as possible without becoming unstable. However, it is realised that it is not possible to design a system that can cope with all conceivable contingencies, so one has to restrict the considered disturbances in the design of the system. Usually, one considers only the most frequent faults in the system. It is also important to consider the consequence of a fault or disturbance when designing a system. Generally it can be said that the more investments that can be made in a system, the more robust the system can be made. One is thus faced with a technical-economical optimisation problem that is very complex. Furthermore, there are a number of parameters that are both very important in the optimisation process and at the same time very hard to quantify. Such a parameter is the value that consumers put on uninterruptable supply of electric power of good quality. This optimisation process has gained a lot of interest during the last few years due to the liberalisation (de-regulation) of the power market taking place all over the world. Theoretically the optimum value of reliability of power supply is when the marginal increase in the value perceived by the customers is equal to the cost of the investment made to achieve this increase in reliability.

Practically it is of course impossible to deduce this optimum, and one has to judge by different methods if the consumers are satisfied with the reliability of the system, and if not if they are willing to pay more to improve it.

To have some more clear and practical rules for system design a number of deterministic rules have been used over the years. One such rule is the so called  $(N - 1)$ -rule, which says that a system should be able to supply customer loads with any component, generator, line, etc., out of service. The disconnection of the component should be preceded by a fault and the transients triggered by this fault should be considered. A more conservative approach would be to apply an  $(N - 2)$ -criterion, which would result in a more reliable but more expensive system.

Modern methods apply probabilistic tools. In many of these approaches one considers both the probability of a fault and its consequences. By assigning a measure, i.e. a number, for this combination of fault probability and consequence a risk based security analysis can be made. Some of these aspects are also discussed in chapter 14.

This section will be concluded by a discussion of different ways to improve the angular stability in power systems. The stabilising effect of the different methods can be verified by studying Figures 11.3 and 11.9. Which method to apply in a given situation depends on a large number of parameters and must be determined from case to case, usually after extensive studies. In some cases, one or several methods can be excluded, e.g. the construction of new lines since the needed permission cannot be granted from the authorities. The most common methods to increase system angular stability are:

- Increase of the inertia constant of the generators. This makes the rotors more difficult to accelerate in connection with faults and the risk for losing synchronism is reduced. In most cases this is a very expensive means and only in special cases it can be applied, e.g. by installing a flywheel on a small hydro unit.
- Increase of system voltage. This increases  $P_{e,max}$  and for given power  $P_m$  the stability margin is increased.
- Reduction of the transfer reactance  $X_e$ . This will also increase  $P_{e,max}$  as in the previous case. This can be achieved by constructing parallel lines, or by installing series capacitors on existing lines or new lines. By installing series capacitors the effective reactance of the line is reduced. This method has been used extensively over the years, e.g. in the Swedish system.
- Installation of fast protections and fast breakers. In this way the time with a fault connected can be reduced and thereby the time during which the generator rotors are accelerated. The ability for the system

to decelerate the rotor swings is increased. Another way is to use automatic re-closure after the fault is cleared, see Appendix A.

- Implementation of fast valving in steam turbines. By fast control of the mechanical power during and after a fault, the acceleration of the rotors can be decreased. It cannot be applied to nuclear power plants by security reasons. The method has not been used to any larger extent, since it is claimed to impose large thermal and mechanical stresses on valves, turbines, etc.
- Installation of braking resistors. These are shunt resistors that are connected by breakers fast after a fault close to a critical generator. The electric load of the critical machine increases and the risk for losing synchronism is reduced.
- Stability control of controllable devices such as High Voltage Direct Current (HVDC), controllable series capacitors, controllable reactive shunt compensation (SVC), etc. These devices are usually too expensive to install just for stabilising the system, but when they are installed, the cost to use their controllability for stabilisation is usually marginal.



# 12

## Power Oscillations in Multi-Machine Systems

*This chapter contains a very brief overview of modelling of multi-machine power systems.*

### 12.1 Classical Model for Systems with Several Machines

The simple model treated in the previous chapter is of limited value for the treatment of realistic systems. The analysis of such a simple model can mainly be motivated by the fact that it provides insight into the problem. Besides, the model can be used for simplified, preliminary computations. In this section, we will extend the model used in the previous section to a system with more than one machine. The same assumptions are made for the modelling:

- Damping is neglected.
- Mechanical power, i.e. turbine power,  $P_m$  is assumed constant.
- The synchronous machines are modelled electrically as constant voltage sources behind the transient reactance  $x'_d$ . The phase angle for the voltage source is assumed to coincide with the rotor angle.
- Loads are represented with impedances that represent the correct load in the state before the disturbance.

The system in Figure 12.1 is passive with  $n$  active sources, constituted by the generators. From these sources, the injected currents can be written as

$$\bar{I} = \bar{Y} \cdot \bar{E} \quad , \quad (12.1)$$

with

$$\begin{aligned} \bar{I} &= (\bar{I}_1, \bar{I}_2, \dots, \bar{I}_n) \quad , \\ \bar{E} &= (\bar{E}_1, \bar{E}_2, \dots, \bar{E}_n) \quad . \end{aligned} \quad (12.2)$$

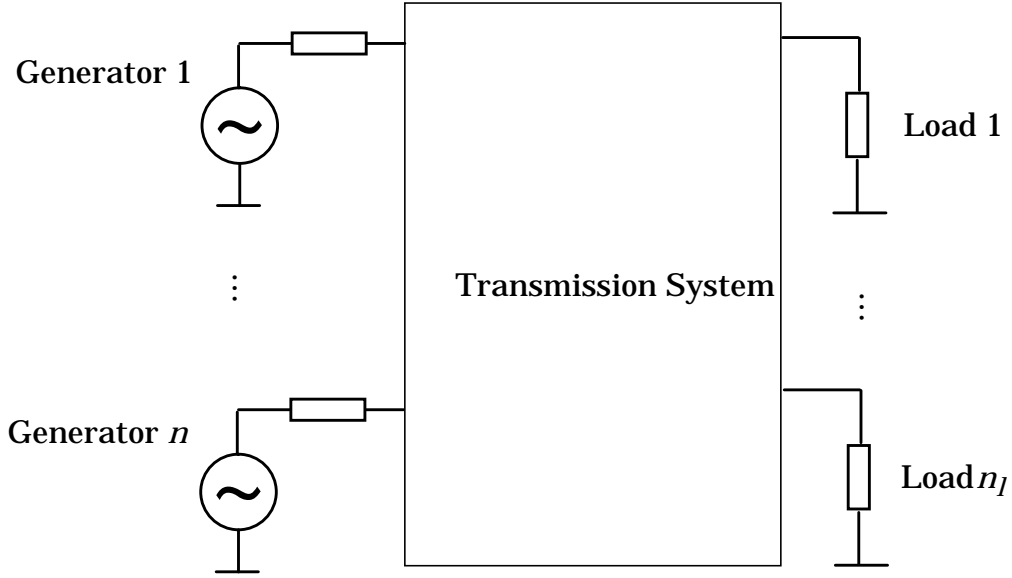


**Figure 12.1.** Schematic Picture of the Classical Model for a Multi-Machine System.

The matrix  $\bar{Y}$  is the bus admittance matrix with the elements

$$\bar{Y}_{ij} = Y_{ij} \angle \delta_{ij} = G_{ij} + jB_{ij} \quad (12.3)$$

and describes the passive net and the loads as they appear seen from the inner emf in the generators. Thus, the loads are included in the bus admittance matrix, which subsequently means that  $G_{ij}$  can be non-zero in a system with loads, even if the line resistances are ignored. The active power from generator  $i$  is

$$P_{ei} = \Re(\bar{E}_i \cdot \bar{I}_i^*) \quad , \quad (12.4)$$

which can be written as

$$\begin{aligned} P_{ei} &= \Re(\bar{E}_i (\sum_j \bar{Y}_{ij} \bar{E}_j)^*) \\ &= E_i^2 G_{ii} + \sum_{i \neq j} E_i E_j Y_{ij} \cos(\delta_{ij} - \theta_i + \theta_j) \\ &= E_i^2 G_{ii} + \sum_{i \neq j} E_i E_j (B_{ij} \sin(\theta_i - \theta_j) + G_{ij} \cos(\theta_i - \theta_j)) \quad . \end{aligned} \quad (12.5)$$

Now, the equations of oscillation for generator  $i$  are

$$\begin{cases} \dot{\omega}_i = \frac{\omega_0}{2H_i}(P_{mi} - P_{ei}) , \\ \dot{\theta}_i = \omega_i , \end{cases} \quad (12.6)$$

with  $P_{ei}$  according to Equation (12.5). Since  $P_{ei}$  also depends on other angles than the one from generator  $i$ , the system is described by  $2n$  coupled differential equations of first order. Hence, the system can be described by the state vector

$$x = (\omega_1, \theta_1, \dots, \omega_n, \theta_n)^T , \quad (12.7)$$

which satisfies the differential equation

$$\dot{x} = f(x) . \quad (12.8)$$

The vector-valued function  $f$  depends on the system's initial state and is nonlinear, cf. Equations (12.5) and (12.6).

Phase portraits for systems with more than two generators become very complicated and cannot be used for practical cases. To get insight into the problem, the linearised system can often be analyzed with respect to small oscillations around an equilibrium point.

The equilibrium points of Equation (12.8) are solutions of  $\dot{x} = 0$ , i.e. of

$$f(x) = 0 . \quad (12.9)$$

$x_0$  denotes a stable solution of (12.9). Small deviations around  $x_0$  can then be written as

$$x = x_0 + \Delta x , \quad (12.10)$$

and Equation (12.8) can be written as

$$\Delta \dot{x} = f(x_0 + \Delta x) . \quad (12.11)$$

For small values of  $\Delta x$ , the right hand side becomes

$$f(x_0 + \Delta x) \approx f(x_0) + \frac{\partial f}{\partial x} \Delta x = \frac{\partial f}{\partial x} \Delta x , \quad (12.12)$$

with the Jacobian matrix  $\frac{\partial f}{\partial x}$ , whose elements are given by

$$\left( \frac{\partial f}{\partial x} \right)_{ij} = \frac{\partial f_i}{\partial x_j} . \quad (12.13)$$

These matrix elements are computed in  $x_0$ . Equation (12.11) can now be approximated by

$$\Delta \dot{x} = \frac{\partial f}{\partial x} \Delta x . \quad (12.14)$$

The solutions to Equation (12.14) are determined by the eigenvalues and the eigenvectors of the Jacobian matrix in Equation (12.13), which has dimension  $2n \times 2n$ , and from these, the oscillatory modes of the system can be determined. Two of the Jacobian matrix's eigenvectors correspond to a translation of all rotor angles and are therefore not of interest. Since the damping has been neglected, the eigenvalues of the Jacobian are purely imaginary and form conjugate complex pairs. Corresponding solutions to the differential equations in Equation (12.14) are therefore purely oscillatory. Thus, there are  $n - 1$  interesting eigenvalues and eigenvectors.

Often, the model is simplified even more, and loads and line resistances are neglected. Then, an unloaded system that only consists of generator rotors and reactances is obtained. The oscillatory modes in that system often give a good picture of the complete system's behaviour during disturbances. Small oscillations in the real system will consist of a superposition of these oscillatory modes. This superposition depends on the disturbance that triggered the oscillations.

## 12.2 General Model for Electro–Mechanical Oscillations

In section 12.1, we introduced a number of simplifications that allowed us to write the equations in such a way that enabled us to use well-known mathematical methods for analyzing the problem. Unfortunately, the model we used has some serious shortcomings that make it less suitable for more detailed studies of the system dynamics. The main shortcomings are:

- The synchronous machine model is too simple. Only two states are used,  $\theta_i$  and  $\omega_i$ , while more states are required for a more satisfactory model. Some quantities will change over time, and different kinds of controllers for voltage and frequency will influence the behaviour. Saturation phenomena in the generator can also be of interest.
- Fast controllable equipment, often based on power electronics, like static compensators (SVC) and high-voltage DC transmission (HVDC), often have a large influence on system stability and therefore have to be modelled in an adequate way.
- The model of the loads is too simple. A large fraction of the loads consists of asynchronous machines and other drives, and their characteristics are not similar to an impedance when exposed to voltage fluctuations. In principle, loads consume as much power as the generators produce. Thus, it is equally important to use realistic load models as it is to model the synchronous machines accurately.

Accurate studies consequently demand more detailed models. A more detailed model delivers, of course, a better description, but the overview is often lost, and the problem can become awkward. In the following chapters, more realistic and, usually, more complicated models will be discussed.

More elaborate models demand the introduction of additional state variables. In the classical model, every generator was represented with two states,  $\theta_i$  and  $\omega_i$ , while a more detailed model requires more states. The modelling of exciters, voltage regulators, and turbine regulators necessitates additional states. Components like SVC and HVDC, with ancillary regulating equipment, have, as a rule, also to be modelled dynamically, which means that new state variables have to be introduced for these components. More realistic load models make the elimination of load buses, which was possible for the classical model, impossible. That means that the load flow equations will constitute algebraic conditions that have to be fulfilled by the state variables.

The dynamic states used for modelling the complete system are

$$\begin{aligned}
 x = & (x_1^1, x_2^1, \dots, x_{n_1}^1, \\
 & \dots \\
 & x_1^n, x_2^n, \dots, x_{n_n}^n, \\
 & x_1^{SVC1}, x_2^{SVC1}, \dots, x_{n_{SVC1}}^{SVC1}, \\
 & \dots \\
 & x_1^{HVDC1}, x_2^{HVDC1}, \dots, x_{n_{HVDC1}}^{HVDC1}, \\
 & \dots) ^T,
 \end{aligned} \tag{12.15}$$

with the states  $x_i$  for generator  $i$ ,  $x^{SVCi}$  for SVC equipment  $i$ , and so on. Further, a vector  $y$ , containing the voltage magnitudes and phase angles which are not included in  $x$ ,

$$y = (U_1, \varphi_1, U_2, \varphi_2, \dots, U_m, \varphi_m)^T, \tag{12.16}$$

is needed. The parameters required for the definition of the system, like line reactances etc., are given by the vector

$$p = (p_1, p_2, \dots, p_k)^T. \tag{12.17}$$

The system dynamics are now determined by the equations

$$\begin{cases} \dot{x} = f(x, y, p, t), \\ 0 = g(x, y, p, t), \end{cases} \tag{12.18}$$

and the initial state of the system at  $t = 0$

$$\begin{cases} x(0) = x_0 , \\ y(0) = y_0 , \\ p(0) = p_0 . \end{cases} \quad (12.19)$$

Disturbances of the system can, for example, be introduced by parameters that change their values at different points in time.

The general model for electro-mechanical oscillations, given by Equations (12.18), has a number of properties worth some comments:

- It is differential-algebraic. The classical model resulted in a pure differential equation. Differential-algebraic systems are much more complicated to analyse than systems which can be modelled by a "pure" system of differential equations.
- The system is non-linear.
- The system is non-time-invariant, i.e. the time occurs explicitly in the equations. This depends on events in the system, e.g. disturbances and connections, but even on protective actions of different kind.

# 13

## Voltage Stability

*Voltage stability has been a limiting factor in many power systems during the last years. Due to a gradual increase in load the reactive power balance can be critical at peak load conditions. This chapter summarizes the basic concepts and provides basic analyzes for two simple test systems. A number of stability indicators are introduced and applied to one of the test systems. The importance of load characteristics and load dynamics are demonstrated.*

IN THE PREVIOUS chapters it was shown that an active power imbalance could give rise to rotor oscillations, which can cause instability if the disturbances are large enough. If all generators in a system rotate with the same electrical angular velocity (in average over a certain time period) the system is said to be synchronously stable. (Sometimes it is said to be in angle stability). This type of stability is strongly connected to the active power balance in the system. As has been seen from the static analysis the reactive power and the voltage are strongly coupled to each other. As a rule of thumb it can be said that if there is net production of reactive power in a node, the voltage is high in the node, while a deficit of reactive power implies that the voltage is low. It could now be asked whether the interplay between  $Q$  and  $U$  can also cause instabilities similar to the angular instability discussed earlier. It turns out that this is the case. The underlying mechanisms for this voltage instability will be dealt with in this chapter together with some methods of analysis.

### 13.1 Mechanisms of Voltage Instability

In chapter 8 voltage instabilities were classified into slow and fast ones. Even if the physical mechanism is the same, i.e. a lack of reactive power, the power system contingencies and power system structures causing them are different. The final break down, collapse, in the system could be quite fast also in a slow voltage instability, and the actual instability can sometimes be disguised, which makes this kind of instability troublesome to detect in a real system. Consequently it can be hard to get reliable indicators to activate preventive actions if the time needed is available.

### 13.1.1 Long Term Voltage Instability

The time scale of the long term, or slow, voltage instability could be tens of seconds to hours. It develops from a gradual lack of reactive power at a node or in a part of the system. Even if the voltage stability phenomenon is closely coupled to the reactive power balance the active power plays a very important role indirectly. Many loads have an inductive power factor that is not unity, and thus an increase in active power will cause an increase in reactive power consumption. Furthermore, the reactive losses in transmission lines are proportional to the square of the active power transmitted, so heavily loaded lines will influence the reactive power balance significantly. A very deceptive role is sometimes played by synchronous machines and other sources of reactive power. These devices can often supply more reactive power than their steady state rating for a limited time, sometimes up to several minutes, and during this period of time the reactive power balance and voltage could be kept at acceptable values. However, when protections in these devices act to avoid that the equipment is damaged, the reactive power output is drastically reduced with a very fast voltage collapse as a result.

The contributing factors to a slow voltage collapse are thus:

- Load increase
- Load recovery after faults
- Reactive losses in power lines due to high power transfer (This could be caused by line outages due to contingencies.)
- Loss of reactive supply (Capacitors, synchronous machines, etc.)

For the second bullet above, the control and dynamics of load tap-changers are very important. A voltage reduction in the high voltage system will propagate to the lower voltage levels. This will usually result in a reduction of the load powers. However, load tap-changers on the transformers will try to restore the voltage on the low voltage side and thereby increasing the load power. This has in most cases a de-stabilising effect on the voltage stability.

### 13.1.2 Short Term Voltage Instability

For the short term, or fast, voltage instability the actual voltage collapse comes very soon after the disturbance, just a few seconds or less. In these instabilities, loads or other devices with special reactive power characteristics are often involved. Such loads are e.g. induction motors that just after fault consume a lot of reactive power. Other loads that could be very detrimental in this context are some types of power electronics based equipment. As an

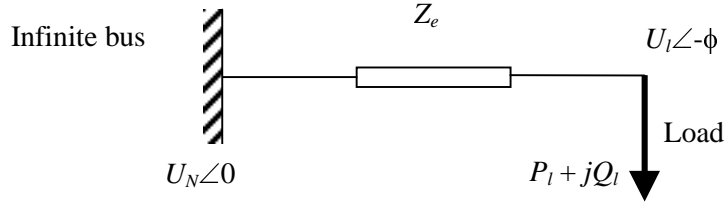


**Figure 13.1.** Simple system for analysis of voltage stability.

example could a line commutated HVDC converter could be de-stabilising in a weak system, and if not properly accounted for in the system design it could lead to system collapse for critical contingencies.

Induction motors are troublesome also in the slow voltage instability. This is particularly the case in countries where the peak load contains a large fraction of air conditioning, which is driven by induction motors. If the voltage gets low, these could stall and hence imply a higher reactive power consumption.

## 13.2 Simple Systems for Analysis of Voltage Stability

The simple model in Figure 11.1 turned out to include all essential properties needed to get an understanding of electro-mechanical oscillations in a power system and of the physical mechanisms that govern the dynamic process. A corresponding simple system for voltage stability is shown in Figure 13.1, which shows how a load is supplied via a line. It shall be emphasised that a detailed analysis of voltage stability in a power system is considerably more complicated than what shall be shown here, but the fundamental mechanisms can be illustrated by the simple system in Figure 13.1.

If it is assumed that the line is lossless, i.e.  $Z_e = jX_e$ , the relations below hold:

$$P_l = \frac{U_l U_N}{X_e} \sin \phi \quad (13.1)$$

$$Q_l = \frac{U_l U_N \cos \phi - U_l^2}{X_e} \quad (13.2)$$

The angle  $\phi$  is not of interest and can be eliminated by moving the non cosine term to the left hand side in (13.2), thereafter squaring both sides of the new equation and of (13.1). After adding the new equations one gets:

$$P_l^2 + \left( Q_l + \frac{U_l^2}{X_e} \right)^2 = \left( \frac{U_l U_N}{X_e} \right)^2 \quad (13.3)$$

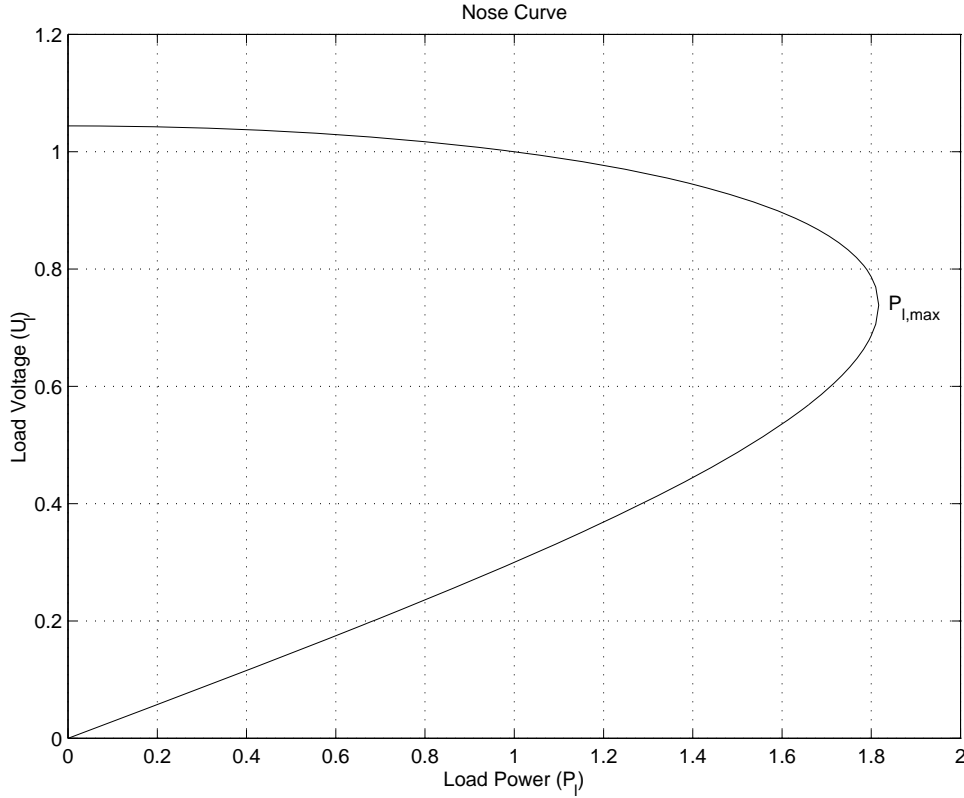


**Figure 13.2.** Relation between active power and voltage magnitude in the load node. The source voltage  $U_N$  is chosen so that nominal voltage gives nominal load power. ( $U_N = 1.044$ ,  $X_e = 0.3$  p.u., and power factor of the load = 1.)

It is now assumed that the reactive load varies in a given way with  $P_l$  and  $U_l$ , e.g. so that the load has constant power factor:

$$\frac{Q_l}{P_l} = k \quad (13.4)$$

If the relation between  $P_l$  and  $U_l$  is plotted in a diagram, Figure 13.2 is obtained, where it is assumed that  $k$  in eq. (13.4) is zero, i.e. the power factor = 1.

The type of diagram shown in Figure 13.2 is often called a “nose curve” by obvious reasons, or a PU-curve. From this figure three observations can be made concerning the number of (theoretically) possible operating points:

1. For  $P_l < P_{l,max}$  there are two solutions.
2. There is exactly one solution for  $P_l = P_{l,max}$ .

3. There is no solution for  $P_l > P_{l,max}$

These observations will now be discussed briefly. For values on  $P_l$  less than  $P_{l,max}$  it was concluded that there are two solutions. Physically the upper solution corresponds to “high” voltage and “low” current, while the lower one corresponds to “low” voltage and “high” current. In the power system the upper solution is of interest, since it yields lower losses. Furthermore in most situations this solution has, which will be shown in section 13.3, other properties which makes it attractive. For  $P_l = P_{l,max}$  there is exactly one solution. The value on  $P_{l,max}$  depends on  $X_e$  and  $U_N$ , but also on the power factor for the load. The more reactive power the load draws the less will  $P_{l,max}$  be. For loads larger than  $P_{l,max}$  there is obviously no solution,<sup>1</sup> and it is consequently clear that the system is unstable if a load greater than  $P_{l,max}$  is connected.

The analysis made above was quite simplified. It was assumed that the load power  $P_l$  could be varied as an independent parameter. However, for a realistic physical load the load power will be a function of the load voltage  $U_l$ , i.e.  $P_l = P_l(U_l)$ . This function is often referred to as the load (voltage) characteristics. The behaviour of the function  $P_l(U_l)$  depends on the time scale considered. In a shorter time scale it is the physical processes involved in the load device that determine the characteristics, while in a longer time scale various control systems must also be taken into account. It turns out that in a the shorter time scale many loads could be modelled as

$$P_l = P_{l0} \left( \frac{U_l}{U_{l0}} \right)^{k_p} \quad (13.5)$$

for not too large variations around the operation point  $U_l = U_{l0}$ , with  $k_p$  typically  $\approx 1 - 2$ . In the longer time scale control systems strive for keeping the load power constant for many load devices. Load modelling is very important in voltage stability analysis, but the detailed knowledge about load models in real systems is often very rudimentary. Much work is being done in the field, but still more work is needed.

Another simple system that could exhibit voltage unstable behavior is shown in Figure 13.3. In this system there are two fairly strong systems, 1 and 2, interconnected by long transmission lines. Between the two areas 1 and 2 there is a small system connected, denoted by index  $m$  in Figure 13.3.

---

<sup>1</sup>Mathematically the point  $P_l = P_{l,max}$  is called a bifurcation point with the active load as parameter. At this point the two solutions coalesce to one, which will disappear when  $P_l$  is further increased. It can be worth mentioning that it is not always true that the maximum available load power is a bifurcation point, but this depends on the independent parameter in the system. In the studied case  $P_l$  is the parameter, but sometimes it can be the load impedance or another parameter, e.g. numbers of connected asynchronous machines. In these cases maximum available load power and the bifurcation point do not necessarily coincide. See also the discussion in section 13.3

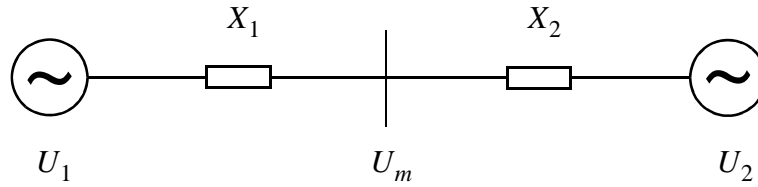


**Figure 13.3.** Another simple system equivalent for studying voltage instability.

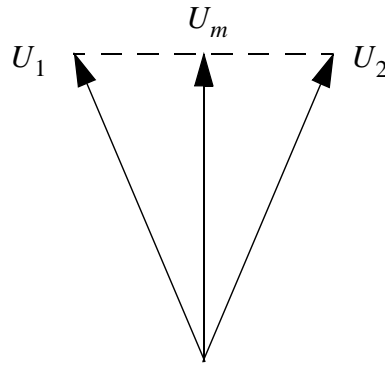


**Figure 13.4.** Voltage phasors for the system in Figure 13.3.

For simplicity it is assumed that  $X_1 = X_2$ ,  $U_1 = U_2$ , and that no load is consumed at the intermediate bus. The voltage  $U_m$  will then be

$$U_m = U_1 \cos(\phi/2) \quad (13.6)$$

where  $\phi$  is the angle between the voltages  $U_1$  and  $U_2$ , see Figure 13.4. If now the angle  $\phi$  is increased due to an increase in the transmitted power or in a fault increasing the reactance between areas 1 and 2, the voltage  $U_m$  will decrease. If there is no reactive power resources at this point it might lead to a voltage collapse in this area, that could in worst case influence the whole system.

### 13.3 Analysis of Voltage Stability

The simple system of Figure 13.1 will now be analyzed for a few cases. In the analysis of voltage stability a few indicators have been introduced to simplify

the stability analysis. These indicators are based on small signal properties of the system and are consequently derived from linearized models. As concluded from the analysis of synchronous stability, linear analysis is often very powerful, but must be used with care since it only captures the local behavior of the system around an operating point. To determine the global behavior the full non-linear model must be employed.

### 13.3.1 Stability Indicators

In this section voltage stability indicators of the system in Figure 13.1 will be discussed. Similar indicators with similar properties exist also for larger systems and these are often used in voltage stability studies of real systems.

#### Voltage Sensitivity Factor

The Voltage Sensitivity Factor  $VSF$  is one of the most used indicators or indices of voltage stability. It is defined for a given node  $i$  as

$$VSF_i = \frac{\Delta U_i}{\Delta Q_i} \quad (13.7)$$

The physical interpretation of  $VSF$  is that it measures the change in voltage magnitude at a given node as a consequence of a reactive power injection in that node. Since all voltage control in a power system is based on that a reactive power injection results in voltage increase, it is clear that a stability criterion is

$$VSF_i > 0 \quad (13.8)$$

Furthermore, it is reasonable to require that an injection of reactive power in any node will not decrease the voltage in any node in the system. This property is often called *voltage regularity*. The  $VSF$ -indicator will be demonstrated on the system in Figure 13.1 later on.

#### $\Delta U/\Delta E$ -indicator

Another indicator that is more closely related to the voltage control in a power system is given by  $\Delta U/\Delta E$ , where  $U$  is the voltage magnitude of a given bus and  $E$  is a voltage that is controllable, e.g. at the terminals of a synchronous machine. Also in this case the requirement of stability is given by

$$\frac{\Delta U}{\Delta E} > 0 \quad (13.9)$$

#### $\Delta Q_g/\Delta Q_l$ -criterion

This criterion relates the reactive power consumed at the load(s) to the reactive power generated by the synchronous machines. In Figure 13.1 it

thus relates the reactive power injected at the infinite bus, here called  $Q_g$ , to the reactive power consumed by the load  $Q_l$ . The stability criterion is

$$\frac{\Delta Q_g}{\Delta Q_l} > 0 \quad (13.10)$$

It can be shown that all the stability criteria above are equivalent in most realistic systems. Which one to use is then dependent on which system variables that are known and controllable in a given situation. The three criteria have also that in common that at the transition point to instability they tend to infinity before going negative.

### 13.3.2 Analysis of Simple System

To gain a better understanding of the mechanisms governing voltage stability a few different cases will be analysed. The system in Figure 13.1 will be used in all cases.

#### Influence of System Parameters

Here the influence of a few system parameters will be investigated. The nose curve in Figure 13.2 was drawn for a lossless system, i.e.  $\theta = 90^\circ$ , and the power factor of the load being equal to unity. In Figure 13.5 the power factor has been varied, and in Figure 13.6 nose curves for a number of different values of the impedance angle is plotted. In all the cases the magnitude of the source voltage  $U_N$  has been adjusted so that when the load is 1 p.u. the load voltage  $U_l = 1$  p.u. From Figure 13.5 it can be concluded that the power factor has a significant influence on the nose curve, and thereby on the voltage stability. If the reactive consumption of the load could be compensated at the load point, this results in higher  $P_{l,max}$  but also in a better voltage regulation around the nominal operating point.

The conclusion drawn from Figure 13.6 is that the impedance angle  $\theta$  does not influence the nose curve significantly for realistic values of high voltage systems. A  $X/R$  ratio of 10 results in  $\theta \approx 84^\circ$  and the deviation from the curve corresponding to  $\theta = 90^\circ$  is insignificant. Thus, in the following it will be assumed that  $\theta = 90^\circ$ .

#### Influence of Load Characteristics

The voltage characteristics of the loads have a very large impact on the voltage stability as will be shown in the following. It should be pointed out that the actual dynamics occurring in a real system during the course of events to be discussed here could be very complicated and that the description given here is simplified to emphasise the fundamental dynamics in the system. The very detailed interplay between load dynamics and voltage control might cause that the actual course of events turn out to be different.

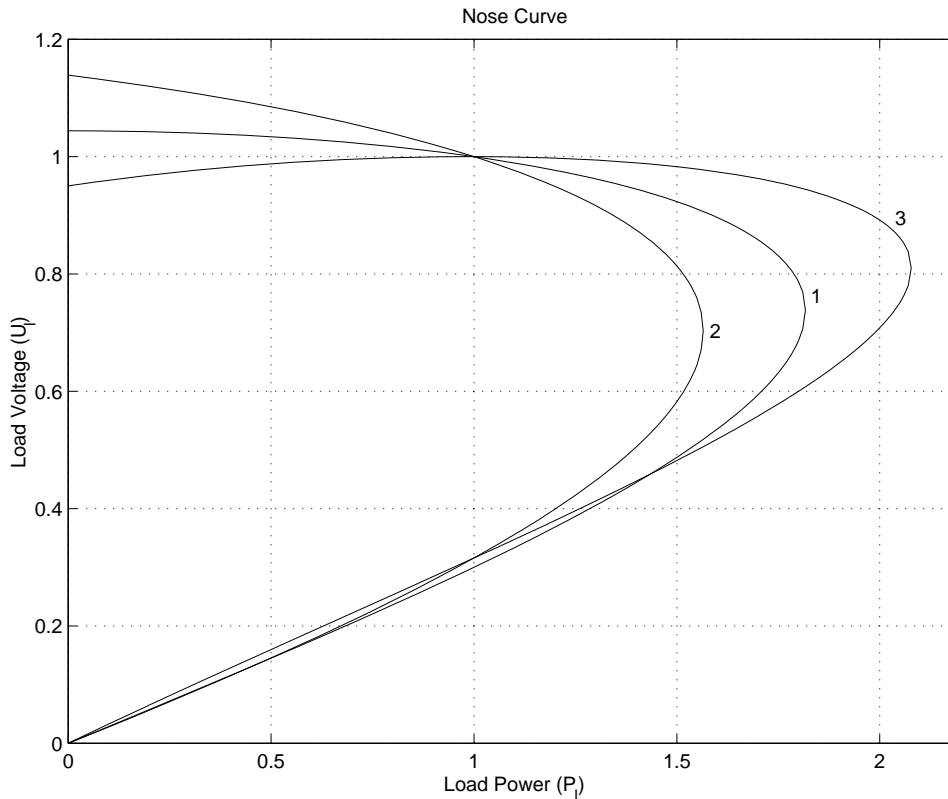


**Figure 13.5.** Nose curves for different values of the power factor of the load of the system in Figure 13.1. Curve 1: Power factor = 1. Curve 2: Power factor = 0.95 (inductive). Curve 3: Power factor = 0.95 (capacitive)

### Load Admittance Influence on Load Power

In Figure 13.7 the load characteristics of an impedance load, i.e. with  $k_p = 2$  in eq. (13.5) has been plotted together with two different nose curves. A very important property of a load is the load power controllability, i.e. the possibility to increase or decrease a load power by controlling suitable parameters. If it is assumed that the physical load in Figure 13.7 is a heater, this control is achieved by changing the resistance (conductance) of the load. Assuming that the voltage is constant the load power can then be increased by decreasing the resistance of the load, i.e. to increase the conductance of the load. In a more general case this is usually expressed as an increase in load power which is achieved by increasing the load admittance. Increasing the load admittance in a general case, when the load is more complicated than a simple resistor as in the heater case, should be interpreted as connecting more load devices of the same kind at the load node. Actually this

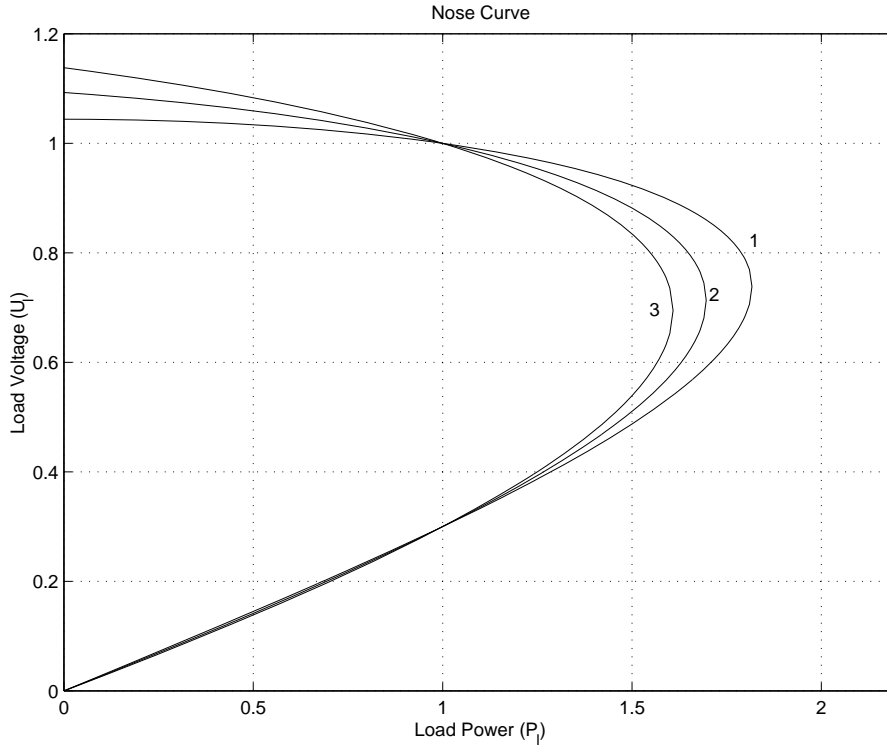


**Figure 13.6.** Nose curves for different values of the impedance angle  $\theta$  of  $Z_e$  of the system in Figure 13.1. Curve 1:  $\theta = 90^\circ$ . Curve 2:  $\theta = 80^\circ$ . Curve 3:  $\theta = 70^\circ$

has formed the basis for one definition of voltage stability:

*A system is said to be voltage stable if an increase in load admittance results in an increase in load power.*

Let us now revert to Figure 13.7. If the nose curve of the system is according to curve 1 it is seen that an increase in load admittance, dashed load curve, gives an increase in load power. Correspondingly a decrease in load admittance, dotted curve, for the operating point on nose curve 1, gives a decrease in load power. Thus the system is voltage stable according to the definition above for the undisturbed (nominal system). If a disturbance occurs increasing the line impedance drastically, the nose curve will be according to curve 2 in Figure 13.7. The new operating point will be the intersection between the load curve and the nose curve resulting a lower load power and a lower voltage. If there is a controller trying to restore the load power to nominal it will increase the load admittance (dashed load curve), which will result in a voltage decrease and a load power decrease. This could be explained in the following way. The load admittance increase results in an increase

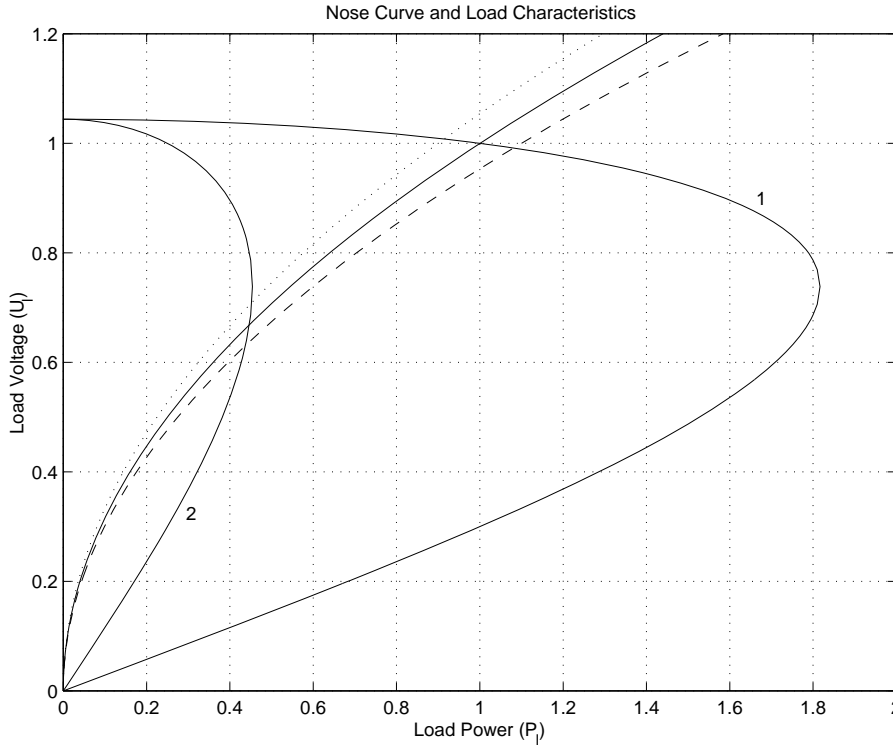


**Figure 13.7.** Nose curve for undisturbed system, curve 1, and for a system after a contingency resulting in increase of  $Z_e$ , curve 2. Load characteristics for impedance load at nominal operating point, solid curve. Load curve with 10% increase in load admittance, dashed curve. Load curve with 10% reduction in load admittance, dotted curve.

of the load current. This current increase is however so large that the load voltage drops so much that the load power decreases. In the nominal operating point of nose curve 1, the voltage drop due to the current increase is however so small that the net effect is an increase in the load power. The situation is clearly unstable for nose curve 2, and the system will collapse. In Figure 13.7 the voltage after the disturbance, nose curve 2, is very low and in a real system protections would have been activated. It should also be noted that since  $P_{l,max}$  of nose curve 2 is much lower than the nominal power, the load power could never recover to the pre-fault value. Generally it can be seen that an increase in load admittance will give an increase in load power if

$$\frac{dP_{ld}}{dU} > \frac{dP_l}{dU} \quad (13.11)$$

where  $P_{ld}$  refers to the load device, i.e. the load characteristics, and  $P_l$  to the load power of the nose curve.

### VSF Criterion

The *VSF* criterion was introduced above and that will now be analysed for different load characteristics. This criterion is closely related to how the voltage control will act in the system. It is rather straightforward to calculate *VSF* for different load characteristics and operating points on the nose curve. From such an analysis the following can be concluded:

- For constant power loads, i.e.  $k_p = 0$  in eq. (13.5), operating points on the upper half of the nose curve are stable, i.e.  $VSF > 0$ , while those on the lower part are unstable or  $VSF < 0$ .
- For loads with  $1 \leq k_p$ , i.e. including constant current and constant impedance loads,  $VSF > 0$  for all operating points, indicating voltage regularity.
- For  $0 \leq k_p < 1$  operating points on the upper part of the nose curve are stable. In addition a part of the lower part is also stable ranging from  $P_{l,max}$  to lower  $P_l$  values. This interval increases with  $k_p$ .

Since in a longer time scale most loads could be approximated by constant power loads, permanent operation is feasible only at the upper part of the nose curve. During transients operation on the lower part could be acceptable.

### Load Dynamics

The discussion in this paragraph relates to the discussion concerning load admittance, but deals with a somewhat different disturbance. The system in Figure 13.1 is considered again. It is now assumed that a voltage increase of 5% occurs in the sending end system, i.e.  $U_N$  is increased by 5%. In Figure 13.8 the nose curves and load characteristics corresponding to an impedance load are depicted. The load is controlled in such a way that the load power should be constant, which e.g. could be the case for a thermostat controlled heater. The voltage increase resulted in a load power increase and consequently the load power control orders a decrease in load admittance. This decrease in load admittance results in the dashed load characteristics in Figure 13.8, and the system can settle to a new operating point at the desired load power, i.e. 1 p.u., but at a slightly higher voltage. An analysis of the behavior of the system shows that, if the sending end voltage is slightly decreased, the system will settle at 1 p.u. load power at a slightly lower voltage.

Now assume that the system is operating on the lower part of the nose curve, see Figure 13.9. According to the *VSF* criterion this operating point is stable. The same disturbance as in the previous case is considered. From Figures 13.8 and 13.9 it can be concluded that both systems are stable

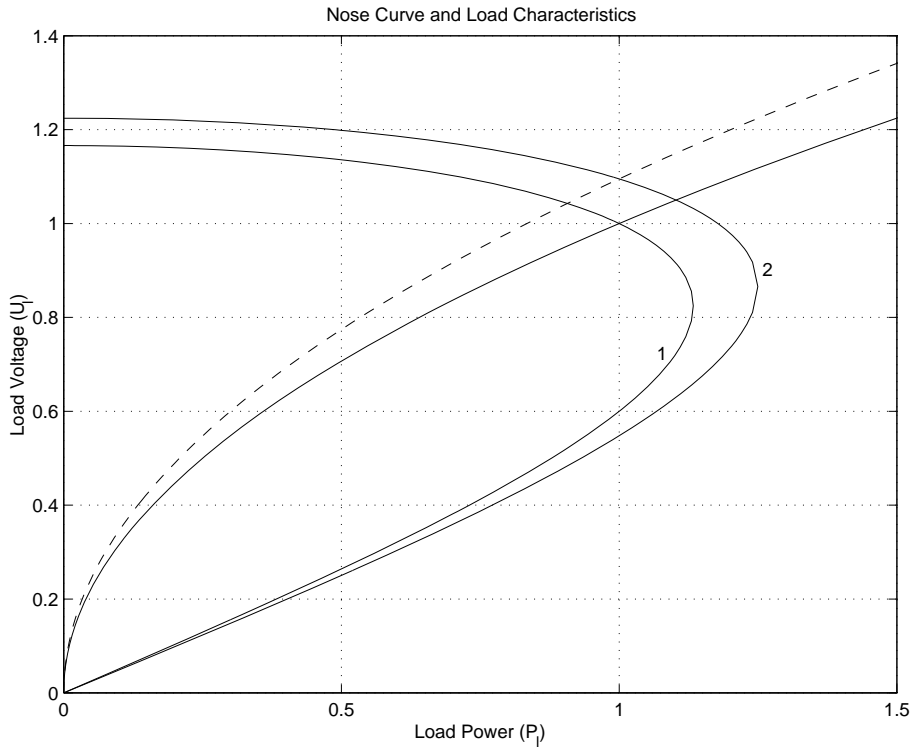


**Figure 13.8.** Nose curve for undisturbed system, curve 1, and for a system where the sending end voltage has been increased by 5%, curve 2. Solid load characteristics corresponds to load admittance before voltage increase. Dashed load characteristics corresponds to decreased load admittance to give load power = 1 p.u. for system after disturbance.

according to the  $\Delta U/\Delta E$  criterion since an increase in the sending voltage causes an increase in the load voltage. It is seen that voltage increase in Figures 13.9 implies a load power increase. The same load power controller as in the previous case would order a decrease in the load admittance to decrease the load power. Such a load admittance decrease is represented by the dashed load characteristics in Figures 13.9. But, the load admittance decrease results in a load power increase. If there are no restrictions on the action of the controller it will continue to decrease the load admittance until the point "A" of Figure 13.9 is reached. A similar analysis shows that a voltage decrease in the sending end system will result in that the load admittance will increase until (theoretically) the point (0,0) is reached. It is thus clear that the initial operating point of Figures 13.9 is unstable.

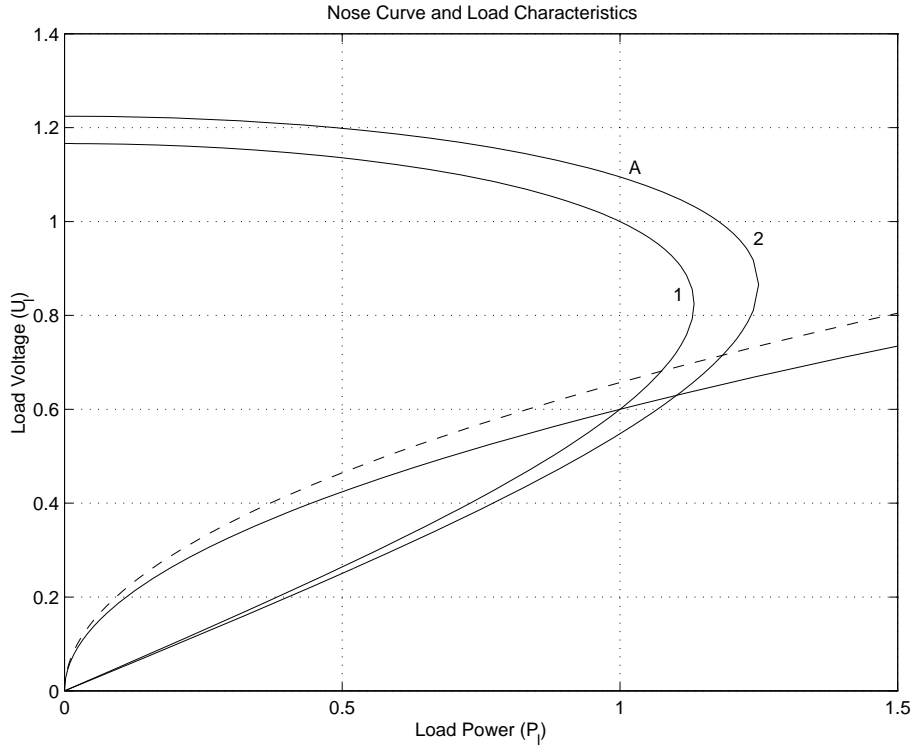


**Figure 13.9.** Nose curve for undisturbed system, curve 1, and for a system where the sending end voltage has been increased by 5%, curve 2. Solid load characteristics corresponds to load admittance before voltage increase. Dashed load characteristics corresponds to decreased load admittance.

### QU curves

Finally another method sometimes used to analyse voltage stability will be demonstrated. In the system of Figure 13.1 one can calculate the amount of reactive power that must be provided to the network for a given load power for different load voltages. If this is done for the system of Figure 13.1 assuming  $P_l = 1$  p.u., a curve according to Figure 13.10 is obtained. The same data as in Figure 13.2 have been used. Since Figure 13.2 was calculated with unity power factor of the load, the load voltages corresponding to  $Q = 0$  of Figure 13.10 should correspond to the voltages giving  $P_l = 1$  p.u. in Figure 13.2. This is easily verified. Furthermore, the *VSF* criterion for stability says that an reactive power injection should result in a higher voltage. In the *QU* curve this corresponds to a positive derivative, which are for load voltages higher than  $\approx 0.6$  p.u.

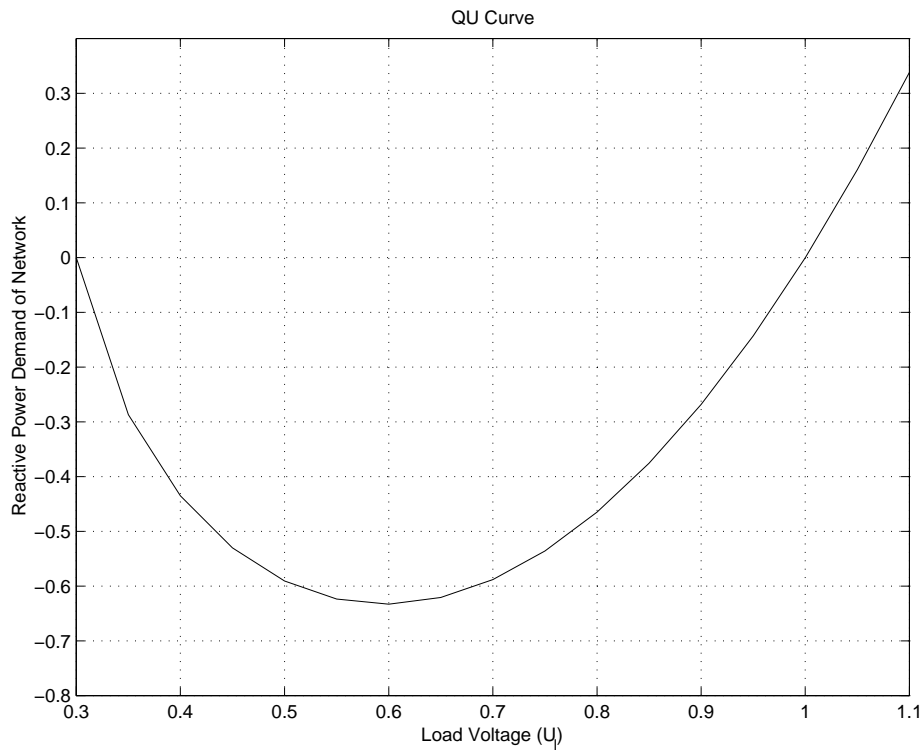


**Figure 13.10.**  $QU$  curve for the system of Figure 13.1. ( $U_N = 1.044$ ,  $X_e = 0.3$  p.u.,  $P_l = 1.0$  p.u.)



# 14

## Control of Electric Power Systems

*This chapter gives an introduction to control of power systems. Both the faster local controls and slower centralised controls are briefly discussed.*

A POWER SYSTEM is planned, designed and built to supply the consumers with electrical energy considering:

- Economy
- Quality
- Supply security (Reliability)
- Environmental impact

The last point has become more and more important during the latest years. This can be seen from the fact that most of the larger companies nowadays have special departments responsible for that the companies follow laws and regulations within the environment area. The three first points above constitute the basis of the optimisation that the power companies must make regarding their investments and daily operation. It is evident that economical considerations must be regarded when deciding issues about quality and supply security for the system. The higher quality and supply security that is required, the more expensive the electrical energy becomes. Methods based on mathematical analysis and decision making theory (operations research) have been worked out to handle this optimisation problem, which contains several considerations/adjustments that are hard to formulate in a stringent mathematical form. As cheap and safe access to electrical energy is of great importance for almost all activities in a modern society, it is not surprising that the decisions makers in the power industry were pioneers to utilise advanced optimisation methods and other analysis tools for expansion and investment planning.

In this compendium we will limit ourselves to discussing how a power system can be controlled to fulfill the constraints regarding quality. A very short introduction is also given about the overall control in a power system, which besides its aim to fulfill the quality even plays an important role in the supply security.

Three important factors that define power quality are:

- Frequency variations
- Voltage variations
- Waveform of voltage and current

The two first factors will be dealt with in this course, but the last point is getting greater importance because more nonlinear components are connected to the electrical system, e.g. power electronics. These can give rise to harmonics.

It has been shown earlier that the frequency is a very good indicator on the active power balance in a power system. The frequency is constant when the same amount of electrical power is produced as consumed by the loads, including system losses. If this is not the case frequency changes will occur. It can also be noted that the frequency is the same in the whole system at steady state. This depends on that the active power easily can be transported in the system (that is why it has been possible to build the power systems of today's size). It is often said that the active power is a global quantity, unlike the reactive power which is a local quantity, since reactive power cannot be transmitted over longer (electrical) distances. (This is because of that  $X$  normally is much greater than  $R$  in a power system, at least for transmission and sub-transmission networks.)

The frequency of the system is reduced when a load increase is not compensated for by a corresponding increase of the turbine power of the connected generators. The power deficit decelerates the generator rotors and consequently the frequency is reduced.

Frequency reductions also arise when production is lost, e.g. as a consequence of failures in the system which lead to that protections disconnect the failed equipment. Too large reductions of the frequency could lead to system collapse, since a lot of equipment in the power stations, e.g. power supply systems, do not tolerate too low frequencies. A load reduction in the system which is not compensated for by a reduction of turbine power leads to a frequency increase.

The permitted stationary frequency deviation in interconnected power systems is at normal operation typically 0.2 % or 0.1 Hz. There are also sometimes requirements on how large the difference between actual, physical time and the time corresponding to the integrated frequency from the system can be. This time difference is normally not permitted to be larger than 10s.

It is also important that the voltage deviations in the system is limited. This is of importance for the connected loads, but a "good" voltage profile is also essential for keeping the losses low and for utilising the reactive reserves to establish a secure operation of the system. Voltage control is, as been pointed out earlier, a more local control than the frequency control. If the

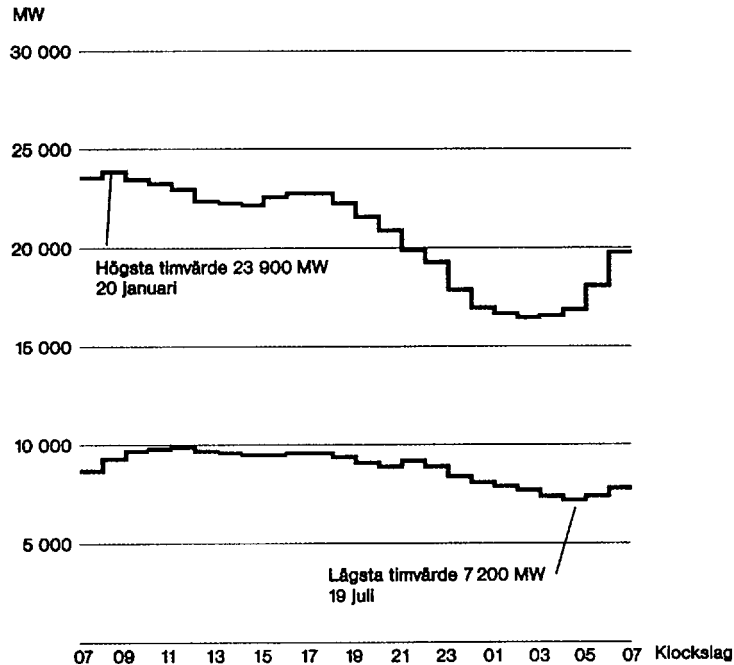


**Figure 14.1.** Typical variation of the load in a power system. The upper curve shows the highest hourly average values over the year and the lower curve the lowest hourly average value.

voltage deviates from the set value in a node, the control action must be made in this or a nearby node.

## 14.1 Control of Active Power and Frequency

Since the stored energy in the system is relatively small, the constant of inertia for a typical generator is  $\approx 4$  s, the electrical energy must be produced in the same moment as it is consumed by the loads. Since the load varies, a certain power reserve must constantly be available. In addition for the daily variation, see Figure 14.1, there are continuously spontaneous load variations up to  $\approx 2\%$  of the total load during a minute. The generation reserves are generally divided into different groups according to their properties: spinning, supplementary and back-up, see Figure 14.2. The reserves are at operation planning divided into normal operation and disturbance reserve after the cause of the needed reserve.

At the operation planning of the power system forecasts over the expected load are carried out continuously. Forecasted values can never ex-

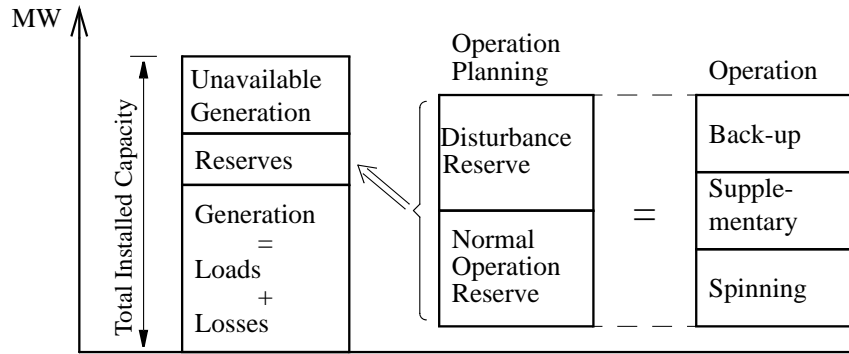


**Figure 14.2.** The different generation reserves in a power system.

actually coincide with real values, therefore a reserve which can compensate the difference is required. Therefore frequency variations arise, which must be compensated for. Both power imbalances due to incorrect load forecasts and to occasional load variations are controlled with the normal operation reserve.

Events which can lead to utilisation of the disturbance reserve are: generator trips or line trips. Disturbances of that kind can lead to frequency reductions and reserves must often be put into operation.

In the operation the reserves are divided after needed time for activation, see Figure 14.2. To keep reserves is expensive and therefore it is of interest to minimise the needed effort of the reserves for maintaining the wanted reliability and security.

### 14.1.1 Spinning reserve

The spinning reserve is co-ordinated in the Nordic system and is above all located in hydro units with turbine control, see Figure 14.3. The turbine control is activated within some seconds if the frequency deviates from the normal and changes then the turbine setting for the regulating generators by changing the guide vane opening to the turbines. When the system frequency is changed the power demand of certain loads is also changed, specially for motors, in such a way that a frequency increase leads to increased power consumption and a frequency decrease gives lower power consumption. This frequency dependence of the load stabilises the frequency. Components for heat- and light production are fairly insensitive to frequency variations.

The resulting change in active power,  $\Delta P$ , at a frequency change in the system is:

$$\Delta P = \Delta P_g - \Delta P_l \quad (14.1)$$

where:  $\Delta P_g$  = the total change in output power from the generators par-

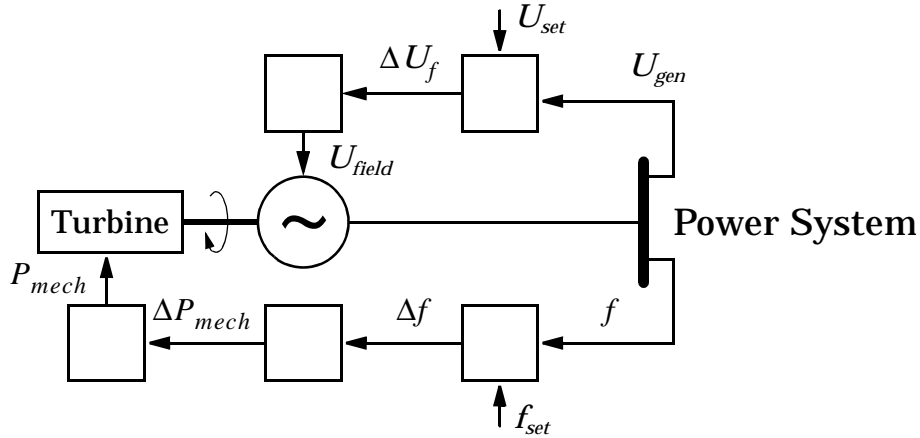


**Figure 14.3.** Generator unit with voltage regulator and turbine regulator for frequency control.

ticipating in the frequency control,  $\Delta P_l$  = the total frequency dependent load power change. The frequency dependence of the load can often be approximated as

$$\Delta P_l = D\Delta f \quad (14.2)$$

where  $D$  is a constant. The value on  $D$  is typically 0 – 4 %/Hz, but large variations occur depending on the kind of load.

The frequency control is performed so that, at least for small frequency deviations, the total change in output power of the frequency controlling generators are (in steady state) proportional to the frequency change,  $\Delta f$ . The relation between changes in active power and frequency deviations can then be written

$$\Delta P_g = -R\Delta f \quad (14.3)$$

The constant  $R$  is determined by the setting of the turbine control of the frequency controlling generators, and is named the *systems frequency regulation constant* or *frequency droop* and is normally given in MW/Hz. The frequency regulation for a system is established so that the frequency does not fall outside given limits at certain dimensional disturbances which can occur, e.g. trip of the largest generator in the system.

It shall be noted that the variation of frequency, computed from the above relations, are the steady state values which are obtained after the frequency controllers have responded. The transient frequency deviation during the process following a large disturbance can be considerably larger than the stationary one, up to some Hz. In Figure 14.4 it is shown how the frequency can vary after a disturbance in the system. As seen the maximal frequency deviation is considerably greater than the stationary

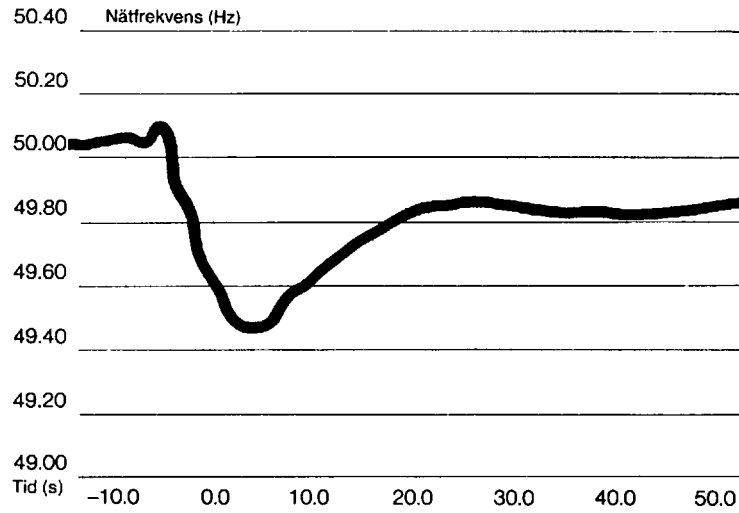


**Figure 14.4.** The transient frequency response after a production loss. The diagram is a recording from the Nordic system at a loss of a 1000 MW unit on the 24 November 1983.

one. The transient behaviour of the frequency is highly dependent on the characteristics of the turbine regulators of the generators, and in this respect the hydro turbines and steam turbines are totally different. Shortly it can be said that the transient frequency deviation is considerably larger if the frequency control is performed by hydro power. This is due to that the hydro turbine is a non-minimum-phase system.

### 14.1.2 Supplementary Reserves

Supplementary reserves must also be available to cope with fast changes in the generation plan at large forecast deviations or at permanent outages when the spinning reserve has been used and must be restored. From the remaining deviation of frequency and the knowledge about the system frequency droop it is straightforward for the system operators to compute how much “new” power production must be connected to restore the system within the prescribed limits. This can either be done by connecting new production or by increasing the turbine power at generators in operation. In some systems this is handled manually, but in some countries, e.g. in continental Europe and USA, this is at certain power companies accomplished by special slow automatic controllers, so-called Automatic Generation Control (AGC). This regulation is considerably slower than frequency control and must be designed not to interact with the frequency control in an adverse

way.

### 14.1.3 Back-Up Reserves

The slow reserve shall be available within about 2 h. It is needed for security reasons to restore the fast reserve when this has been used. The slow reserve can consist of thermal power which is kept at stand by. This implies that pressure and temperature is kept on a level which permits synchronisation and load recovery within 2 hours. Co-generation back-up units for which it is possible to increase the electrical power can also be used.

## 14.2 Control of Reactive Power and Voltage

### 14.2.1 Reactive Power Control

In steady state operation both active power balance and reactive power balance must be maintained. The reactive power generated by synchronous machines and capacitances must be equal to the reactive power of the loads plus the reactive transmission losses. If the active power balance is not kept, the frequency in the system will be influenced, while an imbalance in reactive power will result in that the voltages in the system differ from the desired ones.

If the power system is operated in the correct way, the voltage drops on the lines are usually small. The voltages in the nodes of the system will then almost be the same (flat voltage profile). In this case the transmission system is effectively used, i.e. primarily for transmission of active power, and not for transmission of reactive power.

As known from the Static Analysis the voltage in a system is strongly affected by the reactive power flow. Consequently the voltage can be controlled to desired values, by control of the reactive power. Increased production of reactive power gives higher voltage nearby the production source, while an increased consumption of reactive power gives lower voltage. Therefore it is of great interest to study which components and devices which can be used to regulate the reactive power in a power system. While the active power is entirely produced in the generators of the system, there are several sources of reactive power. In the other hand the reactive power cannot be transported over long distances in the system, since normally  $X \gg R$  in a power system.

Important producers of reactive power are:

- Overexcited synchronous machines
- Capacitor banks
- The capacitance of overhead lines and cables

Important consumers of reactive power are:

- Inductive static loads
- Under-excited synchronous machines
- Induction motors
- Shunt reactors
- The inductance of overhead lines and cables
- Transformer inductances
- Line commutated static converters

For some of these the reactive power is easy to control, while for others it is practically impossible. The reactive power of the synchronous machines is easily controlled by means of the excitation. Switching of shunt capacitors and reactors can also control the reactive power. If thyristors are used to switch capacitors and/or thyristors are used to control the current through shunt reactors, a fast and step-less control of the reactive power can be obtained. Such a device is called SVC (Static Var Compensator).

As has been shown earlier it is most effective to compensate the reactive power as close as possible to the reactive load. There are certain high voltage tariffs to encourage large consumers, e.g. industries, and electrical distributions companies to compensate their loads in an effective way. These tariffs are generally designed so that the reactive power is only allowed to reach a certain percentage of the active power. If this percentage is exceeded, the consumer has to pay for the reactive power. The high voltage network is in that way primarily used for transmission of active power.

The reactive losses of power lines and transformers depend on the size of the reactance. In overhead-transmission lines the reactance can be slightly reduced by the use of multiple conductors. The only possibility to radically reduce the total reactance of a transmission line is to connect a series capacitor, see 6.5.1 in the part "Static Analysis".

### 14.2.2 Voltage Control

The following factors influence primarily the voltages in a power system:

- Terminal voltages of synchronous machines
- Impedances of lines
- Transmitted reactive power
- Turns ratio of transformers

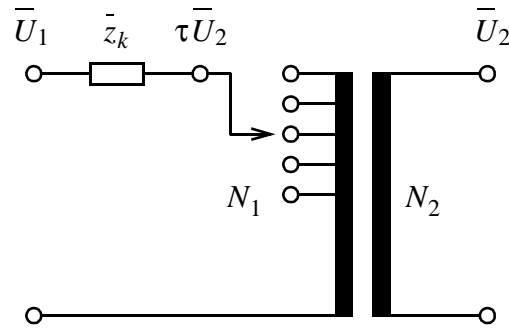


**Figure 14.5.** Transformer with variable turns-ratio (tap changer).

A suitable use of these leads to the desired voltage profile.

The generators are often operated at constant voltage, by using an automatic voltage regulator (AVR). The output from this controls the excitation of the machine via the electric field exciter so that the voltage is equal to the set value, see Figure 14.3. The voltage drop caused by the generator transformer is sometimes compensated totally or partly for, and the voltage can consequently be kept constant on the high voltage side of the transformer. Synchronous compensators are installed for voltage control. These are synchronous machines without turbine or mechanical load, which can produce and consume reactive power by controlling the excitation. Nowadays new installations of synchronous compensators are very rare.

The impact of the impedances of the lines on the reactive power balance, and thereby the voltage, have been analysed in the Static Analysis. These are generally not used for control of the reactive power. Series capacitors are generally installed to increase the active transmission capacity of a line.

From the static analysis it is also known that the reactive power transmitted has a great impact on the voltage profile. Large reactive transmissions cause large voltage drops, thus these should be avoided. Instead, the production of reactive power should be as close as possible to the reactive loads. This can be achieved by the excitation of the synchronous machines, which have been described above. However, there are often no synchronous machines close to the load, so the most cost-effective way is to use shunt capacitors which are switched according to the load variations. An SVC can be economically motivated if fast response or accuracy in the regulation is required. Shunt reactors must sometimes be installed to limit the voltages to reasonable levels. In networks which contain a lot of cables this is also necessary, since the reactive generation from these is much larger than from overhead lines. ( $C$  is larger and  $X$  is smaller.)

An important method for controlling the voltage in power systems is by changing the turns ratio of a transformer. Certain transformers are

equipped with a number of taps on one of the windings. Voltage control can be obtained by switching between these taps, see Figure 14.5. If switching during operation can be made by means of tap changers, this possibility of voltage control is very effective and useful. Normally the taps are placed on the high voltage winding, the upper side, since then the lowest current needs to be switched.

If  $N_1$  is the number of turns on the upper side and  $N_2$  is the number of turns on the lower side, the turns ratio of transformer is defined as

$$\tau = \frac{N_1}{N_2} \quad (14.4)$$

Then the relation between the voltage on the high voltage side,  $U_1$ , and on the low voltage side,  $U_2$ , at no load is

$$U_2 = \frac{U_1}{\tau} \quad (14.5)$$

If the voltage decreases on the high voltage side, the voltage on the lower side can be kept constant by decreasing  $\tau$ , i.e. by switching off a number of windings on the high voltage side. When the transformer is loaded eq. (14.5) is of course not correct, since the load current gives a voltage drop over the leakage reactance of the transformer,  $z_k$ , but the same principle can still be applied at voltage control.

Transformers with automatic tap changer control are often used for voltage control in distribution networks. The voltage at the consumers can therefore be kept fairly constant even though voltage variations occur at the high voltage network. Time constants in these regulators are typically some ten seconds.

Sometimes the turns ratio cannot be changed during operation, but just manually when the transformer is off load. In this case one can only change the voltage level in large but not control the voltage variations in the network.

### 14.3 Supervisory Control of Electric Power Systems

The frequency- and voltage control described above are performed by local controllers, but overall and central control is also needed to secure safe and economical operation of the power system. This control is performed from control centres which generally are hierarchically organised. Often there is a national centre on the top, which supervises the national transmission system and co-ordinates the frequency control. In certain cases this centre can also co-ordinate the operation of different power companies, which in that way can optimise their operation. The next level contains a number of regional control centres which co-ordinate and supervise the regional networks

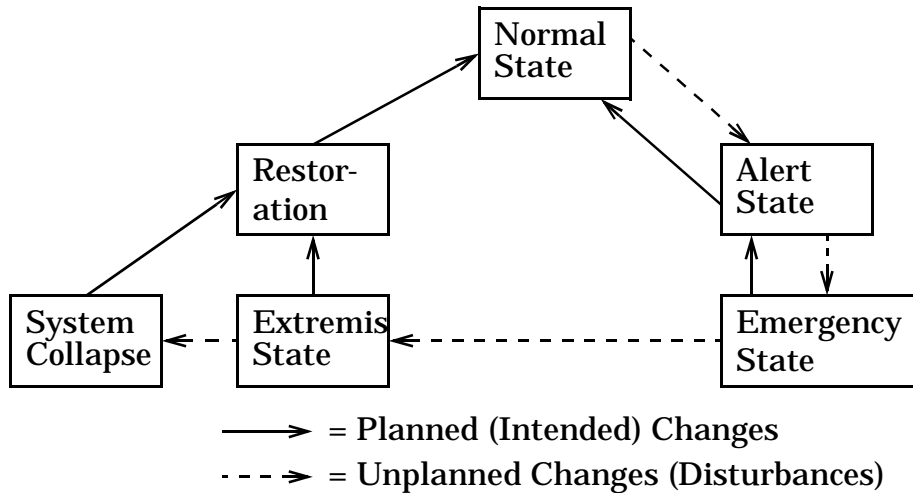


**Figure 14.6.** The different operating states of a power system.

and control the generation within that region. The next level of operation centre has the task of controlling the operation for one or several power stations. The information flow between these different levels is very large and there is an extensive communication system parallel with the electrical power system to handle this. Computers are extensively used to perform the overall control of the power system, but also the operators make important decisions in the control process.

The different states that a power system can be found in is often described according to Figure 14.6. *Normal operation* is the state which is desired for a system. Besides that all quantities in the system are within the limits given by the equipment and the system, there are margins so that the system can tolerate certain predetermined disturbances, e.g. loss of lines and generation, without endangering the system security. When the system is in *alert operation* all quantities are still within the allowed limits, but the margins which existed for normal operation have been lost as a consequence of some disturbance(s). In alert operation power can be supplied as usual, and the consumers do not notice that any disturbance has affected the system. In this state the goal for the control is to bring the system back to normal operation through connecting equipment to establish margins to cope with new disturbances. *Emergency operation* can occur if further disturbances occur or if a large disturbance strikes the system. Some quantities, e.g. voltages or power flows on the lines, are now outside the permitted limits. Still there is no shortage of power, but fast actions must be taken otherwise further equipment will be tripped by different protections. If it is not succeeded to bring the system to alert operation and gradually

	<b>Operating Margins</b>	<b>Rating Limits</b>	$P_{gen} = P_{load} + P_{loss}$
<b>Normal State</b>	OK	OK	OK
<b>Alert State</b>	No	OK	OK
<b>Emergency State</b>	No	No	OK
<b>Extremis State</b>	No	No	No

**Table 14.1.** Characteristics of the different operating states of a power system.

to normal operation, there is a risk to end up in *extremis operation*. In this state there is not enough power to supply the connected loads, and the frequency is decreasing. Load shedding is usually needed to save the system. First of all such load is shed that easily can be connected again without any larger damages to the consumers, for example electrical heaters or domestic loads. As a last resort, loads which demand long time for restoration, e.g. process industry, are shed.

If this defence is not successful, the system, or often parts of the system, will collapse, i.e. be de-energised, which is a state which must be avoided by all means. If this state should be reached the system must as fast as possible be brought back, often part by part, to normal operation. This process is called *system restoration*. The transitions which are marked with unbroken lines in the Figure 14.6 are initiated and performed from different control centres. (The broken lines denote undesired disturbances.) The central control plays an important role to get the system into normal operation.

In Table 14.1 the characteristics of the different operating states of a power system are summarized.

# Appendix A

## Phase-Shifting Transformers

*In three-phase transformers it is possible to arrange the windings in such way that not only the voltage magnitudes between the primary and secondary sides are different but also the phase angles. In this appendix a number of winding arrangements are described that could accomplish such a phase shift.*

FOR SINGLE-PHASE TRANSFORMERS the relation between the primary and secondary side voltages is a real number, known as the turns-ratio, during sinusoidal steady state conditions. In three phase systems the windings can be arranged in different ways, and in some of these configurations a phase-shift is also introduced between the primary and secondary side. Consider the two three-phase transformers in Figure A.1. The transformer at the top has both the primary and secondary windings connected in a Y, called a Y-Y or wye-wye connection and denoted Yy. Obviously there is only a transformation of the magnitude of the voltages between the two sides. In the transformer at the bottom however, the primary side is delta connected and the secondary side is connected in Y, often denoted Dy or  $\Delta y$ . In addition a phase shift is here introduced between the primary and secondary windings, in this case  $30^\circ$ . Obviously other multiples of  $30^\circ$  phase shifts can also be obtained.

An obvious way to incorporate the phase-shift in the transformer model would be to allow for a complex turns-ratio, i.e.  $t = a \cdot e^{j\varphi}$ , as explained in subsection 2.2.2. As also shown there, a phase shift of a transformer has an influence on the power flow, predominantly the active power flow, if one or more parallel paths exist. It is also shown that the magnitude of the turns-ratio, i.e.  $a$  in the expression above, influences mostly the reactive power flow. A phase-shifting transformer would thus be a tool to control the active power flows on parallel paths.

However, the transformers introducing multiples of  $30^\circ$  phase shift would in most cases be too crude for a meaningful power flow control. In realistic systems phase-shifts up to maximum  $10^\circ - 20^\circ$  or so would be very powerful. In addition it would be desirable to be able to control the phase-shift depending on the loading conditions in the network. Thus a transformer according to Figure A.2 where the  $\Delta U_r$  etc. can be controlled, both in mag-

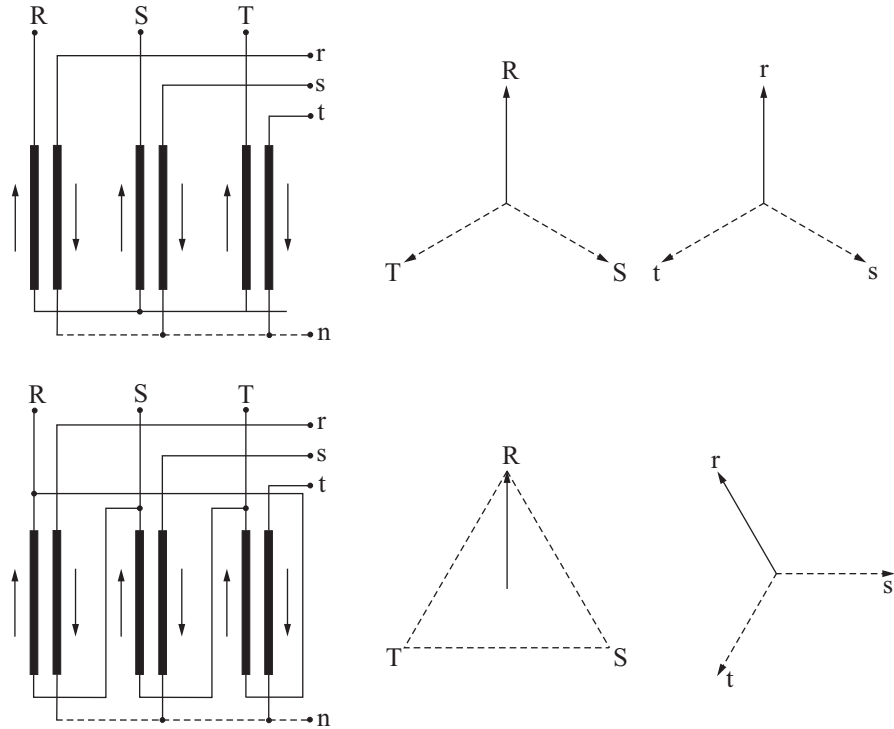


**Figure A.1.** Two different configurations of three-winding transformer.

nitude and in phase, would be of value. This is the so called regulating transformer.

The regulating function of these transformers is achieved through a tap changer that can change the turns on one or more windings and thereby changing the turns-ratio. Depending on the design both the magnitude and the phase of the turns-ratio could be changed. It is obvious that a tap-changer in the transformer connection in Figure A.1 would only change the magnitude of the turns-ratio. (It is assumed that the tap-changers on the three phases are identical and operated identically.) Such arrangements could thus only be used for voltage control. This is one of the main methods to control the voltage in the distribution systems.

In order to introduce a controllable phase-shift to control the active power flow more complicated winding configurations must be introduced. There are several ways of achieving this, and the solution chosen depends on a number of parameters, such as phase-shift range to be controlled, voltage difference between the primary and secondary sides, power rating, etc. Phase-shifting transformers, or phase-shifters, are quite rare in comparison to non phase-shifting transformers<sup>1</sup>. However, phase-shifters play an im-

<sup>1</sup>With non phase-shifting transformers are here meant transformers where a possible

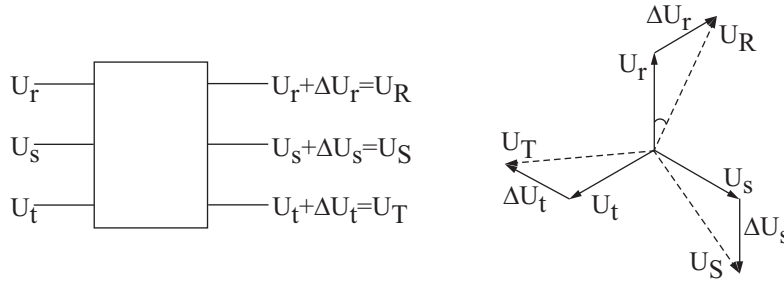


**Figure A.2.** Basic principle of a regulating transformer.

portant role particularly in highly meshed systems where power transfers over long distances take place. Phase-shifters can then re-direct the power flows to circuits that are not so highly loaded. Another function can be to direct the power flow to high voltage lines from highly meshed networks at lower voltage levels. In Europe and North America several phase-shifters are installed for power flow control. Since the traditional tap-changers are mechanical devices, with a typical minimum time interval between subsequent switchings of several tens of seconds, these controllers can only be used for steady state power flow control. Tap-changers with thyristor switches are today available, and with these much faster switchings can be achieved. Thereby also dynamic power swings could be damped. For this purpose also completely power electronics based controllable devices are developed, so called FACTS devices (FACTS = Flexible AC Transmission Systems), which normally offer a much higher degree of controllability.

To obtain a phase-shift, a voltage in quadrature to the phase voltage must be added. Therefore, phase-shifters are also called quadrature transformers or quadrature boosters. Figures A.3 and A.4 show two examples of how phase-shifters can be designed. In Figure A.3 the voltage  $\Delta U$  is inserted by a series transformer and the phase-shift is always accompanied by a certain change in magnitude. For the transformer in Figure A.4 an almost pure phase-shift can be obtained for small phase-shifts.

---

phase-shift does not influence the power flow. Transformers connected Yd are commonly used as generator step-up transformers and as transformers feeding distribution networks. However, since no parallel paths exists, or the parallel transformers are identical, the phase-shift does not play any role for the power flow.

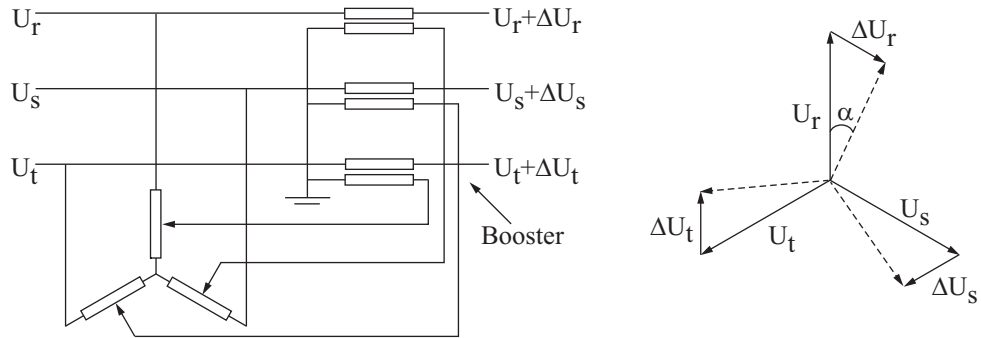


**Figure A.3.** Phase-shift obtained by a series boost transformer.

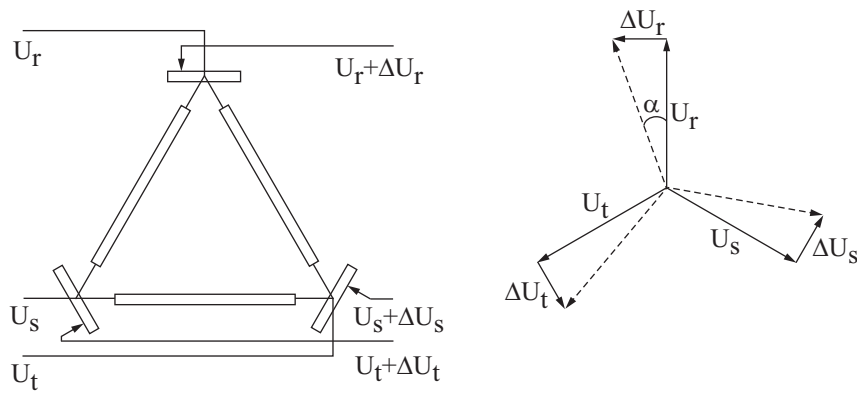


**Figure A.4.** Phase-shift obtained by a quadrature voltage.

# Appendix B

## Protections in Electric Power Systems

*In this Appendix a brief summary of how protections are designed and how they function is given. The very important distance protections and their operating principles are discussed. Some special protections and system wide protections that are of relevance for power system stability is briefly reviewed.*

**D**IFFERENT TYPES of protections are installed to protect the equipment in an electric power system. Their task is to disconnect failed or overloaded equipment or parts of the system to avoid unnecessary damages on equipment and personnel. The purpose is also to limit the impact of failures on the parts of the system that have not failed. Special types of protection are the “system protections”. Their task is to prevent collapse (black out) of the system or parts of the system.

An intensive development of protections based on modern information technology is going on both regarding hardware and software. On the hardware side microprocessors have been used over a long time to implement different functions in the protections, and with the recent developments more and more complicated functions can be implemented in a reliable way. Powerful methods like signal processing, state estimation, and “artificial intelligence”, are being integrated into the protections. In general the functions which earlier were handled with separate relays are increasingly being integrated with other functional units for control and supervision. Furthermore, more complicated criteria for activation of protections can be applied. The interested reader is referred to the literature for further information. The summary here is concentrated on general principles for protections.

### B.1 Design of Protections

A protection for an electric power system comprises the following parts:

- *Measurement device* with current- and/or voltage transformers and other sensors measuring the relevant quantities.
- *Relay* which when certain conditions are fulfilled sends signals to a circuit breaker or another switching device. This relay was earlier a

separate unit, but can in modern protections be a part of a larger unit for protection, supervision and control.

- *Circuit breakers* which execute the given instruction(s) from the relay.
- *Telecommunication system* is mainly used at distance (line) protections to get a faster and more reliable performance.
- *Power supply systems* which shall secure the power supply to the protection system, even with faults in the system.

The requirements on a protection system are that they should be *dependable, secure, selective, sensitive, and fast*.

- *Dependability* means that the protection should react and do its action when a fault occurs for which it is designed to react for. To achieve desired dependability double or even triple sets of certain parts of the protection or of signal paths might be needed. Malfunctions can be divided into "not occurring" operations (which are actions that were supposed to happen but did not) and "unwanted" operations (which are actions that happened although they should not have). Normally not occurring operations are more serious malfunctions than unwanted ones.
- *Security* means that the protection should **not** react when no fault occurs or when a fault for which it is not intended to react occurs.
- *Selectivity* implies that not more than necessary pieces of equipment and apparatuses are disconnected to isolate a fault.
- *Sensitivity* is needed to detect failures which cause small fault currents, e.g. high impedance faults. This implies that the risk for misoperations increases at "small" disturbances, e.g. at energisation of transformers, or at high load operation but normal operation.
- The protection should react *fast* to secure that damages on persons and equipment are prevented or limited.

The protections are often classified according to the object that they protect. An example is shown in Figure B.1. If a failure occurs within an indicated area in Figure B.1 this area should be isolated from the rest of the network.

Many of the protections which protect separate pieces of equipment or parts of a system which occupy a limited physical area are so called current differential protections. These protections measure the difference between two currents, which in normal operation should be equal, and the protection is activated if this deviation exceeds a predetermined value. Both differences in amplitude and phase can trigger the relay. The principle for a current differential protection is shown in Figure B.2.

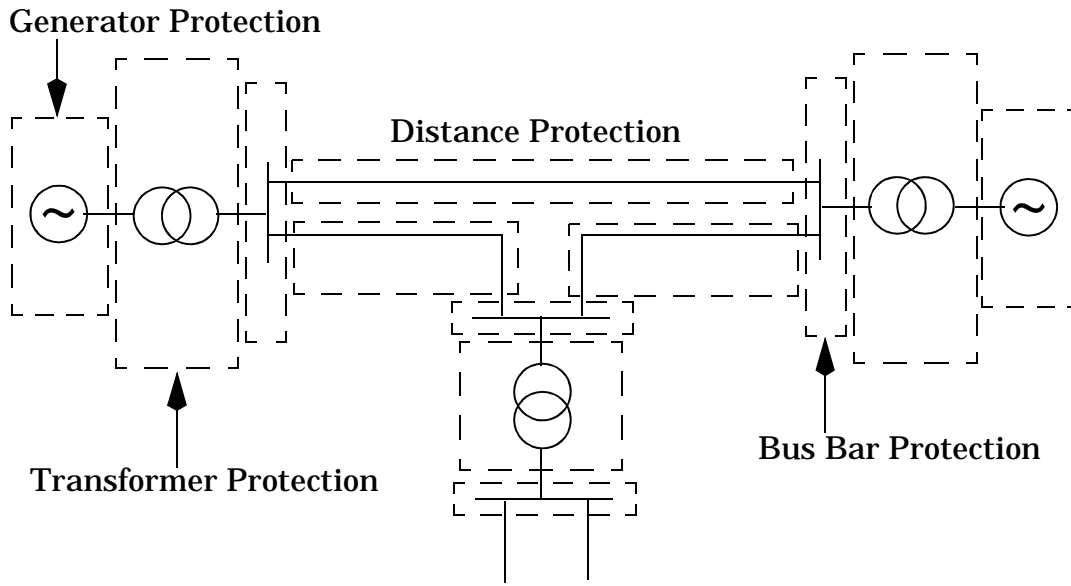


Figure B.1. The different protection zones in a power systems.

## B.2 Distance Protections

### B.2.1 General Principles

So called distance protections are important protections concerning stability and dynamics in a power system. Their task is to disconnect faulted lines or cables. Since large parts of the power system consist physically of lines and these are exposed to different disturbances, e.g. lightning strokes, down falling trees etc., it is important that those faults can be isolated to minimise the impact on the rest of the system. The most common faults are ground (earth) faults, i.e. short circuits between two or more phases and ground (shunt faults). Also interruptions in the lines can occur (series faults). The operating principle of the distance protection is shown in Figure B.3.

Current and voltage are measured in both ends of the line and from these an apparent impedance can be calculated:  $Z = U/I$ . In normal operation this impedance varies within a certain area (large and almost resistive values on  $Z$ ), but if a fault occurs, it will drastically change. The given value depends on where on the line the failure occurs, and from system parameters as line data and short circuit capacity, it can be calculated where the fault has occurred.

For each distance protection there are several protection zones defined in the  $Z$  plane according to Figure B.4. A low value on  $Z$  implies that the fault is close to the measurement. From line data and short circuit capacity

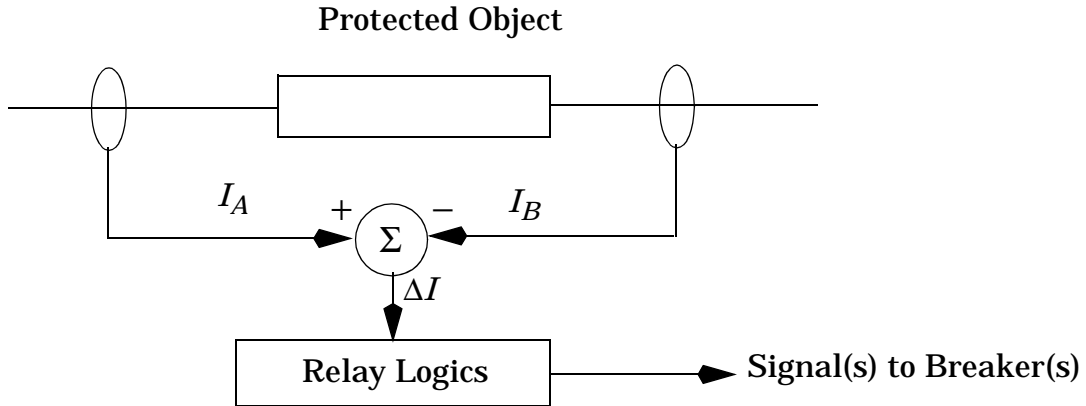


**Figure B.2.** Principles of a current differential protection.

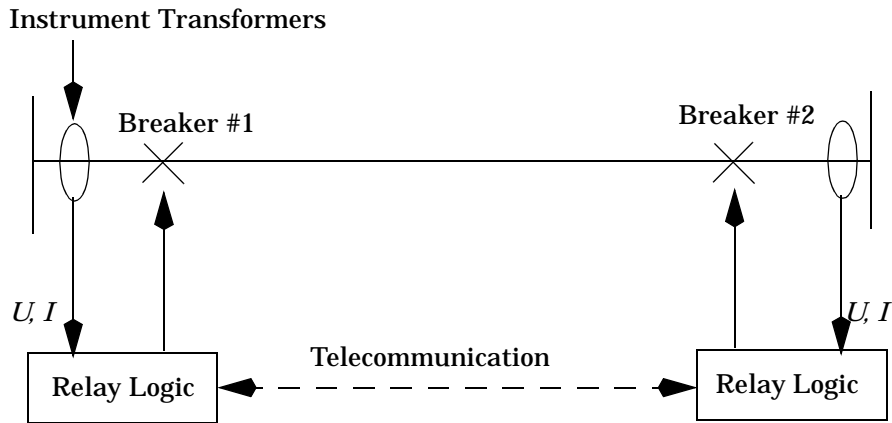


**Figure B.3.** The operating principle of a distance protection.

it can then be decided if the fault is in the protected line, within Zone 1, or not. If that is the case, a trip order is given to the breaker at the same station within some milliseconds, typically 10 ms, after  $Z$  has reached Zone 1. At the same time a trip order is given to the breaker in the other end of the line. This latter trip order is not needed for isolation of the fault, if the protection system in the other end works as it should, but this trip order (transfer trip) increases the security in the system.

If the measured value on  $Z$  is in Zone 2 or 3, it implies that the fault is outside the actual line. This implies that neither breaker 1 nor 2 in Figure B.3 shall be opened. If the breakers, which according to the protection plane should isolate the fault, are not operated by some reason, other breakers which are further away from the fault must isolate it. These secondary

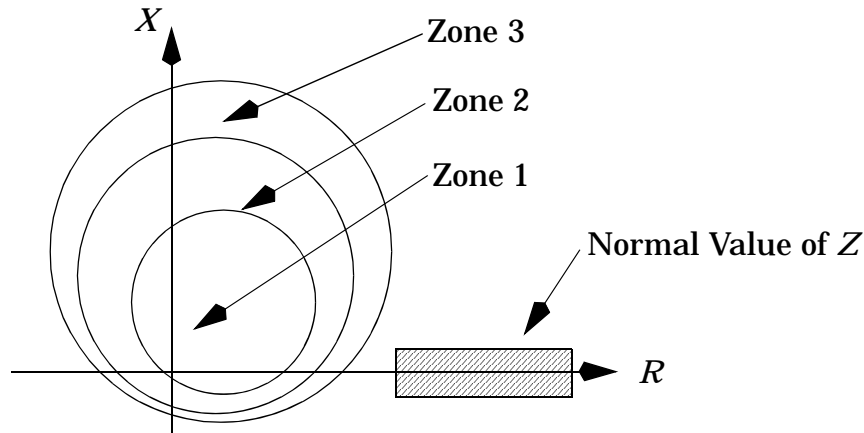


Figure B.4. Different zones in a distance protection.

breakers will be used first after it is clear that the primary breakers have not isolated the fault. Therefore if,  $Z$  is in Zone 2, the breaker does not get the trip order until typically some hundred milliseconds have passed.

To coordinate and tune the settings of the protections to give a fast, reliable, sensitive and selective protection system is a complicated and an important task in an electric power system. In modern protection systems different areas can be defined according to Figure B.4 with in principal arbitrary geometric shapes, which facilitates the work. A plan comprising the different areas of protections and time settings is usually called a *selectivity plan*. The work to establish a selectivity plan is often very time consuming because it should be appropriate for every feasible state of operation, i.e. for different numbers of generators and lines connected and also at different load levels. Often trade-offs must be made to reach acceptable results.

### B.2.2 Automatic Re-Closure

When a ground fault or a short circuit occurs an ionised plasma (arc) that carries the fault current is often formed. This arc remains ionised as long as a the current flows through it. If the fault current is extinguished it is usually sufficient for the plasma to cool down during some hundred milliseconds to rebuild the isolation so that the line can be re-connected. This is used in many systems and the line is automatically re-energised after a given time period after fault clearing. This is the case in many systems, where failed 400 kV lines, or lines at higher voltage levels, are automatically re-closed after 400 ms disconnection. If the failure would still remain, the line is kept disconnected during a larger time period, typically 800 ms, before the next re-closure is done. If the failure would remain after the second re-closure

attempt, more attempts to re-close will not be made. In this latter case the isolation of the line has probably been permanently damaged and it must be repaired before the line can be put in operation again. (This scenario is typical. Due to specific conditions in different countries, deviations can occur.)

Automatic re-closure must be made with certain carefulness when it is made close to large thermal power plants, e.g. nuclear power plants. The connection can in this case cause large stresses on the generator shaft if it occurs at certain phase positions. The re-closure can in this case be done in the remote end of the line seen from the thermal power plant, and then a synchronised re-closure at the other end is made. (With synchronised closure is meant that the voltage over the breaker is zero when it is closed.) In that way the transients in the system are drastically reduced, but of course the re-closure takes longer time.

In some systems all fault clearings on the high voltage grid are made on all three phases. In other systems one phase clearing is used. This means that only the faulty phase(s) is (are) disconnected at fault clearing and re-closure.

### B.3 Out of Step Protections

A synchronous machine which has fallen out of step, i.e. its angular velocity does not coincide with the angular velocity of the net, has lost the synchronism with the system, and the machine must be disconnected. In order to supply electrical power to the system it must be phased in to the system later on. During the time period when the synchronous machine falls out of step large current pulses will pass through the generator, and if these become too many they can damage the generator and limit its life time. Furthermore, vibrations that can jeopardise the generator can arise. To protect a synchronous machine which has fallen out of step the synchronous machine is equipped with a *out of step relay*.

Also in this case an impedance is defined from voltage and current. If the operation state of the generator is in the critical impedance zone a clock is started. If the generator then comes into the critical zone repeatedly times, this is a criterion that the generator is falling out of step, and the protection gives a trip order to the generator breakers.

Generators are also equipped with other protections against overload (stator current protection), over-excitation, etc.

### B.4 System Protections

System protections are special types of protection, the primary task of which is not to isolate failed equipment, but to prevent that the total system or

large parts of it collapse. System protections often use information from several different points in the system or quantities which can give a reliable diagnosis of the state of the system. These systems often work in a time scale which is considerably longer than the more device oriented protections which were considered earlier, typically several seconds or minutes. An example of a system protection is load shedding. This is used to avoid that the frequency in the system falls below acceptable values if the generation capacity has dropped in the system. The load shedding then disconnects predetermined loads depending on how much and how fast the frequency is falling. Voltage collapse protection is another system protection, the task of which is to prevent voltage collapse in the system. Load shedding uses only the frequency as input signal, while the voltage collapse protection often uses several different quantities as input signals.